

TENNET TSO B.V.

# Thermal specification of high temperature superconducting cable in short-circuit conditions

---

## Graduation Thesis

Bachelor of Engineering in Applied Physics

**B.A.C.J. Sluijs (10095365)**

**17-12-2015**

Supervisors at The Hague University of Applied Sciences:

Ing. J.L. Van Yperen, Dr. L.H. Arntzen

Supervisors at TenneT TSO B.V.

Prof. Dr. R. Ross, Ing. G.L.P. Aanhaanen



## Preface

The past seventeen weeks have been a great experience. During my internship at TenneT I had the opportunity to study a technology that lies on the frontier of the application of new technologies. As such I had the chance to not only increase my own knowledge but actually provide, what I think, is useful insights on the application of this technology to my supervisors.

Therefore I would like to start with thanking Rob Ross and Gert Aanhaanen for giving me the opportunity to perform this graduation internship at TenneT and for giving me the ability to study this subject. Furthermore I would like to also thank them for their mentorship and support. The visits to suppliers and conferences have also been a valuable addition to this internship.

Apart from my direct supervisors there have been numerous people who have helped me and given me feedback on my work. Of these people I would like to name the following on the risk that I am forgetting some: Marc Dhallé of the University of Twente, Ruud Hunik and Gerben Koopmans of IWO project and my colleges Andre Lathouwers and Jacco Smit. These people all helped me to improve my work, to check my equations and make my work more useful.

## Abstract

The Dutch Transmission System Operator (TSO) TenneT TSO B.V. is planning to build a 2 km to 4 km long 150 kV superconducting cable connection in the Dutch high voltage grid. Superconducting cable systems allow for connections with no external magnetic field which is beneficial due to society's concerns about magnetic fields. These cables also allow for a reduced right of way compared to conventional cable systems. In locations that already have many underground systems, for example city centres, superconducting cables have the added benefit that they don't influence nearby infrastructure, either thermally or magnetically.

The demand TenneT places on this system is that a superconducting cable should behave just like a conventional connection, not only during regular operation, but also in fault situations. This means that the connection should be able to carry a full fault current of 30 kA for 600 ms and immediately resume operation after the fault is cleared. This demand is not yet demonstrated internationally.

To evaluate the feasibility of this demand this study has been performed. A physical model of a cable system is made using Microsoft Excel. The construction of the cable is then optimized for most efficient operation. The fault current recovery is then evaluated for this cable design. In this manner numeral cable specifications are studied and compared. The cable design that is studied is a counter flown cable. This means that each phase has its own cryostat which contains both a forward and a return flow.

It is demonstrated that at a copper cross section of 300 mm<sup>2</sup> all the designs studied offer immediate fault recovery. Some of the designs offer this recovery at a copper cross section of 250 mm<sup>2</sup>. Depending on the cable configuration and system parameters this is the minimum amount of copper required to offer fault current recovery.

Not only the fault current survivability is calculated for the different cable designs, also the no load and zero load cooling power that is required is calculated. A worst case, realistic case and best case scenario are drafted. For these scenario's the cooling power required is respectively, 329 ± 5 kW, 187 ± 5 kW and 126 ± 5 kW at nominal load and 244 ± 5 kW, 148 ± 5 kW and 112 ± 5 kW at no load.

A comparison is made between these superconducting cable systems and conventional connections. It is shown that the superconducting cable systems can only be competitive in connections that have a high load all of the time. This is due to the high no load losses of superconducting cable systems. For a 1000 A connection the continuous load should be above 550 A for the best case scenario and 650 A for the realistic scenario.

For a 2 km cable that offers immediate fault recovery the realistic scenario is that of a heat intrusion from the exterior of 4 W·m<sup>-2</sup> and a critical current of 3000 A. Such a cable would have a copper cross section of 300 mm<sup>2</sup>, a dielectric field strength of 10 kV·mm<sup>-1</sup> and a former diameter of 36 mm. This cable would operate at a pressure drop over the cable length of 5·10<sup>5</sup> Pa and will have double sided cooling.

The cooling power of longer cable lengths are shown to not scale linear, this can be explained by the fact that longer cables require more cooling and thus a larger diameter. This larger diameter in turn will result in a larger surface area and thus even more heat intrusion from the exterior.

The study shows that the desired behaviour of a system is achievable. There is however only one cable design studied. It is therefore recommended to study other cable designs and determine whether these designs also comply with the demands stated, put possibly at lower losses. It should also be noted that the results of this study can only be used to determine the ballpark dimensions and performance of a superconducting cable system. If such a system would be constructed a more in depth study should be performed.

## Index

Preface .....	3
Abstract .....	4
Introduction.....	9
1 Basic superconductivity principles .....	11
1.1 General principle .....	11
1.2 Applications .....	12
2 Application of superconducting cables in the power grid.....	14
2.1 Benefits .....	14
2.2 Considerations .....	15
3 Layout of a superconducting cable system .....	17
3.1 Cable design .....	17
3.2 Terminations.....	19
3.3 Cooling stations.....	20
4 Overview of relevant physics .....	21
4.1 Thermal equations .....	21
4.2 Pressure equations .....	24
4.3 Electrical equations .....	26
5 Model of a superconducting cable .....	32
5.1 Counter flow design .....	32
6 Cable specifications .....	37
6.1 Short circuit conditions .....	37
6.2 Model results .....	38
7 Conclusion and discussion .....	42
7.1 Results .....	42
7.2 Recommendations .....	42
8 Bibliography .....	44

Appendix A. Material properties .....	47
A.1    YBCO conductor .....	47
A.2    Copper .....	49
A.3    Nitrogen .....	52
A.4    PPLP .....	54
A.5    Multi-Layer Insulation.....	55
Appendix B. Solving the system of equations using excel .....	56
B.1    User interface .....	56
B.2    Calculations and functions.....	58
Appendix C. Model results.....	59
C.1    Dry PPLP .....	59
C.2    Wet PPLP .....	71
Appendix D. Sensitivity Analysis .....	77
D.1    Number of elements .....	78
D.2    YBCO properties.....	80
D.3    Copper properties .....	81
D.4    Nitrogen properties .....	82
D.5    Orders of magnitude of heat transfer.....	83
D.6    Critical current at adiabatic temperature.....	83
D.7    RC time.....	83
D.8    Conclusions .....	84
Appendix E. Graduation Assignment.....	85



## Introduction

The Dutch Transport System Operator (TSO) for systems with a voltage above 110 kV is TenneT TSO B.V. As a TSO TenneT is responsible for the security of supply of electricity in the Dutch high voltage grid.

Since the public opinion is increasingly against overhead lines TenneT is exploring alternatives. Not only the visual impact of overhead lines is an issue, concerns about magnetic fields also increase and pose a problem in the realisation of new connections. One of these alternatives is for example the 380 kV cable project already incorporated in the South-Holland grid near Delft.

A new technology that is gaining increased international attention is the application of superconducting cables in the high voltage grid. These cables allow for high transport capacity with no external magnetic field in a small right of way. Superconducting cables are constructed from a superconducting material and (sub)cooled to liquid nitrogen temperatures of 66 to 90 K.

Some demonstration projects of this technology already exist, the most notable are the 600 m, 138 kV LIPA project in New York, United States and the 1 km, 10 kV Ampacity project in Essen, Germany. To push this technology and acquire hands on experience with the systems and cryogenics TenneT is planning a demonstration project in the 150 kV grid. The system will be designed for a 2 to 4 km long connection of which the location still has to be decided upon.

A special requirement of the TenneT cable is that the cable should exhibit immediate fault recovery and the ability to carry a full fault current. This is a demand that is not demonstrated in any system internationally. Existing cables have either a fault current limiting effect or do not offer immediate fault recovery.

To determine a superconducting cable design that allows for these requirements this study is performed. The main research question is how such a cable design would look like. Secondary questions are how much heat is generated during nominal and fault current operation.

In this paper a brief overview of superconductivity and its benefits will be given. The paper will zoom in on the application, benefits and concerns of superconducting cables in the high voltage grid. After this the governing physics of a superconducting cable system are drafted and a model of a superconducting cable is made. Using the model the operational parameters and fault current  $r$  of several cable designs are calculated. A comparison of the designs is made and expected parameters of such a cable design are shown.

Whilst reading this paper please keep in mind that the objective of the study is to determine the ballpark of the expected system parameters. The ranges in which the results vary is therefore wide and only allow for an estimation of expected performance. To determine exact specification and performance of such a system a more detailed model and calculation should be made.



# 1 Basic superconductivity principles

Superconductivity [1] is the ability of a material to carry electric current without resistance. There is no voltage drop across a superconducting wire when applied to a DC current. Superconductivity was first discovered by Heike Kamerlingh Onnes in Leiden in 1911.

## 1.1 General principle

Superconductors are divided into two groups of superconductors. These groups are type 1 and type 2 superconductors or, low temperature and high temperature superconductors. The main difference between these types of superconductors is the way these materials exhibit superconducting properties. Figure 1-1 shows the year of discovery of several superconductors and the critical temperature from which they exhibit superconducting properties.

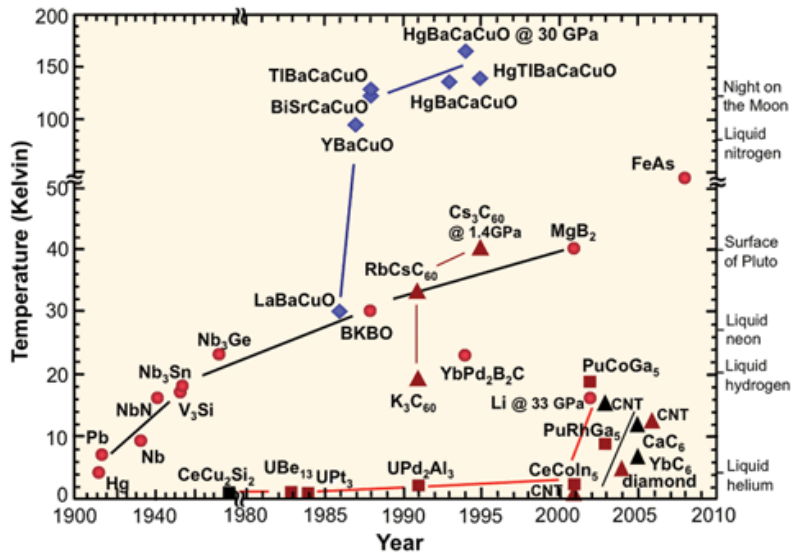


Figure 1-1 Critical temperature and year of discovery of various superconductors [51]

Superconductors require three conditions to be met to become superconducting. These conditions are temperature, current and external magnetic field. All these properties have to be below a critical value. This critical value is different for every superconductor. Figure 1-2 shows an example of the three dimensional field of critical properties that have to be met. The external magnetic field property is mainly an issue in high magnetic field applications and therefore not in the high voltage grid.

### 1.1.1 Type 1 superconductors

Type 1 superconductors are metals that have superconducting properties at temperatures close to absolute zero. These were the first superconductors to be discovered. The principle of these superconductors is relatively well understood and explained by the BCS theory [1]. Type 1 superconductors are only superconducting at low temperatures and with small magnetic fields applied to them. The highest critical temperature for a type 1 superconductor is 9.3 K for Niobium. These superconductors have a discrete superconducting state; either they are superconducting, or they are not superconducting. When these materials are not in superconducting state, they still behave like metal conductors and at lowered temperature still have little resistance. For an example of this, see Figure 1-3.

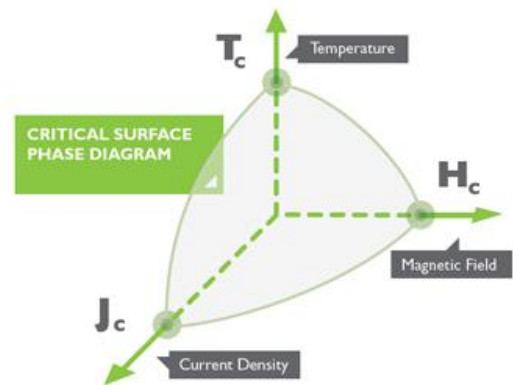


Figure 1-2 Critical quantities [47]

### 1.1.2 Type 2 superconductors

Not only metals can become superconducting, other materials such as alloys and ceramic materials can also possess superconducting capabilities. These kind of superconductors are called type 2 superconductors. The operating principle of this type of superconductors is still not

fully understood. Type 2 superconductors are superconducting at much higher temperatures and are therefore usually called high temperature superconductors (HTS).  $\text{HgBa}_2\text{Ca}_2\text{Cu}_3\text{O}_8$  currently is the superconductor with the highest critical temperature at 138 Kelvin. Commercially available HTS consist of either Yttrium Barium Copper Oxide (YBCO) or Bismuth Strontium Calcium Copper Oxide (BiSCCO). Because these superconductors are superconducting at temperatures above 65 K this allows for cooling with liquid nitrogen. This increases the practical potential of superconductors. For superconducting wires of the first generation BiSCCO is used, for second generation wires YBCO is used.

Apart from the increased critical temperature, type 2 superconductors may also have a higher critical current. Another difference with type 1 superconductors is that type 2 superconductors don't have a discrete superconducting state. Instead of an on or off behaviour they allow for an increased critical current at lower temperatures. When these materials stop being superconducting they behave like electric insulators and have high electrical resistivity of  $20 \text{ m}\Omega\cdot\text{m}^{-1}$  compared to copper with a resistivity of  $2 \text{ n}\Omega\cdot\text{m}^{-1}$  (See Appendix A). Figure 1-3 shows a type 1 superconductor on the left side and a type 2 superconductor on the right. For the type 2 superconductor the critical current depends on the operating temperature. At increased temperatures the critical current is zero and the conductor will be resistive.

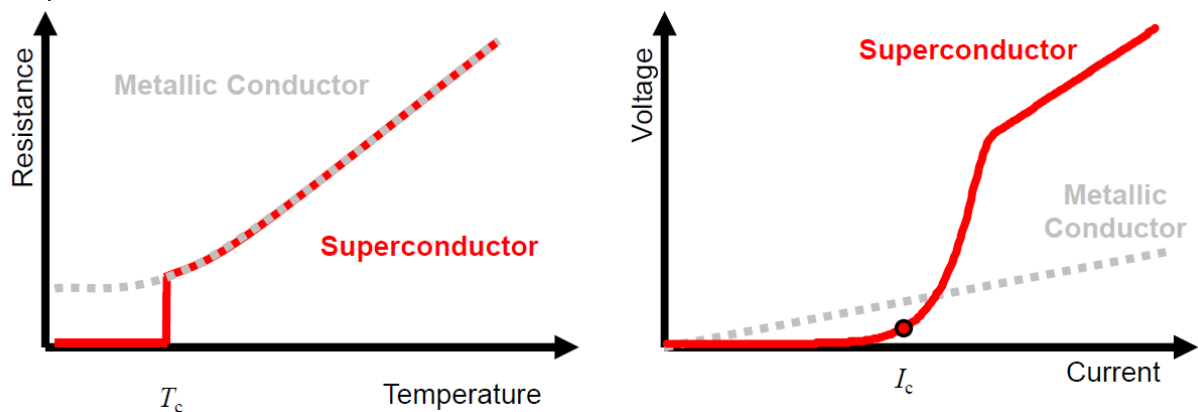


Figure 1-3 Critical quantities of superconductors compared to metallic conductors [2]  
 Left: Type 1 (metallic) superconductor  
 Right: Type 2 superconductor

## 1.2 Applications

Superconductors already have a wide variety of applications. Both type 1 superconductors and type 2 superconductors are used. A limited overview of applications is given in this chapter.

### 1.2.1 Power distribution

Superconductor application in power distribution is in its infancy. There are numerous applications proposed. Superconductors can be used as a replacement for traditional conductors in almost every application. This means superconductors can be used in connections, but also in generators and motors. Power distribution applications use mostly type 2 superconductors.

A new application for superconductors in power distribution is the fault current limiter. By using the property of increased resistivity of superconductors when above their critical current or magnetic field these limiters can be used to decrease the fault currents in a network. This could be beneficial in protecting expensive machines which otherwise would get damaged by the large currents.

### 1.2.2 Other applications

Outside power distribution there are some applications that could not exist without superconductivity. These applications involve powerful magnets. Because the large current capacity of superconducting wires the construction of very strong electromagnets becomes possible. For these applications however, type 1 superconductors are used. These kind of magnets are for example used in Magnetic Resonance Imaging (MRI) machines. They are also used in the Large Hadron Collider (LHC) at CERN to direct the particle beams in the collider. Also the large magnetic fields needed to control the plasma in a tokamak for a nuclear fusion reactor like ITER could not be produced without superconductors. Another application of type 1 superconductors is the maglev train.

## 2 Application of superconducting cables in the power grid

Since this thesis focuses on superconducting cables, the benefits and consideration of the application of superconducting cables in the power grid are further examined.

### 2.1 Benefits

Superconducting cables offer some benefits over conventional cables and lines. These benefits are a reduced right of way, the potential reduction of electrical losses, the prevention of heat production and the reduction of the magnetic field around the cable.

#### 2.1.1 Magnetic fields

A superconducting cable can be constructed in such a way that it does not expel a magnetic field. Since magnetic fields are of concern in regulations and for the social acceptance of power cables and lines this is a mayor improvement. The reduction of magnetic field is achieved by a superconducting shielding layer. Because this requires a double amount of superconducting material this is a costly demand. For this reason it is mainly a cost issue whether or not this property is desired. Because superconducting cables can be placed close together, even without the superconducting shielding magnetic fields can still be reduced by placing the cables in a trefoil configuration as in Figure 2-1.

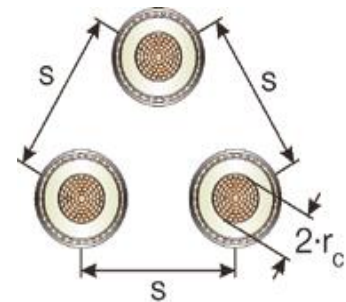


Figure 2-1 Trefoil conventional configuration [52]

#### 2.1.2 Right of way

Superconducting cables allow for a much smaller right of way. Traditional cables require a certain distance between each cable because of the thermal load on the cable. Superconducting cables can be placed directly next to each other. This is especially important at higher voltage levels. The right of way of a 380 kV connection is shown in Figure 2-3, Figure 2-2 shows the right of way needed for a 150 kV connection.



Figure 2-3 Right of way of a 380 kV conventional connection [55]



Figure 2-2 Right of way of a 150 kV conventional connection [54]

At higher transport capacities traditional cables require more cables since the capacity of a single cable is limited, this increases the right of way even further. Superconducting cables can have different transport capacities at the same size of the cable. At the substation the right of way of a superconducting cable is increased, since the substation also has to accommodate the cooling equipment of the superconducting cable.

Figure 2-4 shows a comparison for the decreased right of way in low voltage applications of superconductivity. For High voltage superconductivity a similar or larger reduction in right of way can be achieved.

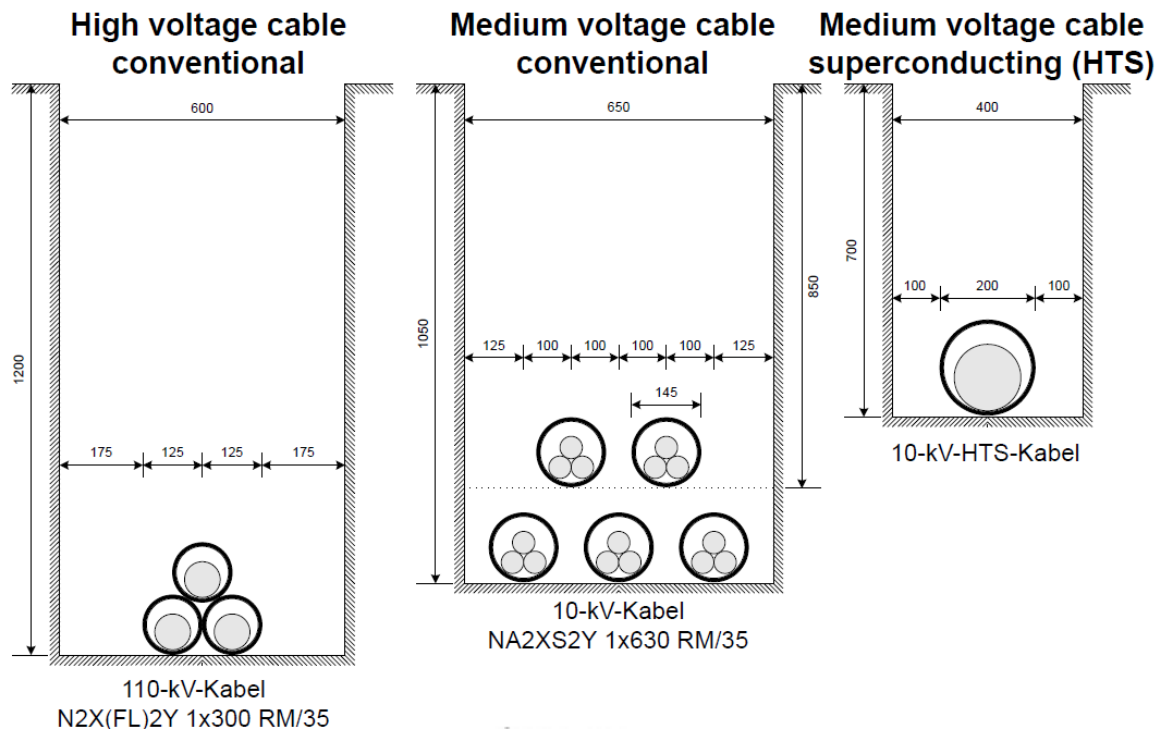


Figure 2-4 Comparison between rights of way for low voltage HTS applications [3]

### 2.1.3 Losses

The reduction of losses in superconducting cable systems can be a benefit of superconductors. This is however particularly the case for DC systems. Superconducting cables do not exhibit resistive losses in DC systems. In AC systems they do however have losses. Depending on cable and cooling efficiency the cable could allow for lower losses than conventional technology. The losses in conventional cables scale with the load of the cable, no load is only the dielectric losses, and high load equals high  $I^2R$  losses. Superconducting cables have higher no load losses since the cable has to be cooled even at no load, at high load the losses will only increase slightly since the superconducting cable has zero resistance. The reduction of losses thus depends on the load factor of the cable. A conventional 150 kV, 1000 A connection (3 phases) at full load has losses of  $187 \text{ kW}\cdot\text{km}^{-1}$  for overhead lines and  $130 \text{ kW}\cdot\text{km}^{-1}$  for cables. At zero load the dielectric losses in conventional 150 kV connections are negligible.

## 2.2 Considerations

One of the key requirements of a superconducting cable formulated by TenneT is that it operates in a similar way as a traditional cable. The application of superconductivity has to be of no consequence on the operating mode of the power grid. This means that from an operating point of view a superconducting cable should be indistinguishable from a conventional cable or line. These considerations mainly concern the behaviour of superconducting cables in regard to short-circuit (or fault) current conditions.

### 2.2.1 Current limiting effects of superconductors

Since superconductors have high resistance at currents higher than their critical current, superconductors exhibit some properties that might be considered positive but need to be considered in a meshed grid. Fault detection systems rely on a high enough fault current to distinguish a fault current from the nominal current. If a superconducting cable would limit the fault current, the fault current might not be high enough to be detected and the fault would not be switched off. It is thus a requirement that the superconducting cable allows for a large enough fault current to flow.

### 2.2.2 Fault recovery time

Conventional cross-linked polyethylene (XLPE) cables are immediately available after a fault current has cleared. Superconducting cables might heat up during a fault and might not be at superconducting temperature immediately after the fault has cleared. This is not acceptable, the superconducting cable should be designed in such manner that immediate fault recovery is guaranteed.

A situation where this design is especially of importance is given in Figure 2-5. In this figure a load is supplied by two parallel conductors. When a fault occurs in the upper cable it is switched off and the other cable will continue supplying the load.

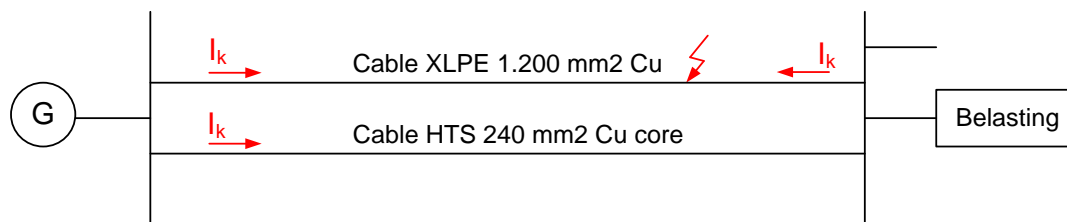


Figure 2-5 Example of short-circuit in neighbouring cable

In a situation when the other connection is superconducting it might heat up because it also feeds the fault. When the conductor is heated and the conventional conductor is switched off, the load is not supplied anymore. The cable should be capable of handling a fault current of 30 kA for 600 ms and return to operation within 3 cycles. In a 50 Hz network this means a recovery time of 60 ms.

### 3 Layout of a superconducting cable system

The superconducting system consists of several components. Apart from the cable itself there are also special cable terminations and cooling stations.

#### 3.1 Cable design

Superconducting cables are constructed in various configurations. Depending on voltage level and operation different types may be preferred.

In general there are four different types of cables. [4] Each will be briefly explained and a more in depth explanation of the single phase, coaxial cables will be given.

##### 3.1.1 Multiphase and warm dielectric cables

The difference between the cable types is the scenario in which they are used. The first cable system is the Triax™ or concentric cable. [5] These cable systems use a single cryostat in which all three phases are wound around a single axis. Figure 3-1 shows a concentric cable. The cable is constructed around a liquid nitrogen filled core. This core is surrounded by the phase 1 superconductor. The second layer is a copper layer for fault current protection. The third layer is a dielectric insulation. Phase 2 and three are similarly constructed. The outer layers of the cable consist of a copper shield, liquid nitrogen, thermal insulation and an outer cover. These cables are used for medium voltage applications. At higher voltages the dielectric would get too large to construct a cable of this design. This design is therefore not applicable in this study.

Another cable type is the single phase PE (warm dielectric) insulated cable. This type of cable is called warm dielectric because the dielectric is outside the cryostat, in contrast to cold dielectric cables where the dielectric is also nitrogen cooled. Warm dielectric cables are useful if spatial constraints are an issue, mainly when retrofitting cables. In new installations cold dielectric cables are preferred [6]. This cable is like conventional XLPE cables except of course for the fact that it is cooled with liquid nitrogen and uses a superconducting core instead of a copper core. The similarity is both conventional XLPE and single phase PE superconductor are not coaxial and use regular PE dielectric insulation. The downside of these cables is that as a result of their design they have an external magnetic field unlike coaxial cable designs. Because the cable design required by TenneT is a design without an external magnetic field, this type of cables is not a viable option.

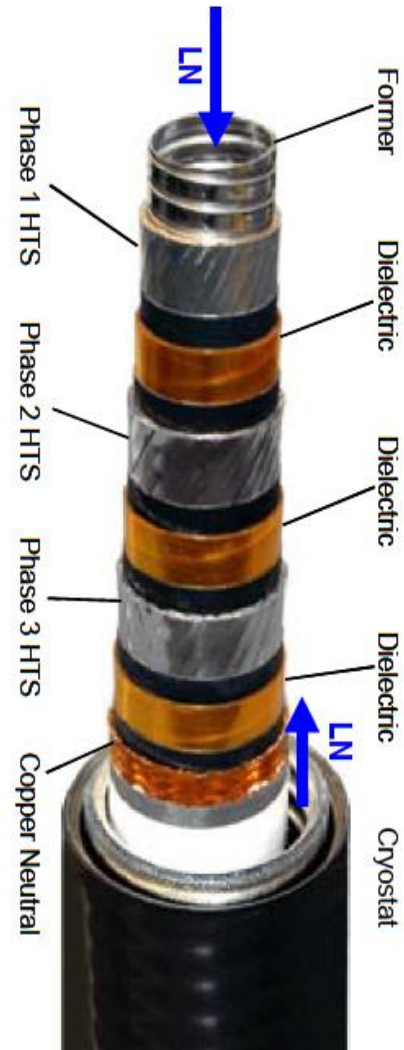


Figure 3-1 Concentric cable [56]

### 3.1.2 Single phase coaxial cables

The cables studied in this paper are from the single phase coaxial design. These designs are suitable for higher voltages and emit no magnetic field. There are two different designs using the coaxial layout. The shared cryostat design (Figure 3-2), and the multiple cryostat design (Figure 3-3). The main difference between these designs is, the layout of the cryostat. The shared cryostat design encapsulates all three phases within a single liquid nitrogen filled cryostat. The multiple cryostat design uses a single liquid nitrogen filled cryostat for each phase. Each phase uses a separate cable surrounded by a separate cryostat. This design is similar to the layout of conventional XLPE cables as these cables also use a single cable per phase.

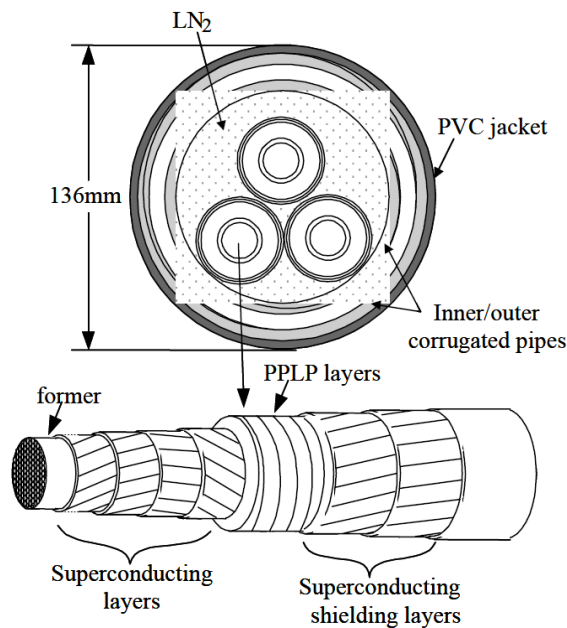


Figure 3-2 Single phase shared cryostat cable [48]



Figure 3-3 Single phase multiple cryostat cable [4]

The inner layers of these coaxial cables are both very similar. The difference between the cables lies in the cryostat. The inner layer of the cable consists of a copper (or alloy) solid former. This former is used to carry the current in case the superconductor is in resistive operation (overcurrent/high temperature/high external field). Surrounding the copper former is a layer (or multiple layers) of superconducting material. The construction of these layers is explained in Appendix A.1. Surrounding the copper material is a polypropylene laminated paper (PPLP) dielectric. This dielectric is submerged in liquid nitrogen. The next layer is a shield layer which consists of superconducting material. The outer layer of the cable is the copper shield layer.

In shared cryostat cables the copper shielding is surrounded by a protective layer. The three phase cables share a bath of liquid nitrogen which in turn is insulated by an inner pipe, vacuum and outer pipe. The entire cable is then surrounded by a PVC jacket.

Multiple cryostat cables have liquid nitrogen surrounding the outer copper shield layer. The nitrogen is encapsulated in the inner cryostat wall. This in turn is surrounded by a thermal insulation and a vacuum. The outer cryostat wall is surrounded by a PE sheath. All three phases use the same layout.

The multiple cryostat design is used in both laboratory and in operational connections [7] [8]. This is because LN2 cooling is provided closer to the superconducting layers. Also the shared cryostat design doesn't allow for evenly distributed cooling of the conductors, because the conductors will move in a configuration as illustrated in Figure 3-2. This might be mitigated by using spacers in the cable design. Single cryostat cables offer improved thermal insulation over multiple cryostat cables because the circumference of the single cryostat cables is lower than when multiple cryostats are used.

Apart from the cable design, the return flow of the nitrogen is also a concern. There are several ways to accommodate the return flow of the nitrogen. This can be done by a separate smaller return feed for the nitrogen. Another method is a hollow former for the flow. This design is common in Triax or DC cable systems, but can also be used in multiple or single cryostat design cables. Multiple cryostat also allow for one phase to serve as a forward flow and the two other phases as the return flows. This configuration doesn't require a hollow former, but will have different flow speeds and pressure drop depending on the flow direction. This setup is used in the American LIPA project [9] and can be seen in Figure 3-4.

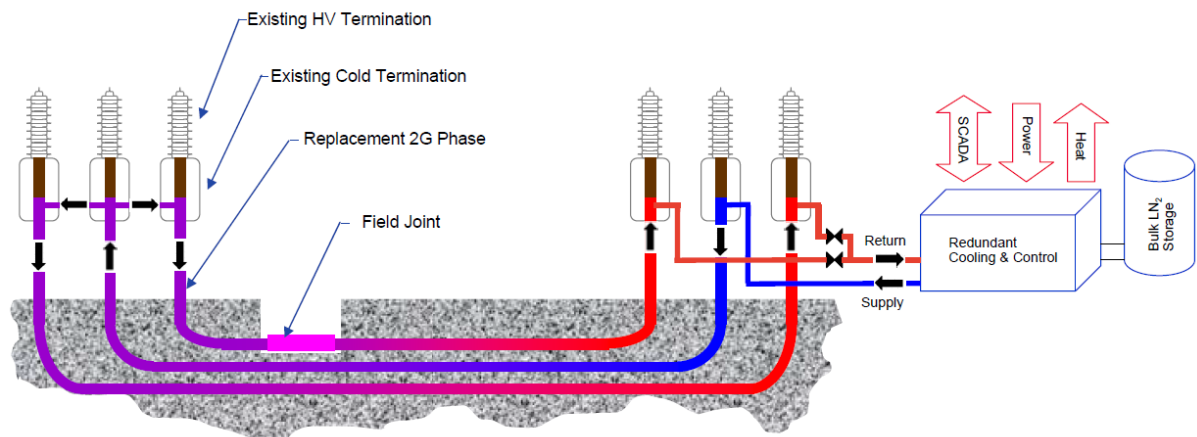


Figure 3-4 Flow paths of LIPA cable [9]

### 3.2 Terminations

The connection between the cable and the substation is made with a termination. The termination of a superconducting cable is not only a termination for the electrical circuitry, it is also a termination for the thermal circuit. This makes the terminations of a superconducting cable a point of interest. Inside the termination the connection between copper conductor and superconductor is made. Also the connection between room temperature and cryogenic temperature is made.

Since the termination connects the copper conductor to the superconductor it is operated at cryogenic temperature. Cryogenic losses in each termination are  $43 \text{ W}\cdot\text{kA}^{-1}$  [10]. Especially in short connections the terminations are an important contribution to the total heat loss.

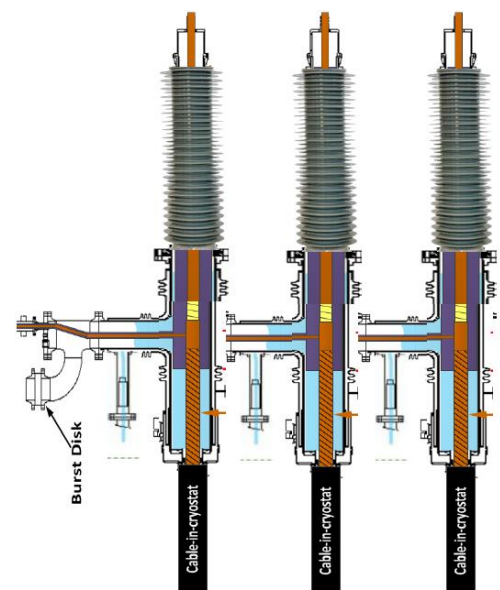


Figure 3-5 Termination design for 150 kV by NKT [53]

Terminations can be designed with their own cooling circuit, this is beneficial because heat generated in a termination doesn't have to be carried all the way through the cable cooling system. When single ended cooling is used one side of the terminations has to be cooled with nitrogen from the cable loop. This heat loss has to be incorporated in the cable cooling design.

### **3.3 Cooling stations**

The terminations on one or both ends of the cable are connected to cooling stations where the liquid nitrogen is cooled down to the desired temperature and pressurised to the desired pressure. The pressurisation is done with a compressor (or pump). The cooling is done with a cryogenic refrigerator. Multiple designs of such devices exist.

#### **3.3.1 Open cycle**

The open cycle cooling station uses a nitrogen storage tank that has to be regularly filled. Reaching the desired temperature is achieved by boiling of nitrogen. The drawback of such a system is the dependency on regular deliveries of nitrogen. Its benefits are a low investment cost and no technical complicated parts.

#### **3.3.2 Closed cycle**

Closed cycle cooling stations re-cool the same nitrogen over and over. The benefit of this approach is no dependency on external suppliers. The drawback of these systems is the higher investment costs and the increased technical complexity. Several different designs of cryo-coolers are available. This paper won't cover the designs and considerations regarding the different type of cryo-coolers. But technical data from suppliers indicate a cooling penalty of 20 should be expected [11]. This means that every watt of cold requires 20 watts of electrical power for cooling.

## 4 Overview of relevant physics

This chapter will cover the different sections of physics that are relevant in modelling a cable system. Every relevant quantity will first be described on its own. These quantities are the thermal, pressure and electrical equations. After these quantities are described an all including model will be made. The goal of this model is to determine the heat profile along the superconducting cable. This is necessary to determine the temperature change that is allowable in the conductor when a short circuit occurs. The system boundary that is considered is the inner cryostat wall, the cryostat itself is therefore outside of the considered system.

### 4.1 Thermal equations

The thermal equations are the equations governing heat transfer. These equations will ultimately define the thermal behaviour of the system, the main goal of this research.

#### 4.1.1 Specific heat capacity

The specific heat capacity is the amount of heat a material needs to absorb to increase its temperature 1 K. It is given by equation (1). The specific heat capacity is relevant to determine the temperature change that occurs in a short circuit condition. It also determines the heat that can be extracted by the liquid nitrogen cooling.

$$q = mc \frac{dT}{dt} \quad (1)$$

With

$q$	Heat absorbed per unit of time	(W)
$m$	Mass of material	(kg)
$c$	Specific heat capacity	(J·kg <sup>-1</sup> ·K <sup>-1</sup> )
$\frac{dT}{dt}$	Rate of heating	(K·s <sup>-1</sup> )

#### 4.1.2 Conduction

Conduction is the heat transfer from one material to another through a barrier of a third material. The amount of heat transferred for a cylindrical configuration is given by equation (2). Since the heat transfer between the layers of the superconducting system is one of the main questions this equation is important in assessing the heat transfer between these layers.

$$q = \frac{-2\pi k L \Delta T}{\ln\left(\frac{r+d}{r}\right)} \quad (2)$$

With

$q$	Heat conducted per unit of time	(W)
$k$	Conductivity coefficient	(W·m <sup>-1</sup> ·K <sup>-1</sup> )
$L$	Length of the cylinder	(m)
$\Delta T$	Temperature difference across the cylinder	(K)
$r$	Inner radius of the cylinder	(m)
$d$	Thickness of the cylinder	(m)

#### 4.1.2.1 Multiple layers

For conduction problems with multiple layers the thermal conductivity can be summed and an average thermal conductivity can be deduced

$$q = \frac{-2\pi L\Delta T}{\frac{1}{k_1} \ln\left(\frac{r_1 + d_1}{r_1}\right) + \frac{1}{k_2} \ln\left(\frac{r_2 + d_2}{r_2}\right) \dots + \frac{1}{k_n} \ln\left(\frac{r_n + d_n}{r_n}\right)} \quad (3)$$

$$k_t = \frac{\ln\left(\frac{r + d}{r}\right)}{\frac{1}{k_1} \ln\left(\frac{r_1 + d_1}{r_1}\right) + \frac{1}{k_2} \ln\left(\frac{r_2 + d_2}{r_2}\right) \dots + \frac{1}{k_n} \ln\left(\frac{r_n + d_n}{r_n}\right)} \quad (4)$$

With

$k_t$  Average thermal conductivity of the cylinder (W·m<sup>-1</sup>·K<sup>-1</sup>)

#### 4.1.3 Convection

Convection equations are analogue to those of conduction. However, whereas conductivity has a known material property  $k$  this is not a known property for convection, for this depends on the type of fluid flow around a material. Convection is governed by Newton's law of cooling (equation (5)). The difference here is that the temperature difference is not across the insulation layer, but between the material and the surrounding liquid. The convective heat transfer determines the efficiency of the liquid nitrogen cooling. Since the desired temperature gradient between the nitrogen and the copper is only small, a large convective heat transfer coefficient is desired.

$$q = -hA\Delta T \quad (5)$$

With

$q$  Heat conducted per unit of time (W)  
 $h$  Convective heat transfer coefficient (W·m<sup>-2</sup>·K<sup>-1</sup>)  
 $A$  Area of heat transfer (m<sup>2</sup>)  
 $\Delta T$  Temperature difference across the cylinder (K)

#### 4.1.4 Characteristic numbers

Heat transfer phenomena can be characterized by several numbers. These numbers give an indication of the behaviour of the phenomena involved.

##### 4.1.4.1 Hydraulic diameter

The hydraulic diameter is an indication of the ratio between the cross section and the surface of a flow. The hydraulic diameter is defined as follows:

$$D_H = \frac{4A}{S} \quad (6)$$

With

$A$  Cross section (m<sup>2</sup>)  
 $S$  Total surface area (m)

Depending on the cable configuration different hydraulic diameters should be used. Three different configurations are applicable, depending on the flow to be calculated. These configurations are listed in Table 1.

**Table 1 Cable configurations and hydraulic diameter**

Schematic	Layout	Flow path description	Hydraulic diameter equation
	Hollow former, normal pipe	Inside the conductor, no objects in flow path	$D_H = D$
See Figure 3-3	Multiple Cryostat	Around the conductor, flow path obstructed by conductor	$D_H = D_{outer} - D_{inner}$
See Figure 3-2	Single Cryostat	Within the flow path there are three smaller conductors.	$D_H = \frac{D_{outer}^2 - 3D_{inner}^2}{D_{outer} + 3D_{inner}}$

The hydraulic diameter of the conductor depends on the final layout of the cable. For example a combination of hydraulic diameters might be used for the final cable design, since a multiple cryostat design might also use a hollow former.

#### 4.1.4.2 Nusselt number

The Nusselt number gives the ration between the convective heat transfer and the conductive heat transfer of a liquid. This is used to calculate the effectiveness of the nitrogen cooling.

$$Nu = \frac{hD_h}{k} \quad (7)$$

With

$Nu$	Nusselt number	
$h$	Convective heat transfer coefficient	$(W \cdot m^{-2} \cdot K^{-1})$
$D_h$	Hydraulic Diameter	$(m)$
$k$	Thermal conductivity	$(W \cdot m^{-1} \cdot K^{-1})$

Under certain conditions a relationship for the Nusselt number other than equation (7) can be given. One of these relationships is the Gnielinski correlation which is valid for Prandtl numbers between 0.5 and 2000 and Reynolds numbers between 3000 and  $5 \cdot 10^6$  [12]. Typical Nusselt numbers for turbulent pipe flow are in the range of 100-1000 [13].

$$Nu = \frac{\left(\frac{f}{8}\right)(Re - 1000)Pr}{1 + 12.7\left(\frac{f}{8}\right)^{\frac{1}{2}}\left(Pr^{\frac{2}{3}} - 1\right)} \quad (8)$$

With

$Nu$	Nusselt number
$f$	Friction factor
$Re$	Reynolds number
$Pr$	Prandtl number

Using the results from equation (8) in equation (7) yields the convective heat transfer coefficient.

#### 4.1.5 Heat exchanger

For some cable designs the heat exchange between the inner and outer flow is of influence. This heat exchange is given by equation (9). Since the expected thermal difference is only small the arithmetical temperature difference can be used instead of the logarithmic mean temperature difference [14]. The maximum expected temperature difference over the cable is 10 K

$$q = kA \cdot \frac{(T_{w1} - T_{c1}) + (T_{w2} - T_{c2})}{2} \quad (9)$$

With

$q$	Amount of heat exchanged between layers	(W)
$k$	Thermal conductivity between flows	(W·m <sup>-2</sup> ·K <sup>-1</sup> )
$A$	Logarithmic average surface area between flows	(m <sup>2</sup> )
$T$	Temperature at different points along the flow	(K)

## 4.2 Pressure equations

Apart from the thermal equations, pressure also plays an important role. As is explained in chapter A.3 increased temperatures and decreased pressure may result in boiling of the nitrogen. This has to be prevented because such a situation would result in permanent damage of the cable. It is therefore important to create an accurate representation of the pressure in the cable.

### 4.2.1 Bernoulli equation

The main equation governing fluid flows is the Bernoulli equation. It states that the energy (in different forms) entering a pipe has to be the same as the energy leaving the pipe. Equation (10) is the Bernoulli equation, equation (11) is the volumetric flow rate.

$$\frac{1}{2}v_1^2 + gh_1 + \frac{P_1}{\rho} - \frac{1}{2}v_2^2 - gh_2 - \frac{P_2}{\rho} - E'_v = 0 \quad (10)$$

$$A_1v_1 = A_2v_2 \quad (11)$$

With:

$v$	Speed of the nitrogen flow	(m·s <sup>-1</sup> )
$g$	Gravitational acceleration	(m·s <sup>-2</sup> )
$P$	Pressure	(kg·m <sup>-1</sup> ·s <sup>-2</sup> )
$\rho$	Density	(kg·m <sup>-3</sup> )
$E'_v$	Friction losses per unit mass	(m <sup>2</sup> ·s <sup>-2</sup> )
$A$	Cable cross-section	(m <sup>2</sup> )

Since for this cable it is assumed that the height difference between cable ends is negligible, the height difference terms in equation (10) can be ignored. The cable diameter at beginning and end are the same, so following equation (11) the flow at beginning and end of the cable is the same. Using this information gives equation (12).

$$\begin{aligned} \frac{P_1}{\rho} - \frac{P_2}{\rho} - E'_v &= 0 \\ \frac{P_1 - P_2}{\rho} - E'_v &= 0 \\ \Delta P &= \rho E'_v \end{aligned} \quad (12)$$

#### 4.2.2 Laminar and turbulent flows

To determine the energy lost due to friction it is needed to determine whether the nitrogen flow is either laminar or turbulent. This is done by determining the Reynolds number of the flow and the relative roughness of the tubing. The relative roughness of the tubing is dependent on the hydraulic diameter and the roughness of the tubing. Equation (13) gives the Reynolds number and (14) gives the relative roughness.

$$Re = \frac{\rho v D_H}{\mu} \quad (13)$$

$$R_r = \frac{\epsilon}{D_H} \quad (14)$$

With

$Re$	Reynolds number	
$v$	Speed of the nitrogen flow	(m·s <sup>-1</sup> )
$\rho$	Density	(kg·m <sup>-3</sup> )
$D_H$	Hydraulic diameter	(m)
$\mu$	Dynamic viscosity	(kg·m <sup>-1</sup> ·s <sup>-1</sup> )
$R_r$	Relative roughness	
$\epsilon$	Roughness	(m)

For heat transfer situations a turbulent nitrogen flow is preferred because this allows for both conductive and convective heat transfer [15]. Flows are generally turbulent with a Reynolds number over 2500 [14]. An optimal point has to be found where flow is still turbulent for maximum heat transfer, but the friction is low enough to prevent a large pressure drop over the cable.

#### 4.2.3 Friction factor

The friction factor is used to determine the amount of heat generated by the pressure drop in the cable. This is relevant because this heat has to be removed from the cable at the cooling stations.

In this paper the Darcy friction factor will be calculated. For laminar flows the friction factor is given by equation (15). For turbulent flows the friction factor is given by the Colebrook equation (16).

$$f = \frac{64}{Re} \quad (15)$$

$$\frac{1}{\sqrt{f}} = -2 \log_{10} \left( \frac{\epsilon}{3.7 D_H} + \frac{2.51}{Re \sqrt{f}} \right) \quad (16)$$

With

$f$	Friction factor	
$Re$	Reynolds number	
$\epsilon$	Roughness	(m)
$D_H$	Hydraulic diameter	(m)

Since the Colebrook equation is an implicit function and cannot be calculated directly, an approximation is used to find the friction factor. In this thesis the Haaland equation (17) is used [16]. The Haaland equation is valid for flows with a Reynolds number above 3000. For these flows the accuracy of the Haaland equation is within 2%.

$$\frac{1}{\sqrt{f}} = -1.8 \log_{10} \left( \left( \frac{\epsilon}{3.7D_H} \right)^{1.11} + \frac{6.9}{Re} \right) \quad (17)$$

When the friction factor is acquired it can be used to determine the friction losses in equation (12) this is done by using equation (18). These energy losses will contribute to the warming of the nitrogen and have to be extracted from the nitrogen at a cooling station.

$$E'_v = \frac{fLv^2}{2D_H} \quad (18)$$

Multiplying with the density  $\rho$  gives the pressure difference over the cable length. In these calculations it is assumed that there are no sudden bends and corners in the cable. This can safely be assumed because such bends could damage the cable core and will therefore be certainly avoided when installing the cable. Pressure drop due to bends and corners is thus negligible.

The pressure drop has to be compensated with a pump. The required pumping power depends on the efficiency of the pump. Since pump efficiency largely depends on the volume flow and the type of pump the efficiency has to be determined after a volume flow is chosen.

### 4.3 Electrical equations

The electrical equations will focus on calculations of losses. Operating conditions and expected short circuit currents will be considered input parameters. The sources of electrical losses considered are resistive losses in the copper core, dielectric losses for the cable insulation, ac-losses for the superconductor and joint losses at the superconductor wire joints.

#### 4.3.1 AC-losses

Theoretically the superconductor has no resistive losses. This is true for DC currents. For AC currents however, superconductors suffer some losses. These losses consist of hysteresis losses, eddy current losses and magnetic coupling losses [17]. These AC losses will generate some heat in the conductor and this heat will have to be removed. An approximation of the AC loss and thus the heat generated in the conductor is given by the Norris equation (19) [18]. Depending on the cable configuration this heat generation is also applicable to heat generated in the shielding of the cable.

$$q = \frac{\mu_0 I_c^2 f}{\pi} \left( \left( 1 - \frac{I_0}{I_c} \right) \ln \left( 1 - \frac{I_0}{I_c} \right) + \left( 1 + \frac{I_0}{I_c} \right) \ln \left( 1 + \frac{I_0}{I_c} \right) - \left( \frac{I_0}{I_c} \right)^2 \right) \quad (19)$$

With

$q$	AC loss per meter	$(W \cdot m^{-1})$
$\mu_0$	Vacuum permeability	$(V \cdot s \cdot A^{-1} \cdot m^{-1})$
$I_c$	Critical current	(A)
$f$	System frequency	$(s^{-1})$
$I_0$	Transport current	(A)

Using this equation the AC losses now can be calculated. Figure 4-1 shows the transport loss for different critical currents of conductors. It can be seen that the critical current should be higher

than the expected transport current. If expected transport current and critical current are equal, ac losses are high. A higher critical current has the benefit of reducing the AC losses, a cost benefit optimization between cooling cost and purchase cost of the superconductor should be made. For applications with transport currents up to 1000 A, a critical current of 1500 or 2000 should be considered as minimum. A critical current of x A will from here on be noted as I<sub>c</sub> x, for example I<sub>c</sub> 1000 means critical current of 1000 A.

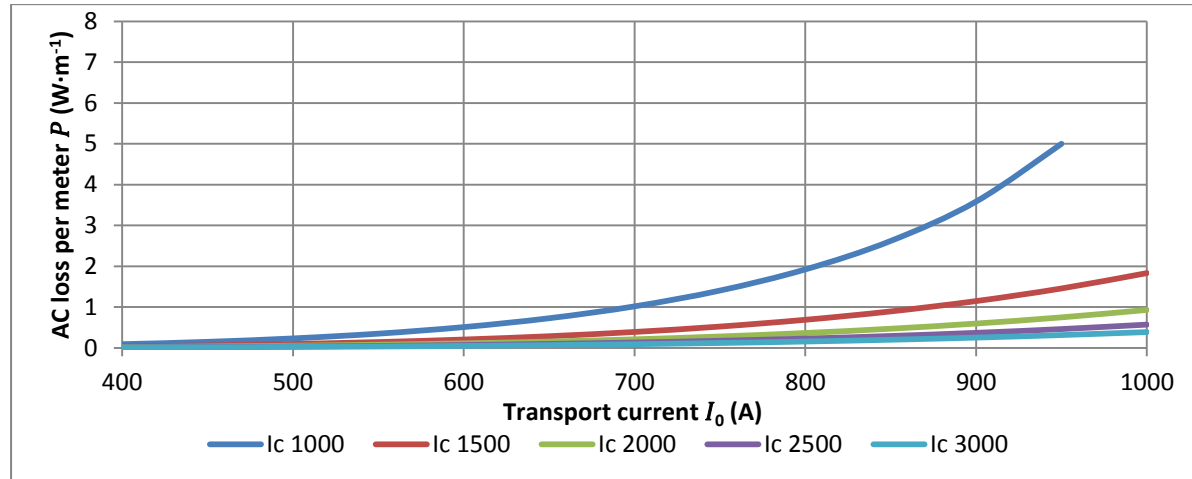


Figure 4-1 AC loss of different conductors

It is demonstrated that using novel production techniques AC losses can be decreased by a factor up to 2 [19]. Therefore a correction factor is introduced. This factor ranges between 0.5 and 1. The representations in this chapter are all done using correction factor 1. An improvement over these values can be expected and is discussed in Appendix A.

#### 4.3.1.1 Temperature dependency

Since the critical current of the superconducting wires is temperature dependent, the AC-losses are also temperature dependent. Because the temperature along the superconducting cable isn't uniform the temperature dependency of the losses has to be taken into account. This is done by making a linear approximation of the temperature dependency. This linear approximation is made because this approach allows for less complicated solving of the final system of equations. This will be explained in chapter 5. For calculations the specified critical current could be used for all temperatures. Figure 4-2 gives a comparison between the three methods for a tape with critical current of 3000A and a current of 1000A. It can be seen that the error made using the linear approximation is much smaller than that of the reference critical current. The linear approximation used is that of equation (20). The approximation that is used is always a worst case approximation. In the temperature range that it is calculated the approximated losses are always higher than the real losses. In other words, the real world performance will be better than the calculated performance. The differences can be found in Appendix D.

$$q = \frac{q_{T_{ref}} - q_{T_{low}}}{T_{ref} - T_{low}} \cdot (T - T_{low}) + q_{T_{low}} \quad (20)$$

With

$q$	AC loss per meter	(W·m <sup>-1</sup> )
$q_{T_{ref}}$	AC loss per meter at reference temperature	(W·m <sup>-1</sup> )
$q_{T_{low}}$	AC loss per meter at system low temperature	(W·m <sup>-1</sup> )
$T_{ref}$	Reference temperature of critical current	(K)
$T_{low}$	Lowest system temperature	(K)
$T$	Temperature at which the loss is to be calculated	(K)

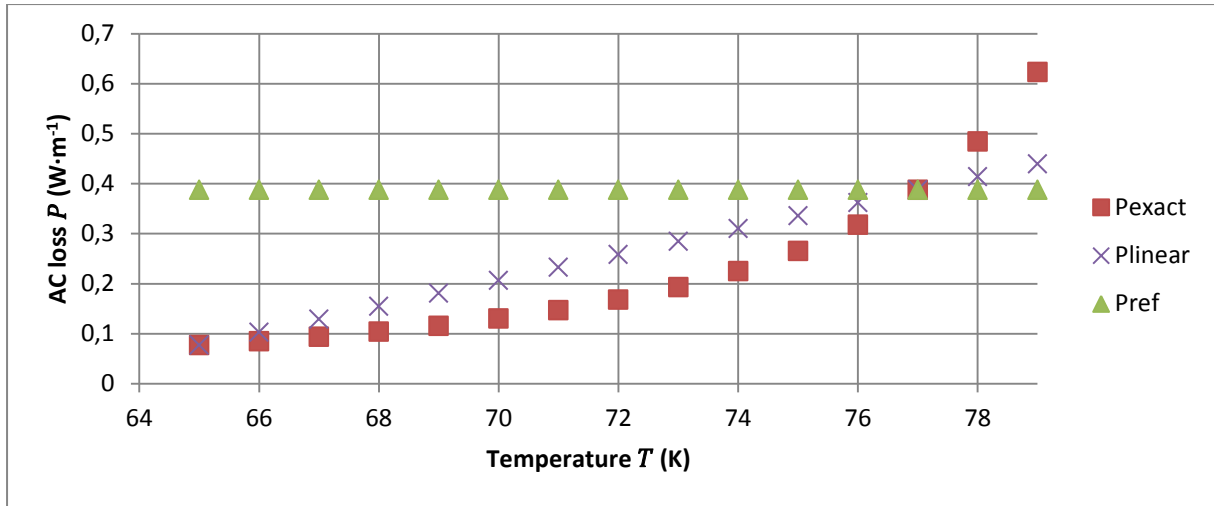


Figure 4-2 Comparison of approximations of AC-loss

#### 4.3.2 Resistive losses

Resistive losses are of significance when the conductor is out of superconducting operation. The resistive losses govern the amount of heat generated by the copper conductor. Equation (21) gives the resistive losses of the conductor. In the calculations it is assumed that when the superconductor is in operation the copper core can be considered a perfect insulator and when out of superconducting state the superconductor can be assumed a perfect insulator. Thus the assumption is when superconducting:  $R_{superconductor} \ll R_{copper}$  and when out of superconducting state:  $R_{superconductor} \gg R_{copper}$ . Using these assumptions heat generated by the copper or the conductor can be neglected depending on operating conditions. As with AC losses these losses might be applicable to the shielding.

$$q = I^2 R \quad (21)$$

With

$q$	Resistive loss per meter	(W·m <sup>-1</sup> )
$I$	Current	(A)
$R$	Copper resistance	(Ω·m <sup>-1</sup> )

Using equations (36) and (21) the resistive losses can be calculated. Figure 4-3 shows resistive losses for different cable cross-sections with currents up to 30 kA. This shows the expected losses in short circuit conditions and the amount of heat the system has to handle.

Figure 4-4 compares different HTS critical currents with copper cross sections at nominal currents. This shows that the combination of the  $I_c 1000$  HTS with 350 mm<sup>2</sup> copper conductor is unlikely because of the better performance of copper in nominal conditions.

Another comparison is the comparison of HTS losses and copper losses in overcurrent situations. Figure 4-5 shows this comparison. It can be seen that the losses of HTS conductors and 300 mm<sup>2</sup> copper transition when the superconductor exceeds its critical current.

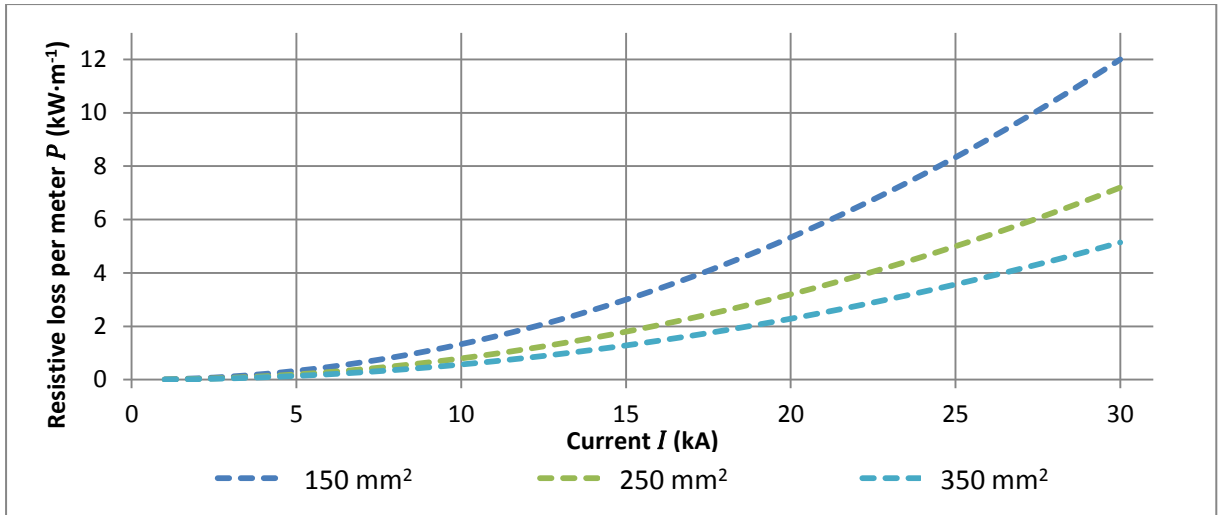


Figure 4-3 resistive losses for different conductor cross-sections in short circuit conditions

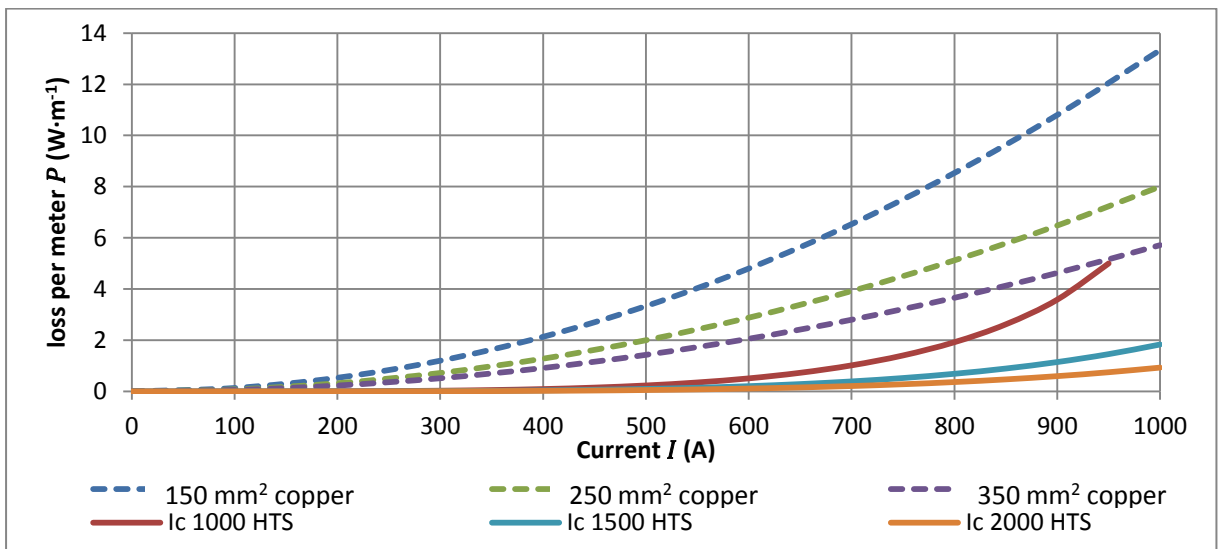


Figure 4-4 Losses of copper core and HTS of different dimensions compared at nominal current

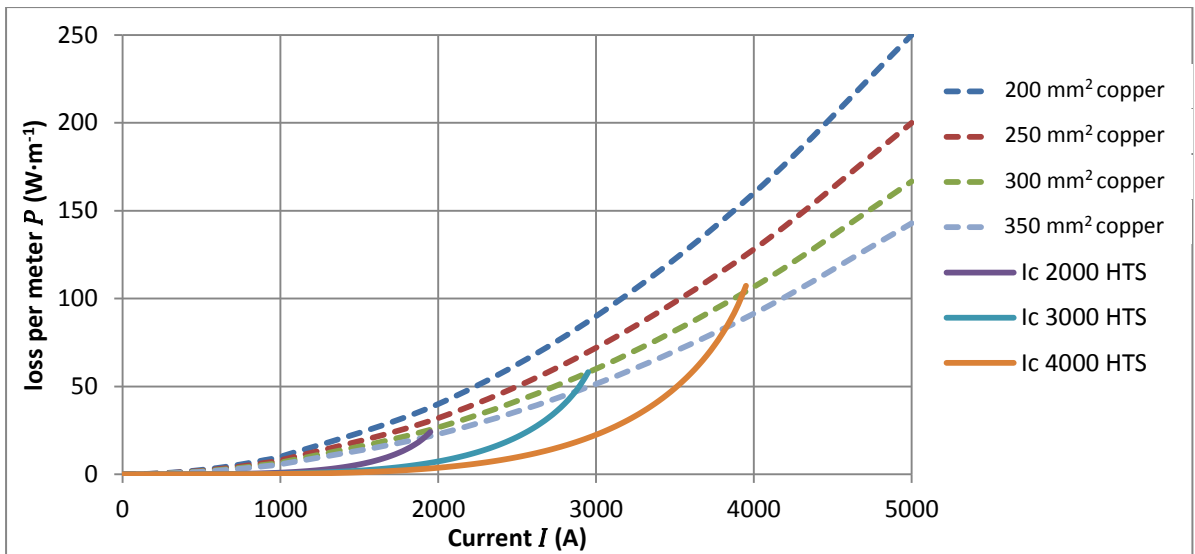


Figure 4-5 Losses of copper core and HTS of different dimensions compared at over current

### 4.3.3 Dielectric insulation and losses

The dielectric losses depend on the voltage level and the dielectric insulation properties.

#### 4.3.3.1 Dielectric insulation

The minimum insulation thickness between inner and outer conductor is calculated as if there is no PPLP between the conductors and only nitrogen. The maximum allowable peak electric field strength before discharge is  $15\text{kV}\cdot\text{mm}^{-1}$  as is explained in chapter A.3.1.1. Cable dielectric insulation is calculated based on the phase voltage.

$$E_{max} = \frac{U}{r \ln\left(\frac{R}{r}\right)} \quad (22)$$

With

$U$	Phase voltage	(kV)
$E_{max}$	Maximum field strength	( $\text{kV}\cdot\text{mm}^{-1}$ )
$r$	Inner radius	(mm)
$R$	Outer radius	(mm)

Using these equations the insulation thickness of the cable can be determined for various allowed electrical fields. This can be seen in Figure 4-6. It should be noted that the cross section is not necessarily that of the copper. A hollow copper strand could also be used, still resulting in the same diameter. The figure also shows that if only a low electrical field is allowed the outer radius is much larger.

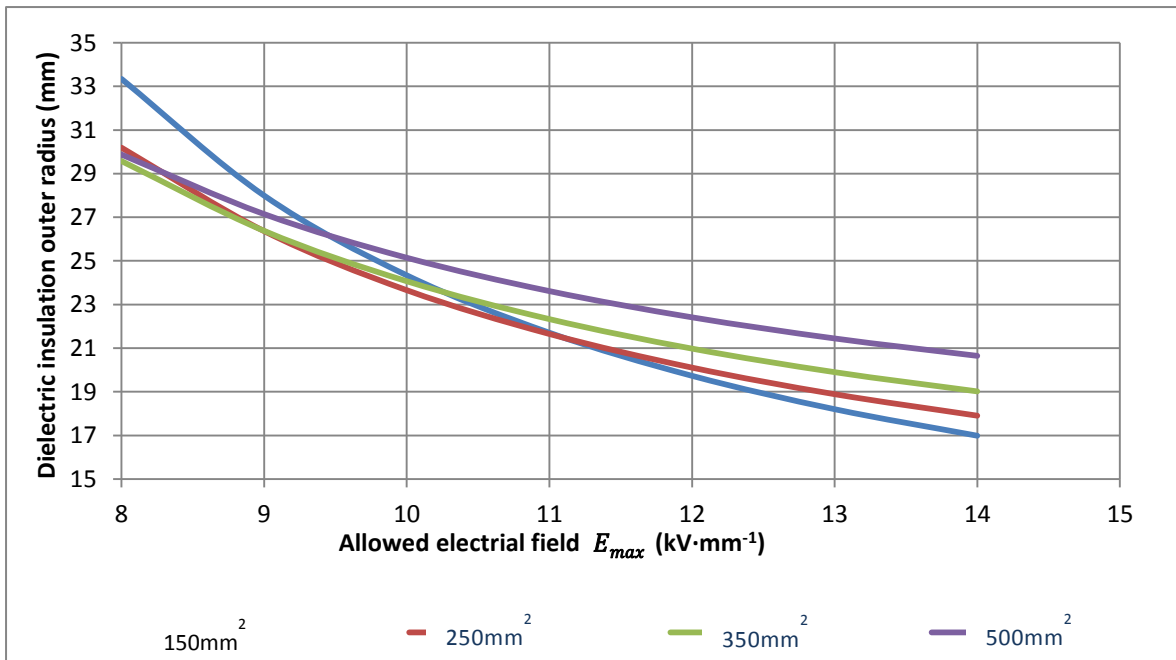


Figure 4-6 Insulation outer radius for different field strength and different core cross-sections

### 4.3.3.2 Dielectric losses

The total dielectric losses are given by equations (23) and (24).

$$C = \frac{2\pi\epsilon_0\epsilon_r}{18 \ln\left(\frac{R}{r}\right)} \quad (23)$$

$$q = \frac{U^2}{3} 2\pi f C \tan(\delta) \quad (24)$$

With

$C$	Capacitance per unit length	(nF·m <sup>-1</sup> )
$\epsilon_r$	Relative permittivity of the insulation	
$\epsilon_0$	Vacuum permittivity	(nF·m <sup>-1</sup> )
$r$	Inner radius	(mm)
$R$	Outer radius	(mm)
$q$	Dielectric loss	(W·m <sup>-1</sup> )
$U$	Line voltage	(kV)
$f$	System frequency	(s <sup>-1</sup> )
$\tan(\delta)$	Dissipation factor	

Using these equations the dielectric losses are calculated and plotted in Figure 4-7.

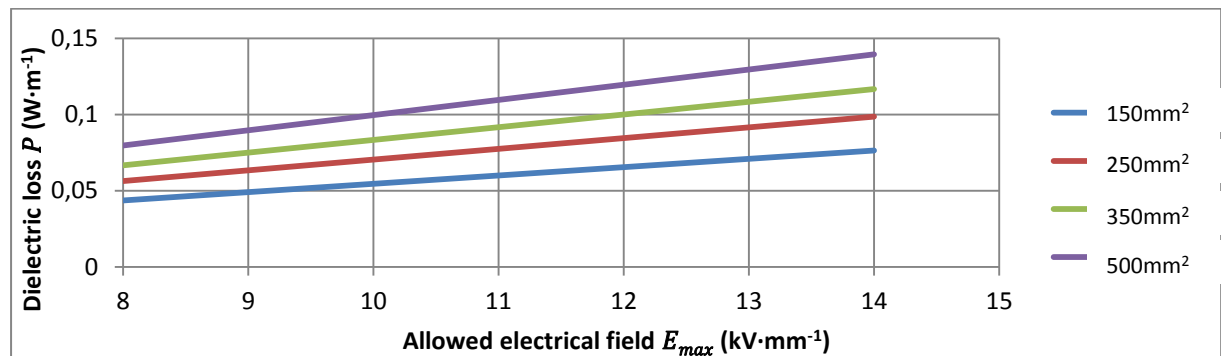


Figure 4-7 Dielectric loss for different electrical fields

For the dielectric losses it is beneficial to use a smaller inner cross-section. Lower electric field strengths allow for lower AC-losses but these fields need larger outer radii of the cylinders. An optimization between these two parameters should be made.

### 4.3.4 Joint losses

Since YBCO wires only can be manufactured in limited lengths the wires have to be jointed at certain intervals. The resistance of a typical wire joint is 20-100 nΩ with a typical critical current of 100 A [20] this amounts to a joint loss of 1 mW for every joint. For a critical current of 1000 A, 10 wires are needed. Single wire length is a minimum of 100 meters. Using this data the worst case joint loss is considered to be 10 mW every 100 meters. This is negligible in comparison to the other losses in the cable.

## 5 Model of a superconducting cable

To model the temperature distribution in the cable the equations and data from the previous chapters will be used. The cable design that is modelled is the hollow former design. The flow pattern for this cable is that of a counter flow cable. This means that every cable has its own closed loop with a forward and return flow. A parallel flow or a solid former cable should be considered in future research. Because of time constraints only the hollow former counter flow cable is modelled.

Design parameters are the desired radius of the former, maximum dielectric field strength, and the desired maximum pressure drop over the cable. From these parameters the mass flow speed is calculated. Using the obtained mass flow rate the heat profile in the cable is then calculated.

The input data for the material properties are described in Appendix A.

### 5.1 Counter flow design

The counter flow design cable has a flow loop for each separate cable. The nitrogen flow enters and returns from each phase. This design is used in triaxial superconducting cables [5]. It is not yet demonstrated as a cooling methodology for single phase cables. The benefits of these cables are the closed loop and equal flows for each phase, a drawback is the increased heat flux between hot and cold flow, especially in single ended cooling designs. Figure 5-1 shows a schematic representation of the cable with the forward and return flow represented as solid lines. The heat exchange through the dielectric is shown with a dashed line. Figure 5-2 shows the results of a modelled cable including the different layers that are included and calculated in the model.

#### 5.1.1 Calculation of flow

The flow speed in the cable is calculated using the equations mentioned in chapter 4.2. It is assumed that for the design of the cable the flow speed in the outer and inner flow are equal. For a constant mass flow rate the surface area of the inner and outer flow are also the same.

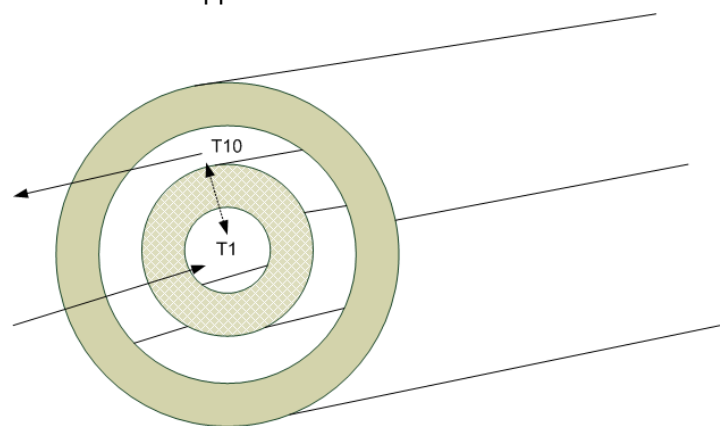


Figure 5-1 Schematic representation of a counter flow cable

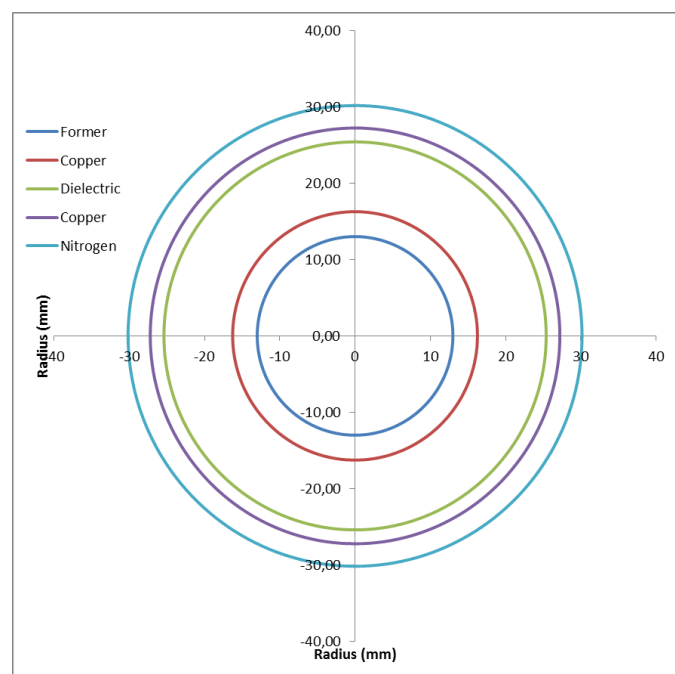


Figure 5-2 Modelled cable including the calculated layers

This approach is safe because of reduction of the surface area for the inner flow would only result in a minimal decrease of the outer radius (because of the larger dielectric radius) and would increase the pressure drop and losses in the inner flow.

Since the outer flow has a larger surface area relative to its area, the pressure drop in the outer flow will be the larger of the two pressure drops. The flow speed that is allowed is thus calculated based on the outer flow pressure drop. This is done by combining equations (12), (13), (17), and (18) and this gives equation (25).

$$\Delta P = \frac{\rho L v^2}{2D_h} \cdot \left( \frac{1}{-1.8 \log_{10} \left( \left( \frac{\epsilon}{3.7D_h} \right)^{1.11} + \frac{6.9\mu}{\rho v D_h} \right)} \right)^2$$

$$v = - \sqrt{\frac{2\Delta P D_h}{\rho L}} \cdot 1.8 \log_{10} \left( \left( \frac{\epsilon}{3.7D_h} \right)^{1.11} + \frac{6.9\mu}{\rho v D_h} \right) \quad (25)$$

With

$\Delta P$	Pressure drop	(Pa)
$\rho$	Density of the nitrogen	( $\text{kg}\cdot\text{m}^{-3}$ )
$L$	Cable length	(m)
$v$	Flow velocity	( $\text{m}\cdot\text{s}^{-1}$ )
$D_h$	Hydraulic diameter	(m)
$\epsilon$	Roughness of the tubing	(m)
$\mu$	Viscosity of the nitrogen	( $\text{kg}\cdot\text{s}^{-1}\cdot\text{m}^{-1}$ )

Equation (25) can't be solved arithmetically and is solved by using the Newton-Raphson method. The function used and its derivative are given by equations (26) and (27).

$$F(v) = v + \sqrt{\frac{2\Delta P D_h}{\rho L}} \cdot 1.8 \log_{10} \left( \left( \frac{\epsilon}{3.7D_h} \right)^{1.11} + \frac{6.9\mu}{\rho v D_h} \right) \quad (26)$$

$$F'(v) = 1 - \frac{1.8 \sqrt{\frac{2\Delta P D_h}{\rho L}} \cdot \frac{6.9\mu}{\rho D_h}}{\ln(10) \left( \left( \frac{\epsilon}{3.7D_h} \right)^{1.11} + \frac{6.9\mu}{\rho v D_h} \right) v^2} \quad (27)$$

From these formula's the flow speed and thus the mass flow rate of the system are determined. Now the pressure loss and the heat generated in both flows can be calculated. It should be mentioned that for single ended cooling the pressure drop over the entire cable (go and return flow) should be calculated.

## 5.1.2 Assumptions

To construct the model some assumptions are made. These assumptions are made because some factors are not known yet and still have to be taken into consideration in the model.

### 5.1.2.1 Heat transfer

For the counter flow design an important design parameter is the amount of heat flux between the inner and outer flow. Since the flow in both the inner and outer tube is turbulent a high convective

heat transfer is achieved between the walls of the tubes and the flows. Therefore the convective heat transfer is insignificant to the total heat transfer. The total heat transfer is determined by the conductive heat transfer coefficient of the copper and the dielectric.

#### **5.1.2.2 Norris correction**

The second assumption concerns the AC losses according to the Norris equation it is shown that by proper tape layout these losses can be reduced. A correction factor for the Norris equation between 0.5 and 1 should be used. Which correction factor is most applicable largely depends on cable manufacturing process. The final results should mention which correction factor is assumed.

#### **5.1.2.3 Magnetic coupling**

The magnetic coupling between conductor and shield is not ideal. This means that not all current flowing through the main conductor is induced in the shield conductor. Hands on experience by TenneT for regular conductors rates this correction factor at 0.9 times the conductor current as shield current [21]. For superconductors the magnetic coupling is assumed to be perfect.

#### **5.1.2.4 Dielectric losses**

In the model it is assumed that dielectric losses are equally distributed between inner and outer flow. This means both flows are heated by the same amount of dielectric losses ( $\frac{1}{2}q_{dielectric}$ ). It is not known what the real ratio of this distribution is. For the voltage of 150 kV the dielectric losses however are low compared with the other losses. For higher voltages, for example 380 kV, these losses become more relevant and it should be considered that the ratio of heat distribution is different.

#### **5.1.2.5 Uniform critical current**

It is assumed in this model that there is no correction in place for the expected critical current. This means that the amount of tapes is the same throughout the length of the cable. In a real cable such compensation could be made to diminish the effect of temperature rise on the AC-losses. This means that hotter parts of the cable design would include more or higher  $I_c$  tapes.

### **5.1.3 System of equations**

To determine the temperature distribution along the cable a set of equations has to be drawn up. This is done by dividing the cable into N segments and solve the system of equations for all those segments. The system of equations is solved using matrix calculations. A higher number of segments gives an increased accuracy of the calculations.

#### **5.1.3.1 Double ended cooling**

Dividing the cable into N sections gives N+1 temperatures for both the inner and outer flow. The total number of temperatures to be calculated is 2N+2. Since each section has its own heat balance this gives 2N equations. These equations are all balancing equations; the heat entering a segment is equal to the heat leaving a segment. Figure 5-3 shows an example of a cable divided into eight segments and having ten different temperatures.

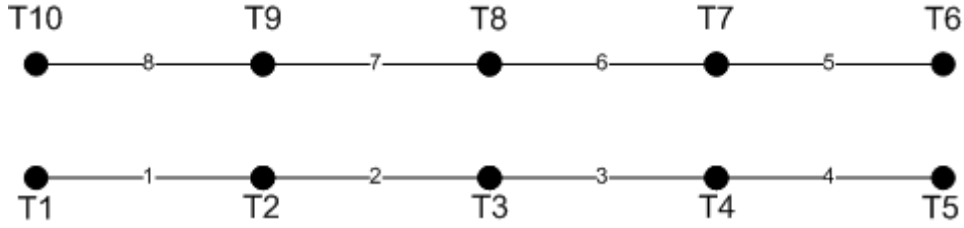


Figure 5-3 Example of 8 segment cable approximation

For the inner segments these equations are as follows:

$$\begin{aligned} \dot{m}C_p(T_{i+1} - T_i) = & q_{pressuredrop} + \frac{1}{2}q_{Dielectric} + \frac{q_{T_{ref}} - q_{T_{low}}}{T_{ref} - T_{low}} \cdot \left(\frac{T_i + T_{i+1}}{2} - T_{low}\right) + q_{T_{low}} \\ & + \frac{kA(T_{2N+3-i} + T_{2N+2-i} - T_i - T_{i+1})}{2} \end{aligned} \quad (28)$$

The equations for the outer sections are similar but have extra heat entering from the outside of the cryostat and a change of signs for the direction of heat transfer between the layers.

$$\begin{aligned} \dot{m}C_p(T_{i+1} - T_i) = & q_{pressuredrop} + q_{thermal} + \frac{1}{2}q_{Dielectric} + \frac{q_{T_{ref}} - q_{T_{low}}}{T_{ref} - T_{low}} \cdot \left(\frac{T_{i+1} + T_{i+2}}{2} - T_{low}\right) + q_{T_{low}} \\ & - \frac{kA(T_{2N+3-i} + T_{2N+2-i} - T_{i+1} - T_{i+2})}{2} \end{aligned} \quad (29)$$

In case of double sided cooling the temperature at  $T_1$  and  $T_{N+2}$  are both known and are the temperatures of the cryocoolers. This leaves a system of  $2N$  equations with  $2N$  unknowns. These equations are then put into matrix form and solved.

With

$\dot{m}C_p(T_{i+1} - T_i)$	Heat removed from the segment	(W)
$q_{pressuredrop}$	Heat entering due to friction losses	(W)
$\frac{1}{2}q_{Dielectric}$	Dielectric loss	(W)
$\frac{q_{T_{ref}} - q_{T_{low}}}{T_{ref} - T_{low}} \cdot \left(\frac{T_i + T_{i+1}}{2} - T_{low}\right) + q_{T_{low}}$	Linearized AC-loss	(W)
$\frac{kA(T_{2N+3-i} + T_{2N+2-i} - T_i - T_{i+1})}{2}$	Heat exchange with opposing nitrogen flow	(W)

### 5.1.3.2 Single ended cooling

The solution to the system of equations for single ended cooling is similar to the solution for double ended cooling. In case of single ended cooling however the entry temperature of the return flow is also an unknown variable. This requires an extra equation. The equation is given by the heat leak from the termination:

$$\dot{m}C_p(T_{N+2} - T_{N+1}) = q_{termination} \quad (30)$$

### 5.1.4 Sensitivity analysis

The different assumptions and material properties used in the model are evaluated in a sensitivity analysis. This analysis can be found in Appendix D. The main conclusions of the sensitivity analysis are an accuracy for the cooling power required of  $\pm 5$  kW and an accuracy of  $\pm 0.7$  K for the cable temperature.



## 6 Cable specifications

Now the heat profile of the cable can be modelled it can be determined what cable design allows for immediate fault recovery. An approximate cooling power required can also be determined. The cable specification is drafted for several cable design parameters. The cable design is then varied to determine a cable design that allows for the least amount of losses and is thus the most beneficial in operation. The cable design should be specified in a way that it allows for immediate fault recovery of the cable. This means that the temperature rise after a short circuit may not exceed the critical temperature of the superconductor for the required nominal current.

### 6.1 Short circuit conditions

The short circuit condition that the conductor should recover from is a 30 kA current with a duration of 0.6 seconds. First the heat generated in the cable is calculated and then the temperature increase in the cable is calculated. To determine the temperature increase it is first determined whether the temperature increase is adiabatic or not, using a thermal electric analogy.

#### 6.1.1 RC-analogy and time constant

Thermal circuits and electrical circuits are very similar. A thermal circuit may be transformed to an electrical circuit [22]. To do this the following equations are used:

$$C_t = mC_p \quad (31)$$

$$R_t = \frac{1}{Ah} \quad (32)$$

With

$C_t$	Thermal capacitance	(J·K <sup>-1</sup> )
$m$	Mass	(kg)
$C_p$	Specific heat capacity	(J·kg <sup>-1</sup> ·K <sup>-1</sup> )
$R_t$	Thermal resistance	(K·W <sup>-1</sup> )
$A$	Area of convective heat transfer	(m <sup>2</sup> )
$h$	Coefficient of convective heat transfer	(W·m <sup>-2</sup> ·K <sup>-1</sup> )

Using equation (31) and (32) the time constant of the RC network can be determined. The heat capacity used is the heat capacity of the nitrogen and the convective heat transfer is between the copper and the nitrogen. Using the time constant it can be determined how much time it takes for a temperature increase in the copper to distribute to the nitrogen. The time constant is given by equation (33).

$$\tau_{RC} = R_t \cdot C_t \quad (33)$$

With

$\tau_{RC}$	Time constant	(s)
-------------	---------------	-----

Since immediate fault recovery is demanded, the time constant of the system has to be in the order of magnitude of milliseconds to satisfy this demand for the heat exchange situation. When the time constant is larger the heating of the copper should be considered adiabatic, without heat exchange with the nitrogen.

### 6.1.2 Adiabatic heating

When it is determined that the process is adiabatic, the heat generated in the copper is calculated using equations (1) and (21). It is then calculated what the final temperature rise of the system will be using equation (1) and the losses at a risen temperature will be calculated to determine the cooling capacity needed.

## 6.2 Model results

The various results and cable designs can be found in Appendix C. Since some design parameters are unknown at this stage there is thus a range of cable specifications that are drafted. It is however shown that for the different specifications a cable design is possible that offers immediate fault recovery and continuous operation.

One of the design parameters that are varied is the heat intrusion from the cryostat. This is done because an exact value of the heat intrusion is not known yet. Furthermore the cable specifications are drafted for a correction for AC (Norris) losses between 0.5 and 0.9. A realistic correction factor for the AC losses is 0.9 and can be considered the minimum achievable. The best case scenario is 0.5 and is achieved in laboratory conditions but it is questionable if this can be achieved in production grade HTS tapes. Since the amount of tape that is used is a cost versus benefits issue the model is run with critical currents of 2000 A, 3000 A and 4000 A. The final parameter that is varied is the thermal conductivity which is varied between  $0.05 \text{ W}\cdot\text{m}^{-1}\cdot\text{K}^{-1}$  for dry PPLP and  $0.25 \text{ W}\cdot\text{m}^{-1}\cdot\text{K}^{-1}$  for wet PPLP. All these variations are modelled for copper cross sections of 200, 250 and 300  $\text{mm}^2$ . It is shown that all variations offer immediate fault recovery at a cross section of 300  $\text{mm}^2$ , whereas some variations already offer this survivability at 250  $\text{mm}^2$ . To estimate the electrical cooling power required a cooling penalty of 20 is used in the calculations.

### 6.2.1 Worst and best case scenario

From the different scenarios a worst case and a best case variation are chosen. A realistic scenario is also chosen. The realistic scenario is that of heat intrusion of  $4 \text{ W}\cdot\text{m}^{-2}$  and critical current of 3000 A with Norris correction of 0.9 and double sided cooling. These parameters are chosen based upon realistic performance described by system manufacturers. Dry PPLP is not a realistic alternative so the wet PPLP values should be considered. Dry PPLP however does perform better since it allows for a smaller thermal conductivity. The results are shown in Table 2.

**Table 2 Worst, best and realistic cooling capacity**

Scenario		Cooling power at nominal current $P$ (kW) $\pm 5$ kW	Cooling power at no current $P$ (kW) $\pm 5$ kW	Heat intrusion $q$ ( $\text{W}\cdot\text{m}^{-2}$ )	Norris Correction	Critical current $I$ (A)	Cooling stations
Dry PPLP	Worst Case	265	183	5	0.9	2000	Single side
	Realistic	158	124	4	0.9	3000	Double side
	Best Case	106	96	3	0.5	4000	Double side
Wet PPLP	Worst Case	329	244	5	0.9	2000	Single side
	Realistic	187	148	4	0.9	3000	Double side
	Best Case	126	112	3	0.5	4000	Double side

Figure 6-1 and Figure 6-2 show the cooling power required for different parameter variations of wet PPLP.

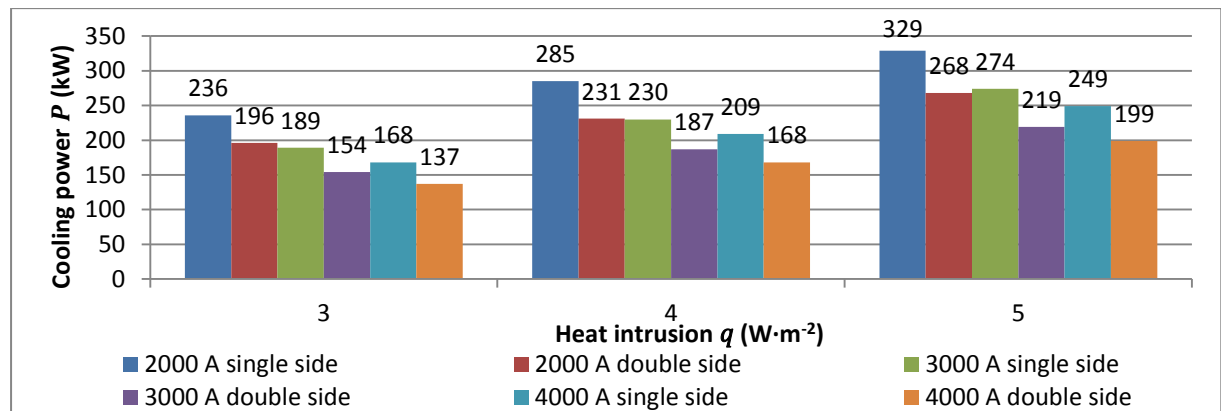


Figure 6-1 Cooling power for thermal conductivity 0.25 W·m<sup>-1</sup>·K<sup>-1</sup> and Norris Correction 0.9

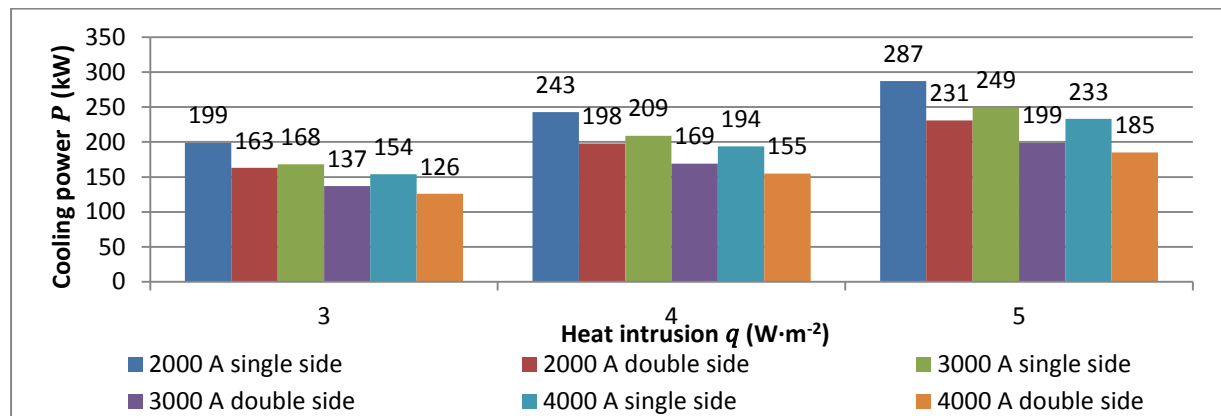


Figure 6-2 Cooling power for thermal conductivity 0.25 W·m<sup>-1</sup>·K<sup>-1</sup> and Norris Correction 0.5

### 6.2.2 Different cable lengths

The wet PPLP realistic variation is also modelled for 3 and 4 km cable lengths with double sided cooling. These results are shown in Table 3. The table shows that the required cooling power doesn't scale linearly with the cable length. This can be explained by the cable outer surface that increases as longer lengths are demanded. This allows for more heat from the outside to enter the cable. The increase in cable radius can be seen in Figure 6-3.

Table 3 Realistic cooling power for different cable lengths

System length (km)	Cooling power at nominal current $P$ (kW) $\pm 5$ kW	Cooling power at no current $P$ (kW) $\pm 5$ kW	Cooling power after fault $P$ (kW) $\pm 5$ kW	Pressure drop at nominal current ( $10^5$ Pa)	Pressure drop at zero current ( $10^5$ Pa)	Former Diameter (mm)	Dielectric Field strength ( $\text{kV}\cdot\text{mm}^{-1}$ )
2	187	148	204	5	4	36	10
3	316	257	331	7	6	43	8
4	462	374	487	8	7	49	8

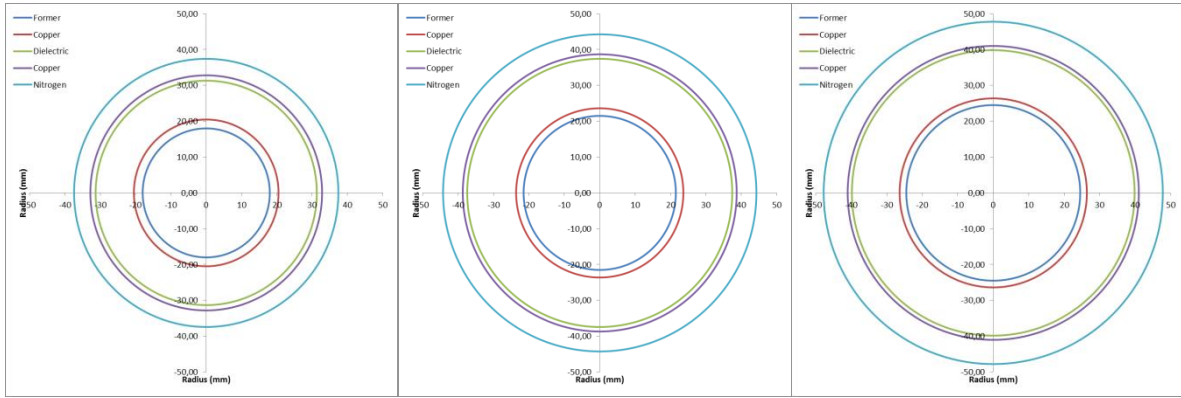


Figure 6-3 From left to right 2, 3 and 4 km cable cross sections

### 6.2.3 Comparison with conventional connections

The three wet PPLP scenarios are compared to a conventional XLPE cable connection and a conventional overhead line. Figure 6-4 shows this comparison. It can be seen that even the best case scenario only becomes beneficial in terms of total losses on connections that have a high load factor. The bump that can be seen in the HTS graphs is due to the increase in the flow speed and thus pressure drop and heat loss because of the increased temperature at that load. This is because there is no gradual increase in pressure drop in the model, only a discrete step. This bump is thus due to the model and not a property of the system.

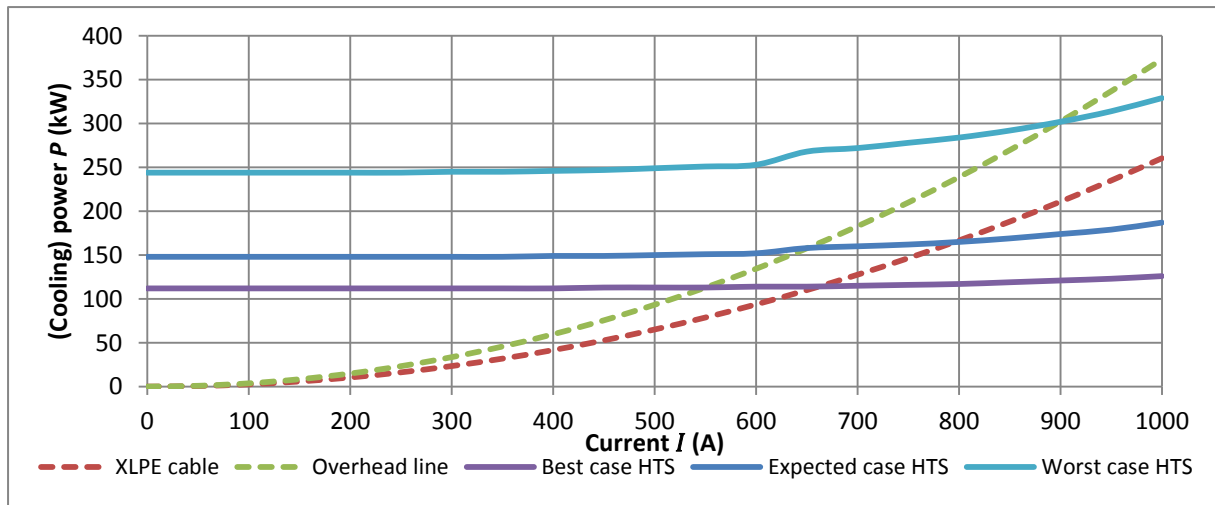


Figure 6-4 Comparison between conventional connections and different HTS scenarios

### 6.2.4 Redundant cooling

For security of supply the cooling system will probably be constructed redundant. One could envision that the redundancy be implemented not on one side of the cable, but on both sides. In this way a cable can be constructed that will operate as a double sided cooled system in normal operation, but will continue to operate as a single sided cooled cable when one of the cooling sites suffers from a fault. To achieve this the cable should be constructed to allow for single sided operation and the operating parameters should be varied depending on the operating mode. For the wet PPLP 2 km scenario these parameters are calculated and shown in Table 4.

**Table 4 Cable configurations and cooling power for redundant single/double sided cooling**

Scenario	Cooling power operation <i>P</i> (kW) ± 5 kW				Pressure drop at double sided operation (10 <sup>5</sup> Pa)	Pressure drop at single sided operation (10 <sup>5</sup> Pa)	Former Diameter (mm)	Dielectric Field strength (kV·mm <sup>-1</sup> )
	Nominal current designed for double sided	Nominal current double sided operation	Nominal current single sided	No current double sided operation				
Worst Case	268	289	329	234	2	4.73	55	8
Realistic Case	187	202	230	175	2	4.58	48	8
Best Case	126	137	154	129	2	4.64	43	8

When these results are compared to the double sided cooling optimal situation there is a penalty of  $11 \pm 5$  to  $21 \pm 5$  kW for respectively the best case and worst case scenario. This penalty however offers the opportunity for the continues operation if one of the two cooling stations fails.

## 7 Conclusion and discussion

### 7.1 Results

In this report the immediate fault recovery of a superconducting cable is explored. A model is constructed for a counter flown single phase cold dielectric superconducting cable. The model results show that various cable constructions offer immediate fault recovery. Immediate recovery is achievable for cables with a copper cross section from  $250 \text{ mm}^2$  and is viable for all designs with a cross section of  $300 \text{ mm}^2$ .

The model is constructed using finite element method in a 2D lumped parameter approach. The model uses 64 elements and is a steady state model. Fault conditions and temperature rise are studied using an RC-analogy.

Exact determination of the required cooling power is limited since material properties of the cryostat are not known yet, but also some system properties are not decided upon yet. One of these properties is the critical current of the system which is of great influence on the cooling power required. Another design parameter is whether single or double ended cooling is used for the system.

For a 2 km long superconducting cable system the expected electrical cooling power required at full load is between  $126 \pm 5 \text{ kW}$  and  $329 \pm 5 \text{ kW}$  for the best and worst case scenario. A superconducting cable will be beneficial in terms of losses only at connections that have a high load factor. Even the best case scenario only is beneficial in terms of losses at connections with a continuous load above 550 A.

A realistic value for a cable system with double sided cooling at the current state of technology is  $187 \pm 5 \text{ kW}$  of cooling power. For such a system the no load cooling power required would be  $148 \pm 5 \text{ kW}$  and after a fault has occurred the required cooling capacity is  $204 \pm 5 \text{ kW}$ . The construction of this cable would consist of a hollow former with a 36 mm diameter, a dielectric field strength of  $10 \text{ kV}\cdot\text{mm}^{-1}$  and would operate at a pressure drop of  $5\cdot 10^5 \text{ Pa}$ .

It is also shown that the required cooling power for longer length systems doesn't scale linear. Longer length cable systems operate at even higher required cooling power since the cable diameter for these systems increase and thereby the heat intrusion from the environment.

### 7.2 Recommendations

Since for this report only a counter flown cable is studied the most important recommendation is to perform a study to other cable designs.

The first design that should be studied is one that uses separate phases for the forward and return flows. Such a cable design would benefit from the absence of thermal influence between the phases. The increased heat gradient between cable core and nitrogen flow after short circuit situations in such a cable should be considered.

Another design that might be considered, especially at 110 kV is the 3 in 1 cryostat design since the total surface area of such a design is smaller than 3 separate cryostats and therefore the heat from the exterior is reduced. At voltages lower than 150 kV this becomes feasible because the phases can be constructed smaller because of the smaller dielectric needed.

Apart from the cold dielectric cables the warm dielectric cable might be useful for long length HTS systems and should be studied. Warm dielectric cables allow for a reduced cryostat surface area because of the smaller cryogenic envelope. The dielectric losses also don't have to be transported by the cryogenic system. A reduction in HTS tapes is possible because of the conventional instead of a superconducting screen. The downside of such a design would be the existence of an external magnetic field, but this impact might be reduced by using a trefoil cable configuration.

For the model that is used there are also some recommendations. For instance, the current model assumes no height difference between cable terminations. In real implementations this might be the case. The pressure drop due to this height differences should be taken into account. Another consideration that can be made is the usage of another conventional core; aluminium is already widely used in conventional cables and could also be used in a superconductor.

## 8 Bibliography

- [1] Hyperphysics, "Superconductivity concepts," Georgia State University, [Online]. Available: <http://hyperphysics.phy-astr.gsu.edu/hbase/solids/supcon.html#c1>. [Accessed Oktober 2015].
- [2] R. Soika, "High Temperature Superconductor Power Cables for High Voltage Applications," in *Supernet Symposium*, Delft, 2015.
- [3] T. Keugel, *Superconducting medium-voltage cables for urban power supply*, Essen: Westnetz GmbH / RWE Deuschlang AG, 2015.
- [4] Nexans, "Superconducting Cable Systems," April 2012. [Online]. Available: [http://www.nexans.de/eservice/Germany-en/fileLibrary/Download\\_540229834/Germany/files/Nexans\\_Superconducting\\_cable\\_systems\\_1.pdf](http://www.nexans.de/eservice/Germany-en/fileLibrary/Download_540229834/Germany/files/Nexans_Superconducting_cable_systems_1.pdf). [Accessed September 2015].
- [5] NKT, "HTS Triax Energy Cable Systems," November 2008. [Online]. Available: [http://www.nktcables.com/~media/Files/NktCables/download%20files/com/HTS-Triax\\_engl\\_061108.pdf](http://www.nktcables.com/~media/Files/NktCables/download%20files/com/HTS-Triax_engl_061108.pdf). [Accessed September 2015].
- [6] S. Norman, M. Nassi, P. Ladie, S. Poehler and R. Schroth, "Design and development of cold-dielectric (CD) high-temperature superconducting cable systems for bulk power transmission at voltages up to 225kV," Cigre, Parijs, 2000.
- [7] Fujiwara, Wang, Ueda, Ishiyama, Yagi, Saitoh and Aoki, "Thermal Characteristics of 275 kV/3 kA Class," *IEEE Transactions on applied superconductivity*, no. 20, pp. 1268-1271, 2010.
- [8] Maguire, Schmidt, Hamber and Welsh, "Development and Demonstration of a Long Length," *IEEE transactions on applied superconductivity*, no. Volume 15, pp. 1787-1792, 2005.
- [9] J. Maguire, F. Schmidt, S. Bratt and T. Welsh, "Lipa II Project," in *DOE Peer Review UPdate*, Arlington, 2008.
- [10] J. Oestergaard, J. Okholm, K. Lomholt and O. Toennesen, "Energy losses of superconducting power transmission cables in the grid," in *Applied Superconductivity Conference (ASC2000)*, Virginia Beach, 2000.
- [11] DH Industries BV, "Technical Specification SPC-4 Stirling Process Cryogenerator," Eindhoven, 2014.
- [12] Bergman, Lavine, Incropera and Dewitt, *Fundamentals of heat and mass transfer*, Jefferson City: Wiley, 2011.
- [13] F. M. White, *Heat Transfer*, Addison-Wesley Longman, 1984.
- [14] Haagse hogeschool, *Theorie diktaat fysische transport verschijnselen*, Delft.
- [15] R. S. Subramanian, "Heat transfer in Flow Through Conduits," 3 Juli 2014. [Online]. Available: <http://web2.clarkson.edu/projects/subramanian/ch330/notes/Heat%20Transfer%20in%20Flow%20Through%20Conduits.pdf>. [Accessed 17 September 2015].
- [16] S. Haaland, "Simple and Explicit Formulas for the Friction Factor in Turbulent Pipe Flow," *Journal of Fluids Engineering*, vol. 105, no. 1, pp. 89-90, 1981.
- [17] M. Ainslie, "Transport AC loss in high temperature superconducting coils," University of

Cambridge, Cambridge, 2012.

- [18] W. Norris, "Calculation of hysteresis losses in hard superconductors carrying ac: isolated conductors and edges of thin sheets," *Journal of applied physics*, vol. 3, no. 4, pp. 489-507, 1969.
- [19] Long, Badcock, Beck, Mulholland, Ross, Staines, Sun, Hamilton and Buckley, "Narrow strand YBco Roebel cable for lowered AC loss," in *8th European Conference on Applied Superconductivity*, Lower Hutt, New Zealand, 2008.
- [20] AMSC, "Guidelines for Hand-Assembled Splicing of Amperium Wire," 2012. [Online]. Available: [http://www.amsc.com/library/AMPSPLICING\\_AN\\_A4\\_0112.pdf](http://www.amsc.com/library/AMPSPLICING_AN_A4_0112.pdf). [Accessed 30 September 2015].
- [21] G. Aanhaanen, Interviewee, *Magnetische koppeling tussen fase en aardscherm*. [Interview]. Oktober 2015.
- [22] A. Robertson and D. Gross, "An Electrical Analog Method for Transient Heat-Flow Analysis," *Journal of Research of the National Bureau of Standards*, vol. 61, no. 2, pp. 105-115, 1958.
- [23] Hyperphysics, "Yttrium Barium Copper Oxide," [Online]. Available: <http://hyperphysics.phy-astr.gsu.edu/hbase/solids/scex.html#c4>. [Accessed September 30 2015].
- [24] Cigre, "Common characteristics and emerging test techniques for high temperature superconducting power equipment," Cigre, 2015.
- [25] J. A. Lleonart, "Study of the Resistive Switching phenomenon in YBCO superconducting samples," Universitat Autònoma de Barcelona, Barcelone, 2014.
- [26] I. Falorio, E. A. Young and Y. Yang, "Quench characteristic and minimum quench energy of 2g YBCO tapes," *IEEE Transactions on applied superconductivity*, vol. 25, no. 3, 2015.
- [27] Naito, Fujishiro, Yamamura, Saito, Okamoto, Hayashi, Goshō, Ohkuma and Shiohara, "Specific heat and thermal diffusivity of YBCO coated conductors," Elsevier, Morioka Japan, 2012.
- [28] M. Bonura and C. Senatore, "High field thermal transport properties of REBCO coated conductors," University of Geneva, Geneve, 2014.
- [29] Hyperphysics, "Resistivity and Temperature Coefficient at 20C," [Online]. Available: <http://hyperphysics.phy-astr.gsu.edu/hbase/tables/rstiv.html>. [Accessed 11 september 2015].
- [30] J. Polinski, "Materials in cryogenics," in *European Course in Cryogenics*, Geneva, 2010.
- [31] Hyperphysics, "Wiedemann-Franz Ratio," [Online]. Available: <http://hyperphysics.phy-astr.gsu.edu/hbase/hframe.html>. [Accessed 14 september 2015].
- [32] E. Marquardt, J. Le and R. Radebaugh, "Cryogenic material properties database," National Institute of Standards and Technology, Boulder, 2000.
- [33] Cryogenic Technologies Group, "Material Properties OFHC Copper," National Institute of Standards and Technology, 3 February 2010. [Online]. Available: [http://www.cryogenics.nist.gov/MPropsMAY/OFHC%20Copper/OFHC\\_Copper\\_rev1.htm](http://www.cryogenics.nist.gov/MPropsMAY/OFHC%20Copper/OFHC_Copper_rev1.htm). [Accessed 14 September 2015].
- [34] Air Liquide, "Gas Encyclopedia Nitrogen," 2013. [Online]. Available: <http://encyclopedia.airliquide.com/Encyclopedia.asp?GasID=5>. [Accessed 15 September 2015].
- [35] M. Kurrat, "HTS Insulation," in *Cigre workshop on high temperature superconductors D 1.38*,

Parijs, 2012.

- [36] Brookhaven National Laboratory, "Selected Cryogenic Data Notebook," Brookhaven National Laboratory, 1980.
- [37] U.S. Department of Commerce, National Bureau of Standards, "Saturated liquid densities of Oxygen, Nitrogen, ARgon, and Parahydrogen," US Government Printing Office, Boulder, Colorado, 1968.
- [38] E. F. Peschke and R. Von Olshausen, *Cable Systems for High and Extra-High Voltage*, Munchen: Publicis MCD Verlag, 1999.
- [39] Y. S. Choi, D. Kim, D. Shin and S. Hwang, "Thermal property of insulation material for HTS power cable," *AIP Conference Proceedings*, no. 1434, pp. 1305-1312, 2012.
- [40] M. Furuse and S. Fuchino, "Analysis and measurement of thermal conductivity of polypropylene laminated paper impregnated with subcooled liquid nitrogen," Elsevier, Japan, 2014.
- [41] Cryotherm GmbH, "Cryo Line Systems," Kirchen, 2015.
- [42] Nexans, "Cryoflex Transfer lines for liquid gases," Hannover, 2012.
- [43] Jang, Lee, Jang, Choi, Lee and Kim, "Superconducting cable with aluminium cryostat". United States Patent US20110207611 A1, 25 August 2011.
- [44] Copper Development Association Inc, "Cryogenic Properties of copper," [Online]. Available: <http://www.copper.org/resources/properties/cryogenic/>. [Accessed 14 september 2015].
- [45] Wikipedia, "Darcy friction factor formulae," 14 September 2015. [Online]. Available: [https://en.wikipedia.org/wiki/Darcy\\_friction\\_factor\\_formulae](https://en.wikipedia.org/wiki/Darcy_friction_factor_formulae). [Accessed 17 September 2015].
- [46] AMSC, "Effects of Temperature and Magnetic Field on Amperium Wire Performance," 2012. [Online]. Available: [http://www.ams.com/library/AMPIcBT\\_AN\\_A4\\_0112.pdf](http://www.ams.com/library/AMPIcBT_AN_A4_0112.pdf). [Accessed 30 September 2015].
- [47] HTS Triax, "Superconductivity," [Online]. Available: <http://www.htstriax.com/superconductivity.html>. [Accessed 30 September 2015].
- [48] Suzuki, Honjo, Takahashi, Masuda, Hirose and Isojima, "Verification tests of a 66KV high-tc superconducting cable system for practical use," Cigre, Parijs, 2002.
- [49] Demko, Lue, Gouge, Stovall, Butterworth, Sinha and Hughey, "Practical aC Loss and Thermal Considerations for HTS Power Transmission Cable Systems," in *2000 Applied superconductivity conference*, Virginia Beach, 2000.
- [50] Superpower, "2015 technology and manufacturing innovations at Superpower," 2015.
- [51] Wikipedia, "Superconductivity," 4 November 2015. [Online]. Available: <https://en.wikipedia.org/wiki/Superconductivity#>. [Accessed 5 November 2015].
- [52] ABB, "XLPE Land Cable Systems Users Guide revision 5," Sweden.
- [53] NKT, "State of the art superconducting cables".
- [54] A. Hak Electron, "150 kv Zoetermeer Bleiswijk," 2013. [Online]. Available: <http://www.a-hakelectron.nl/150-kv-zoetermeer-bleiswijk>. [Accessed November 2015].
- [55] [Art]. Tennet TSO B.V., 2014.
- [56] A. Geschiere, D. Willen, E. Piga, P. Barendregt and I. Melnik, "Optimizing cable layout for long length high temperature superconducting cable systems".

## Appendix A. Material properties

The different materials that are used all have their own set of properties. These properties are important to create a clear image of the thermal and electrical behaviour of the cable. This isn't trivial because of the low temperatures involved with super conduction. In this chapter the different properties of the materials are explained.

### A.1 YBCO conductor

The core part of the superconducting cable is of course the superconductor itself. The superconductor that will be used is a type 2, second generation superconducting wire. These wires are made with YBCO superconducting material. At the time of this report the manufacturer of the wire is not yet decided on and so generic data will be used.

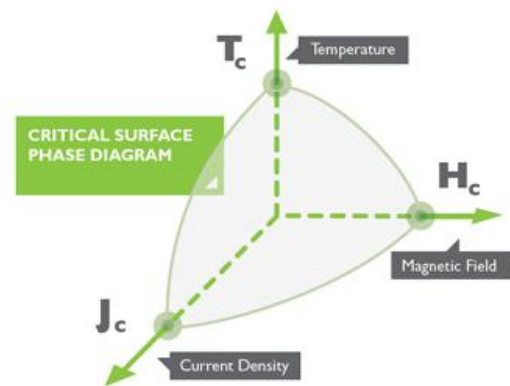


Figure A-1 Critical quantities [47]

#### A.1.1 Critical quantities

Superconducting wires have to meet certain criteria to be in a superconductive state. If any of these criteria isn't met the wire won't be superconducting. Figure A-1 illustrates these criteria. For superconducting power cables the most important quantities are the temperature and current density as explained below.

##### A.1.1.1 Temperature

The critical temperature of the wire is 87 K [23]. This is the highest allowable temperature for the conductor to be superconducting. There is however a strong relationship between the temperature of the superconductor and the maximum current density. This relationship is shown in Figure A-2. Equation (34) gives an approximate relationship between critical current and temperature [24]. For YBCO wires the material coefficient is 0.1.

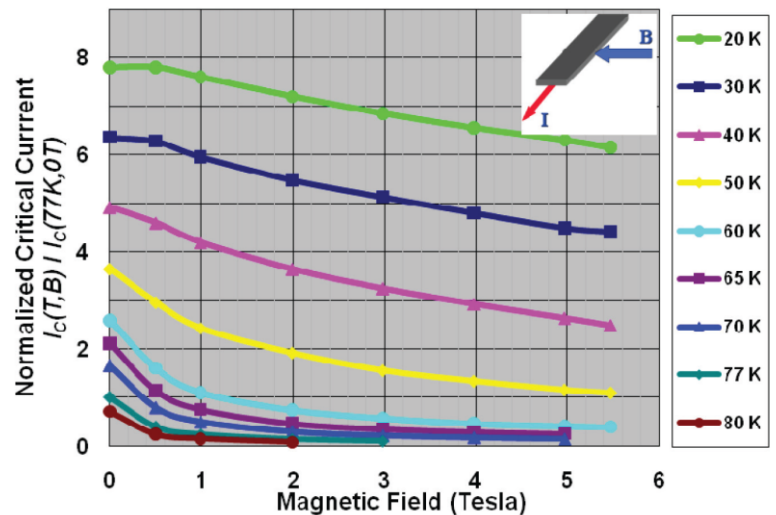


Figure A-2 Relationship between temperature, current density and magnetic field [46]

$$I_c = I_{c(T_{ref})} (1 + k(T_{ref} - T)) \quad (34)$$

With

$I_c$	Critical current	(A)
$T$	Temperature	(K)
$T_{ref}$	Reference temperature	(K)
$k$	Material coefficient	

This relationship implies a critical temperature of 87 K. When above this temperature, the conductor returns to normal state with a resistivity of  $20 \text{ m}\Omega \cdot \text{m}^{-1}$  [25].

### A.1.1.2 Current density

The current density property defines which currents a superconductor can conduct without dropping out of superconductivity. As stated before and can be seen in Figure A-2 the critical current is strongly dependent on operating temperature of the superconductor. The critical current density is also of importance in determining the AC-losses in the superconductor. This will be explained in chapter 4.3. Critical current density is defined as the current density at which the voltage drop over a centimetre of superconducting material exceeds  $1 \mu\text{V}\cdot\text{cm}^{-1}$ .

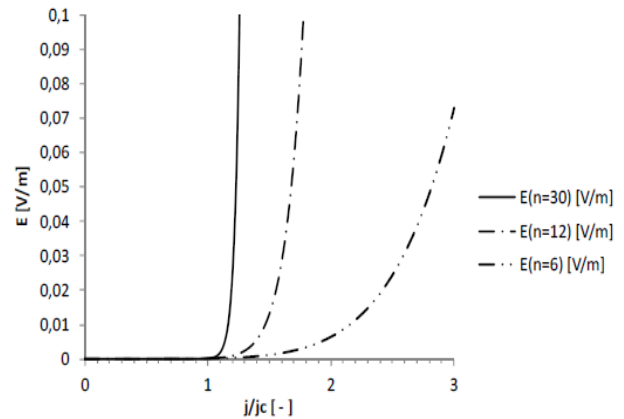


Figure A-3 Current density and voltage drop for different  $n$  superconductors [24]

The voltage drop over a cable depends on the ratio between critical current density and actual current density. This relationship is given by equation (35) [24]. In this equation  $n$  is a conductor property that ranges between 20 and 30 for YBCO conductors [24] [26] [19]. Figure A-3 shows the voltage drop over a cable segment for different  $n$ .

$$E = E_c \left( \frac{I}{I_c} \right)^n \quad (35)$$

With

$E$	Voltage drop	$(\mu\text{V}\cdot\text{cm}^{-1})$
$E_c$	Voltage drop at critical current density	$(\mu\text{V}\cdot\text{cm}^{-1})$
$I$	Current density	(A)
$I_c$	Critical current density	(A)

### A.1.1.3 Magnetic field

An externally applied magnetic field on superconducting wires is mainly of interest in applications where magnetic fields play a significant role, for example transformers, MRI or magnetic levitation. When superconducting wire is used for power cables the magnetic field is negligible. Since all phases are magnetically shielded from each other even the high magnetic fields that could occur in short circuit conditions are not of concern.

### A.1.2 Composition

The main parts of an YBCO wire are stabilizers, the substrate and off-course the YBCO tape itself. An overview of a YBCO tape can be seen in Figure A-4.

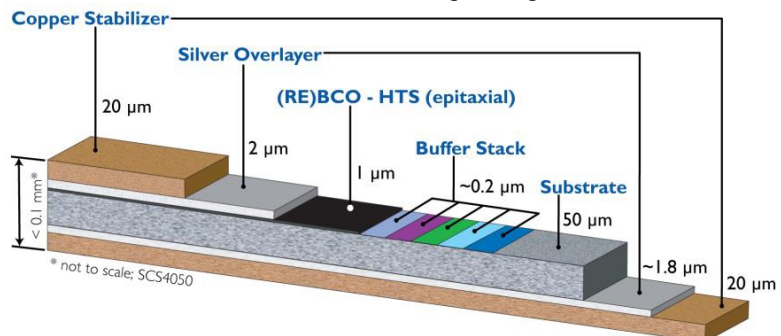


Figure A-4 Composition of a (RE)BCO/YBCO tape [50]

The copper stabilizer serves as a buffer in case of thermal rise or (local) exceeding of the critical current. The substrate is a requirement for the manufacturing process. The YBCO tape itself is only  $1 \mu\text{m}$  in thickness. The width of a typical YBCO wire is between 4 and 12 mm. Continuous length of wires is between 100 and 500 meter length, depending on the desired uniform critical current of the tape.

### A.1.3 Thermal properties

Since the total size of the superconductor is relatively small the thermal properties of the conductor are predominately dictated by the properties of the copper stabilizer and the substrate. Research confirms that the thermal properties of the conductor are dominated by the characteristics of the copper; the substrate is of marginal influence [27] [28].

## A.2 Copper

Depending on the final cable design there might be a copper core (former) and shielding in the cable. Even if this is not the case the YBCO conductor has a copper layer. The copper layer can be lumped in the entire YBCO conductor properties, but for improved accuracy a separate calculation using the copper properties might be used.

### A.2.1 Electrical resistivity

Electrical resistivity of any material is not only dependant on the material properties but also on the temperature it is used. This relation is given by equation (36) and (37)

$$R = \frac{\rho l}{A} \quad (36)$$

$$\rho = \rho_0 e^{\alpha T} \quad (37)$$

With

$R$	electrical resistance of the conductor	( $\Omega$ )
$\rho$	resistivity	( $\Omega \cdot m$ )
$l$	length of the conductor	(m)
$A$	cross section of the conductor	( $m^2$ )
$\rho_0$	resistivity at 0 K	( $\Omega$ )
$\alpha$	temperature coefficient of resistivity	( $K^{-1}$ )
$T$	absolute temperature	(K)

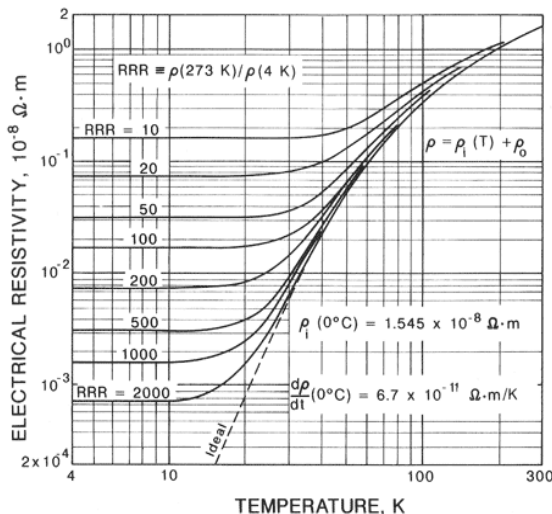


Figure A-5 Resistivity of different purity coppers [44]

Copper has a resistivity of 16.8 n $\Omega$ ·m at a temperature of 293K [29]. The temperature coefficient of copper is 0.0386 K<sup>-1</sup>. Using equation (37) the ideal 0 K resistivity can be calculated and after that the resistivity at different temperatures can be calculated. The ideal resistivity of copper at 0 K is 206 f $\Omega$ ·m. Figure A-5 shows the actual resistivity of different purity coppers. Copper used for power applications is usually of a residual resistance ratio (RRR) between 40 and 50 [30]. Resistivity of copper at superconducting temperatures is 2 n $\Omega$ ·m. At temperatures between 65 and 80 K the benefits of using higher grade copper are minimal.

### A.2.2 Thermal conductivity

Not only the electrical, but also thermal resistivity (or in this case conductivity) is of concern. This parameter determines whether heat is transferred to other layers of the conductor or if the copper

is mainly heating itself. Thermal and electrical conductivity are closely related by the Wiedemann-Franz law [31]. For commercially available copper this theoretical approach is found to be inaccurate [32]. Instead of the Wiedemann-Franz law, the relation in equation (38) between temperature and thermal conductivity is used [33]. This is a logarithmic fit of measured thermal conductivities. From this fit the thermal conductivity at a given temperature can be calculated. The fit is valid from 4 K up to 300 K.

$$\log_{10}(\kappa) = \frac{a + cT^{0.5} + eT + gT^{1.5} + iT^2}{1 + bT^{0.5} + dT + fT^{1.5} + hT^2} \quad (38)$$

With

$\kappa$	Thermal conductivity	(W·K <sup>-1</sup> ·m <sup>-1</sup> )
$T$	Temperature	(K)
$a - i$	Material coefficients	

The smallest available coefficients are those for RRR50 purity copper. These coefficients are given in Table 5.

**Table 5 Coefficients for conductivity, specific heat for RRR50 copper [33]**

Coefficient (units)	Thermal conductivity RRR50 (W·m <sup>-1</sup> ·K <sup>-1</sup> )	Specific heat (J·kg <sup>-1</sup> ·K <sup>-1</sup> )
a	1.8743	-1.91844
b	-0.41538	-0.15973
c	-0.6018	8.61013
d	0.13294	-18.996
e	0.26426	21.9661
f	-0.0219	-12.7328
g	-0.051276	3.54322
h	0.0014871	-0.3797
i	0.003723	0

Figure A-6 shows the thermal conductivity of RRR50 copper at the operating temperatures of the HTS conductor. It can be seen that the difference in thermal conductivity between the lower

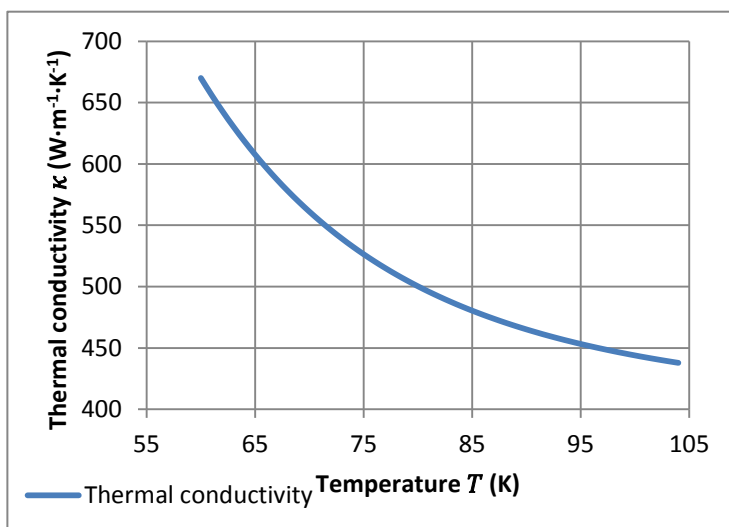


**Figure A-6 Thermal conductivity of RRR50 copper in HTS operating region**

operating limit and the upper operating limit is a factor 1.5. This means that when the copper core heats up, the ability to conduct thermal energy decreases. This is the opposite of the desired behaviour. For this reason the worst case scenario of 500 W·K<sup>-1</sup>·m<sup>-1</sup> is used.

The thermal conductivity of RRR50 and RRR100 are compared in Figure A-7 . It is shown that the more refined RRR100 shows little improvement in thermal conductivity at the

superconducting region between the black bars. The main benefit of more refined copper is at even lower temperatures, between 10 K and 40 K.

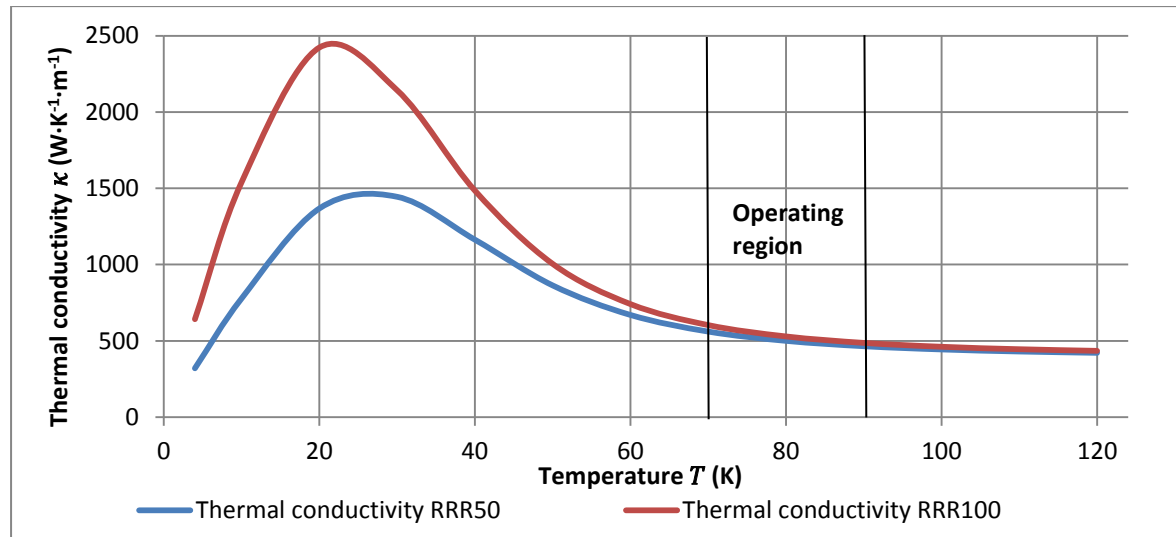


Figure A-7 Thermal conductivity of RRR50 and RRR100 compared

### A.2.3 Specific heat capacity

Not only thermal conductivity and electrical resistivity are temperature dependent, the specific heat capacity of copper is also temperature dependant. Specific heat capacity is independent of the RRR. The equation for determining the temperature dependent heat capacity is given in equation (39). The coefficients are already given in Table 5.

$$\log_{10}(C) = a + b \log_{10} T + c \log_{10}^2 T + d \log_{10}^3 T + e \log_{10}^4 T + f \log_{10}^5 T + g \log_{10}^6 T + h \log_{10}^7 T + i \log_{10}^8 T \quad (39)$$

With

$C$	Specific heat Capacity	$(\text{J} \cdot \text{K}^{-1} \cdot \text{kg}^{-1})$
$T$	Temperature	$(\text{K})$
$a - i$	Material coefficients	

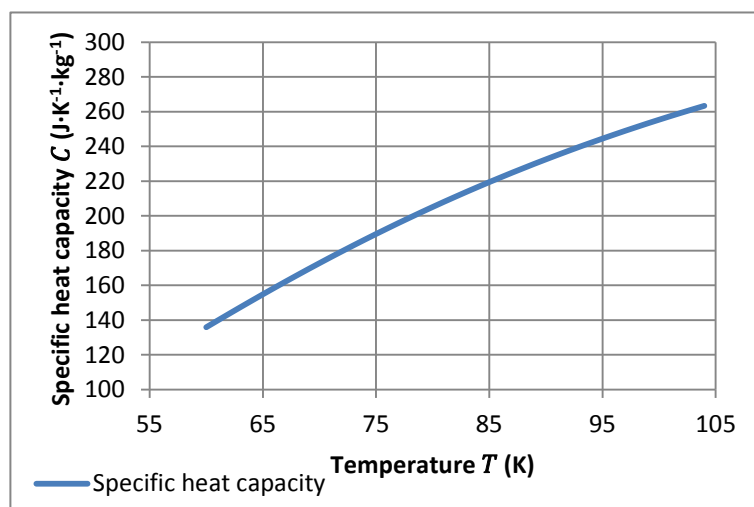


Figure A-8 Specific heat capacity of copper

Figure A-8 shows the specific heat capacity of copper at different temperatures. The heat capacity of the copper is of importance because in fault current situations the copper will function as a cold buffer. Although the heat capacity is still a factor 2 lower then at room temperature the rise of heat capacity at higher temperatures is beneficial for the usefulness as a thermal buffer.

## A.3 Nitrogen

For the cooling of the superconductor liquid nitrogen is used. Because the conductor is surrounded by the liquid nitrogen, not only the thermal, but also the electrical properties of liquid nitrogen are important.

### A.3.1 Solidification and boiling point

The boundaries of the operating temperatures of the superconductor are given by the maximum operating temperature of the superconducting material and the solidification point of nitrogen. The solidification point of nitrogen is  $-210^{\circ}\text{C}$  or  $63.15\text{ K}$  [34], this is the lower operating limit of the system because any solidification will prevent the nitrogen from flowing. The boiling point of the liquid nitrogen depends on the pressure of the nitrogen. The boiling point of nitrogen at different temperatures is shown in Figure A-9. At 1 bar the boiling point of nitrogen is  $78\text{ K}$ . The operating pressure of the system is yet to be determined, but it can already be seen that 1 bar is not practical because at this pressure the boiling point of the nitrogen is the upper limit, instead of the operating region of the superconductor material. To prevent nitrogen boiling at operating temperatures of the superconductor a minimum nitrogen pressure of  $4.3\text{ bar}$  is needed. The critical point of nitrogen is at a pressure of  $34\text{ bar}$  and a temperature of  $126\text{ K}$ . Above this temperature no pressure increase can prevent the nitrogen to boil. This is the maximum operating limit achievable for temperature, although it is not a practical operating point because of the high pressures involved.

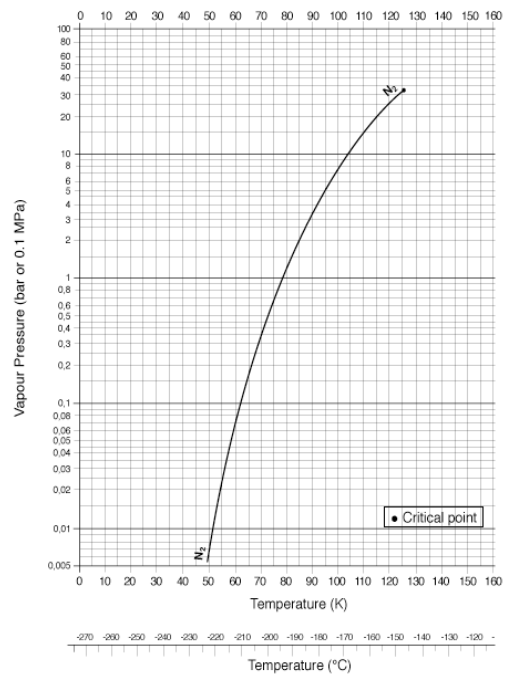


Figure A-9 Boiling point of nitrogen [34]

#### A.3.1.1 Discharge field strength

The reason why boiling of the nitrogen is a problem is because it influences the electrical field within the conductor (electrical)insulation. Gas bubbles influence this field negatively and can introduce partial discharges in the insulation layers. This should be prevented because these partial discharges are destructive. Partial discharges have the potential to destroy the cable. The discharge field strength of liquid nitrogen is  $35\text{ kV}\cdot\text{mm}^{-1}$  without gas bubbles and  $15\text{ kV}\cdot\text{mm}^{-1}$  with bubbles [35]. A field strength between  $8$  and  $12\text{ kV}\cdot\text{mm}^{-1}$  is advised [24].

### A.3.2 Thermal conductivity

Liquid nitrogen is a thermal insulator, its thermal conductivity is around 3000 times less than that of copper. For temperatures between  $68\text{ K}$  and  $88\text{ K}$  the thermal conductivity is between  $1.53$  and  $1.25\text{ mW}\cdot\text{cm}^{-1}\cdot\text{K}^{-1}$  [36]. As can be seen in Figure A-10 the relationship

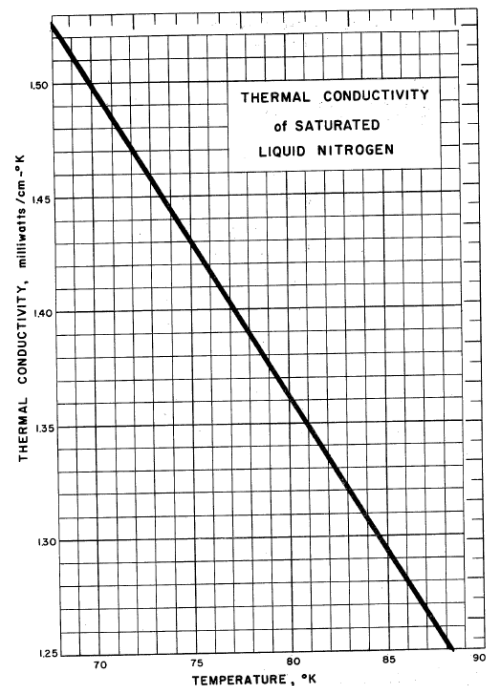


Figure A-10 Thermal conductivity of liquid nitrogen [36]

between temperature and thermal conductivity is linear. It should be noted that this is the thermal conductivity at the boiling point, it is assumed that the thermal conductivity is temperature dependent and not pressure dependent.

### A.3.3 Specific heat capacity

Figure A-11 shows the specific heat capacity of saturated liquid nitrogen. As with the thermal conductivity it is assumed that the heat capacity is temperature dependent and pressure independent. The specific heat capacity lies between  $2.01 \text{ J}\cdot\text{g}^{-1}\cdot\text{K}^{-1}$  at 65 K and  $2.14 \text{ J}\cdot\text{g}^{-1}\cdot\text{K}^{-1}$  at 92 K. Since there only exist small temperature variations in specific heat capacity an average specific heat capacity can be used for heat capacity calculations.

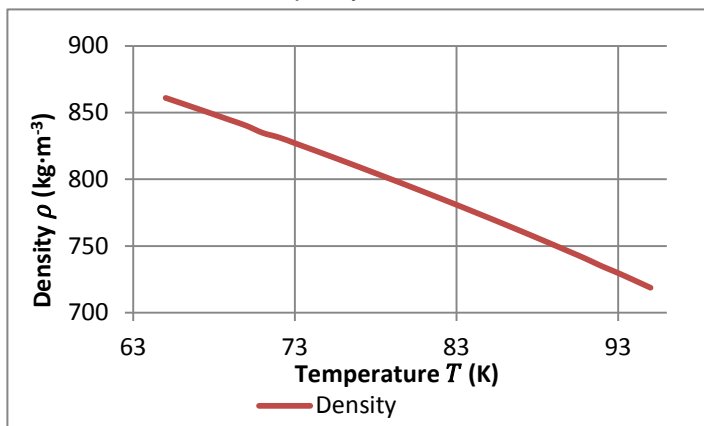


Figure A-12 Density of liquid nitrogen [37]

### A.3.4 Density

The density of nitrogen varies from  $861 \text{ kg}\cdot\text{m}^{-3}$  at 65 K to  $719 \text{ kg}\cdot\text{m}^{-3}$  at 95 K [37] at this interval the relationship between temperature and pressure is practically linear as can be seen in Figure A-12. Again it is assumed that the nitrogen is an incompressible fluid and pressure is not of influence on the nitrogen density. For the model  $840 \text{ kg}\cdot\text{m}^{-3}$  at 70 K is used.

### A.3.5 Viscosity

Viscosity of liquid nitrogen is also temperature dependent. Viscosity varies between 0.28 mPa·s at 67 K to 0.10 mPa·s at 95 K [36]. As can be seen in Figure A-13 the temperature/viscosity relationship is not a linear one over the entire operating range. Depending on the temperature range of operation a linear approximation could be made. For this report however the value of 0.2 mPa·s at 72 K is used.

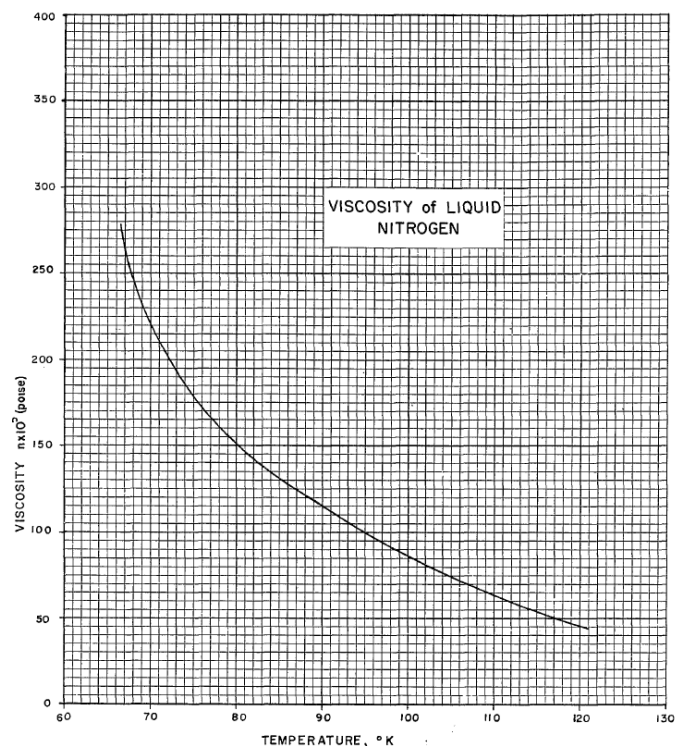


Figure A-13 Viscosity of liquid nitrogen [36]

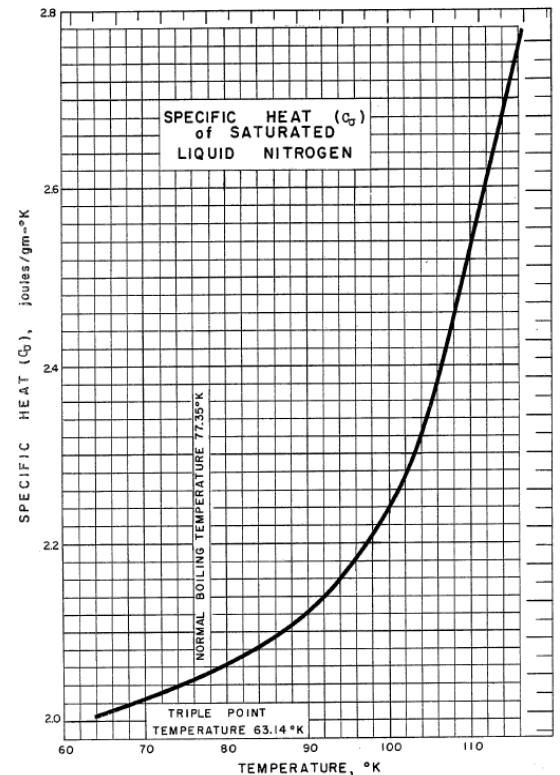


Figure A-11 Specific heat capacity of liquid nitrogen [36]

### A.3.6 Prandtl number

Using the data of liquid nitrogen the Prandtl number of nitrogen at different temperatures can be calculated. The Prandtl number is of importance in the calculation of the Nusselt number for the determination of the ratio between convective and conductive heat transfer.

$$Pr = \frac{c_p \mu}{k} \quad (40)$$

With

$Pr$	Prandtl number	
$c_p$	Specific heat capacity	(J·K <sup>-1</sup> ·kg <sup>-1</sup> )
$\mu$	Viscosity	(kg·s <sup>-1</sup> ·m <sup>-1</sup> )
$k$	Thermal conductivity	(W·m <sup>-1</sup> ·K <sup>-1</sup> )

Using equation (40) and the data available from this chapter the Prandtl number of nitrogen at different temperatures can be calculated. The Prandtl number for different temperatures is plotted in Figure A-14.

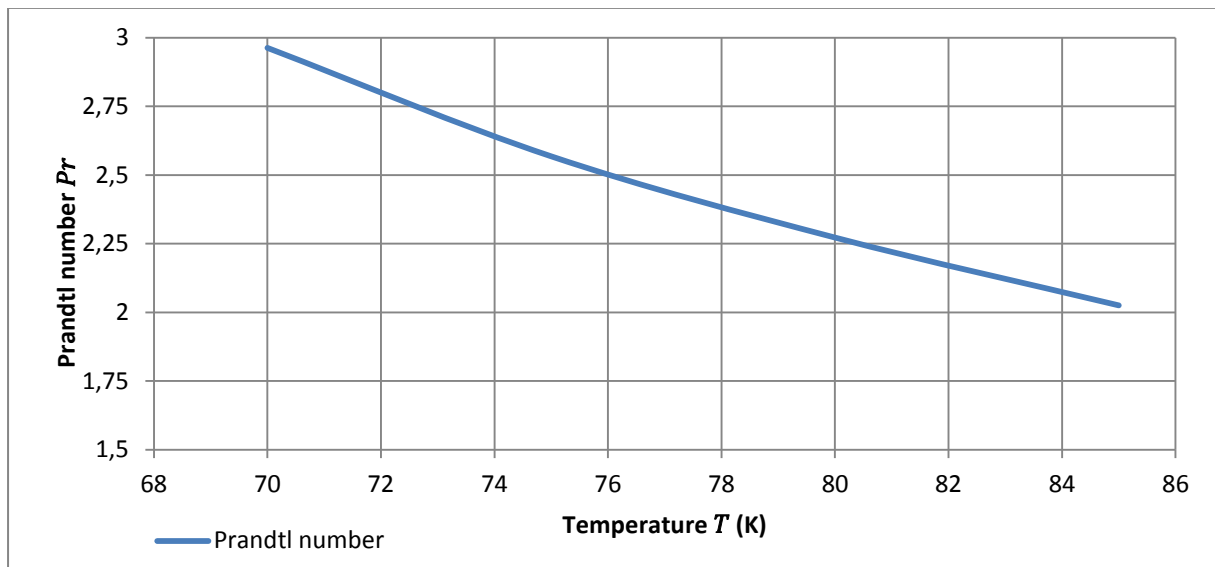


Figure A-14 Prandtl number of liquid nitrogen at different temperatures

## A.4 PPLP

Polypropylene laminated paper (PPLP) is used as a dielectric in high temperature superconductors. The PPLP is immersed in liquid nitrogen, this offers both cooling and dielectric insulation.

### A.4.1 Di-electric constant

The dielectric constant of a material determines the distribution of the electric field. For PPLP this constant  $\epsilon_r$  is 2.6 [38]

### A.4.2 Loss factor ( $\tan \delta$ )

To determine the dielectric loss the loss factor is used. This determines the ratio of heat generated inside the dielectric. The loss factor of PPLP ( $\tan \delta$ ) lies between 0.5 and 0.6 [38]. Since 0.6 is the worst case scenario this will be used in this paper.

#### **A.4.3 Thermal conductivity**

Thermal conductivity of PPLP should be examined in comparison to the thermal conductivity of liquid nitrogen. Dry PPLP has a thermal conductivity of  $0.05 \text{ W}\cdot\text{m}^{-1}\cdot\text{K}^{-1}$  [39]. When the PPLP is immersed in liquid nitrogen its thermal conductivity changes this is due to the thermal conductivity of the nitrogen. The wet PPLP has a thermal conductivity  $0.25 \text{ W}\cdot\text{m}^{-1}\cdot\text{K}^{-1}$  [40] which is higher than that of either PPLP or nitrogen.

### **A.5 Multi-Layer Insulation**

The cryogenic insulation is of the Multi-Layer Insulation (MLI) type. This type of insulation uses closely spaced reflective insulation layers to prevent radiation heat loss. Cryogenic piping comes in two forms, flexible piping and rigid piping. Flexible piping has easier transportation and placement as its main benefits. Rigid piping has better thermal insulation. Both piping systems use MLI insulation as the insulating material.

#### **A.5.1 Thermal losses**

The heat intrusion in thermal insulating piping is measured in  $\text{W}\cdot\text{m}^{-2}$ . Rigid piping is approximately a factor 2 better insulator than flexible piping [41]. The heat intrusion for flexible piping is between  $3.5$  and  $4.5 \text{ W}\cdot\text{m}^{-2}$  depending on piping diameter [42]. Smaller pipes have worse insulation, the larger radius pipes thus allow for smaller heat intrusion.

#### **A.5.2 Vacuum**

The MLI insulation depends on the existence of a proper vacuum between the MLI layers. Vacuum preservation over longer periods of time is still an issue. Nexans guarantees a vacuum in its cryostat for a period of 2 years. Compared to the desired life span of cable systems of 30 years this is an issue that has to be addressed in the construction of a superconducting cable system.

#### **A.5.3 Piping roughness**

The roughness of the piping determines both the pressure drop and the heat generated by the flow itself. The roughness of the piping is between  $0.015 \text{ mm}$  and  $0.030 \text{ mm}$  [43]. The roughness of  $0.030 \text{ mm}$  is used in this paper.

#### **A.5.4 Allowable pressure**

The allowed pressure of the liquid in the piping depends on the manufacturer of the cryostat. For example Nexans specifies an allowable pressure of  $20 \text{ bar}$  [42] whereas Cryotherm specifies  $10 \text{ bar}$  [41]. The working pressure of the cable at any given point should be below this pressure.

## Appendix B. Solving the system of equations using excel

The system of equations is solved using Microsoft Excel, the main motivation of this choice is the availability of Matlab at TenneT. Because Excel is widely available this program is chosen to calculate the model.

### B.1 User interface

Solving the system of equations is done in Microsoft Excel. A user is able to define a set of input parameters after which the worksheet calculates the size and specifications of the resulting superconducting cable system. The results are offered as a function of a 4,8,16,32 or 64 element method. Figure B-1 shows the input section of the worksheet. The orange fields are user input fields, the white fields are material properties or calculated fields and are therefore no alterable input parameters. The results are given in the green fields and are also graphically presented.

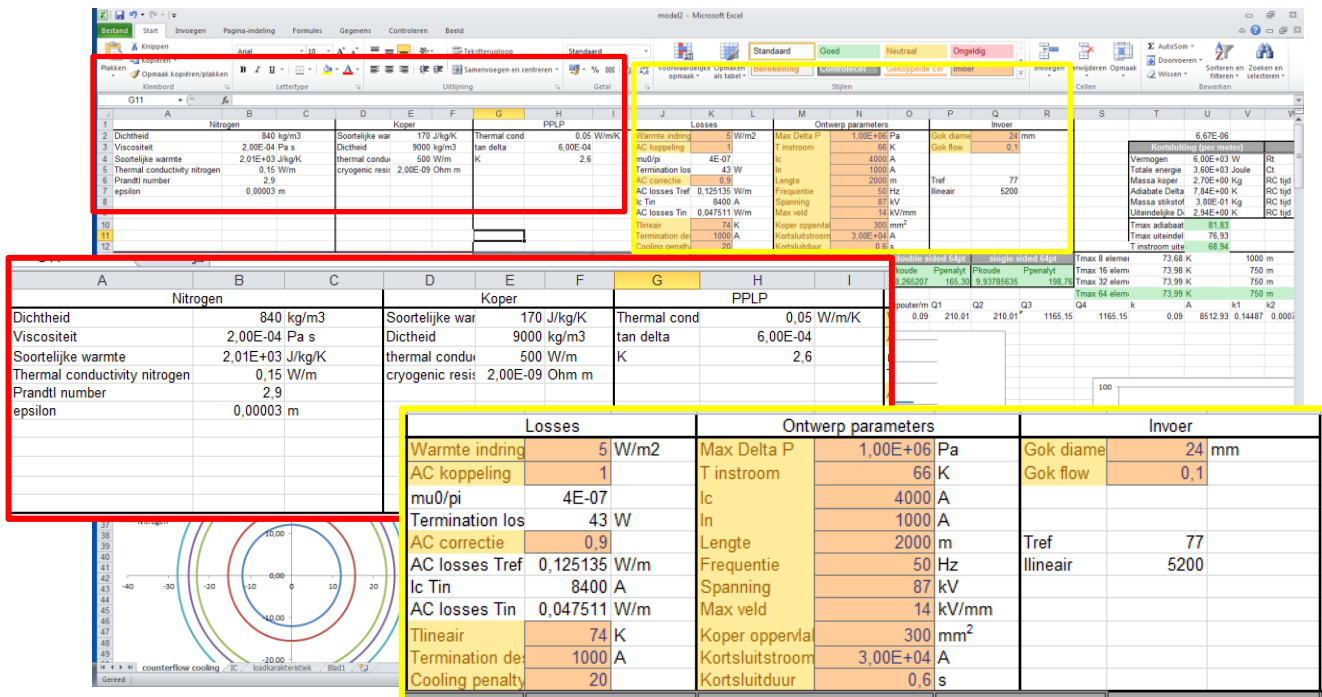


Figure B-1 Overview of input fields of excel worksheet

The results of the calculations are given numerically for the maximum temperature and its location, the cooling capacity required and the temperatures in short circuit conditions. These properties are calculated for both single ended and double ended cooling.

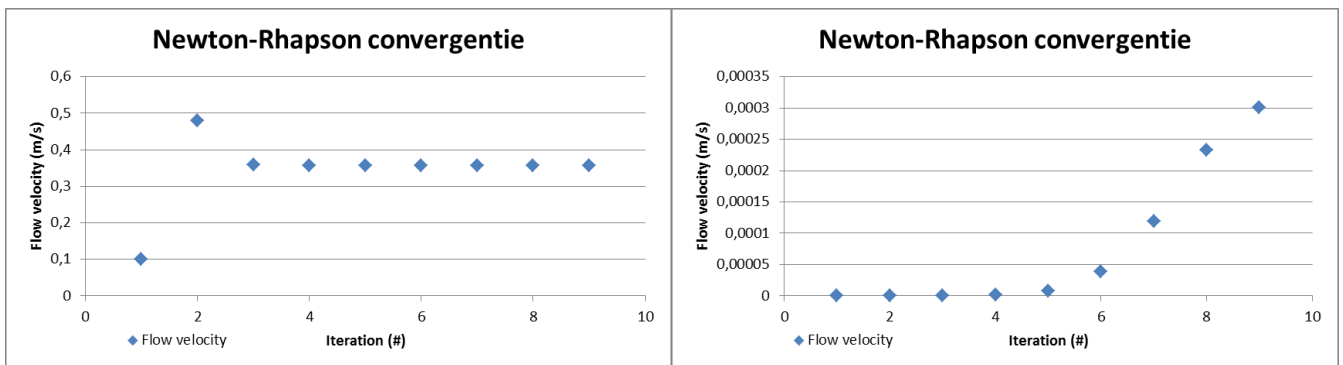


Figure B-2 Example of Newton-Raphson convergence  
left: correctly converging right: non-converging

Some properties are also displayed graphically. The first item that is shown graphically is whether or not the flow that is guessed (input parameter) results in converging of the Newton-Raphson solution. Figure B-2 shows both a correctly converging and a non-converging graphical representation of the Newton-Raphson solution. When a non-converging solution is found another initial guess should be made.

Besides the Newton-Raphson graphical representation a representation of the cable layout is also generated. Figure B-3 shows a cable cross-section, it should be noted that the generated cable cross-section does not take the cryostat into account. The cross-section only shows the interior of the cryostat.

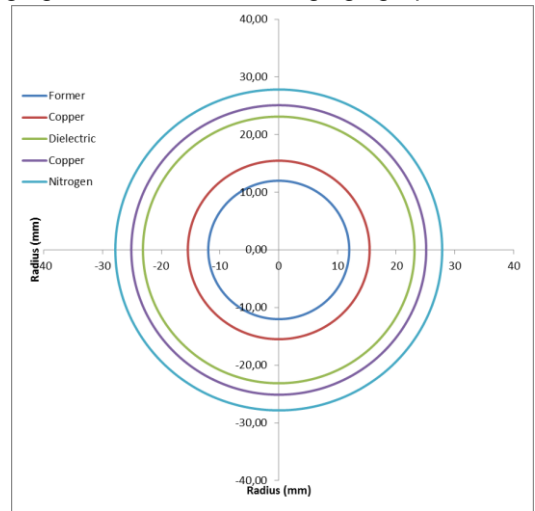


Figure B-3 Cable cross-section generated by Excel

Figure B-4 shows the generated output for a double sided cooling setup with 64 elements. Figure B-5 gives the temperature profile for the same input parameters but uses single ended cooling instead of double ended cooling.

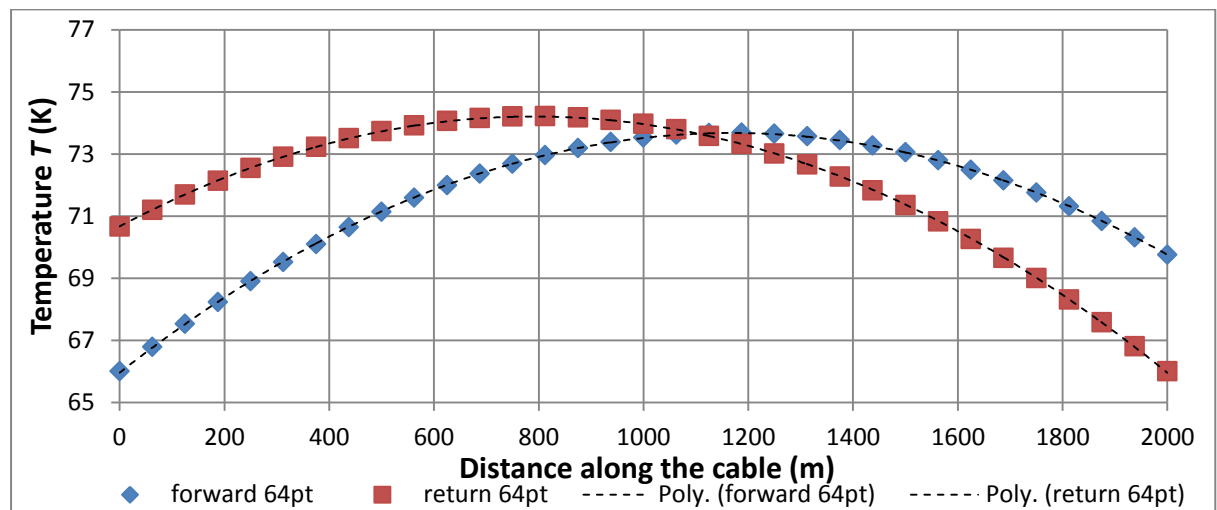


Figure B-4 Heat profile for a cable with double sided cooling

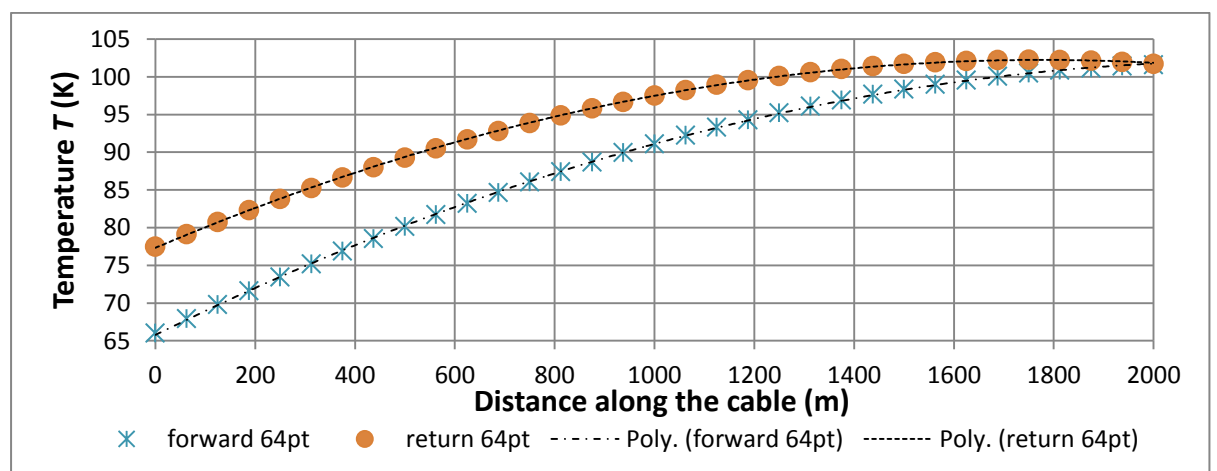


Figure B-5 Heat profile for a cable with single sided cooling

## B.2 Calculations and functions

The calculations in the excel worksheet are based upon the equations given in chapters 4 and 5. For a given set input parameters the excel worksheet first calculates the radii of the different segments of the cross section. The input that is used for these calculations is the allowed electrical field strength and the hollow former radius.

Now the different radii are known the excel worksheet calculates the thermal conductivity between the layers of the system according to equation (4). Using 9 iterations with the Newton Raphson method the flow velocity that allows for the maximum allowable pressure drop is calculated according to equations (26) and (27).

From this flow velocity now the mass flow rate, Reynolds number and Nusselt number are calculated using equations (7), (8) and (13). The convective heat transfer to the flow is also calculated. This is done separately for the inner flow and the outer flow because of the different ratio between surface area and flow area.

The AC losses are calculated depending on the linearization range that is given by the user. These values are then put into equation (28) and (29) and these equations are put into matrix form. This results in a 64 x 64 input matrix and a 64 x 1 matrix.

The matrices are solved using the Excel function "Productmat" and "Inversemat". The "Inversemat function is used on the input matrix. When this matrix is multiplied with the result matrix using "Productmat" the resulting 64 x 1 matrix gives the temperatures along the cable. These matrices are shown in Figure B-6. From these results the total heat load is calculated using the temperature difference between input and output and the mass flow rate.

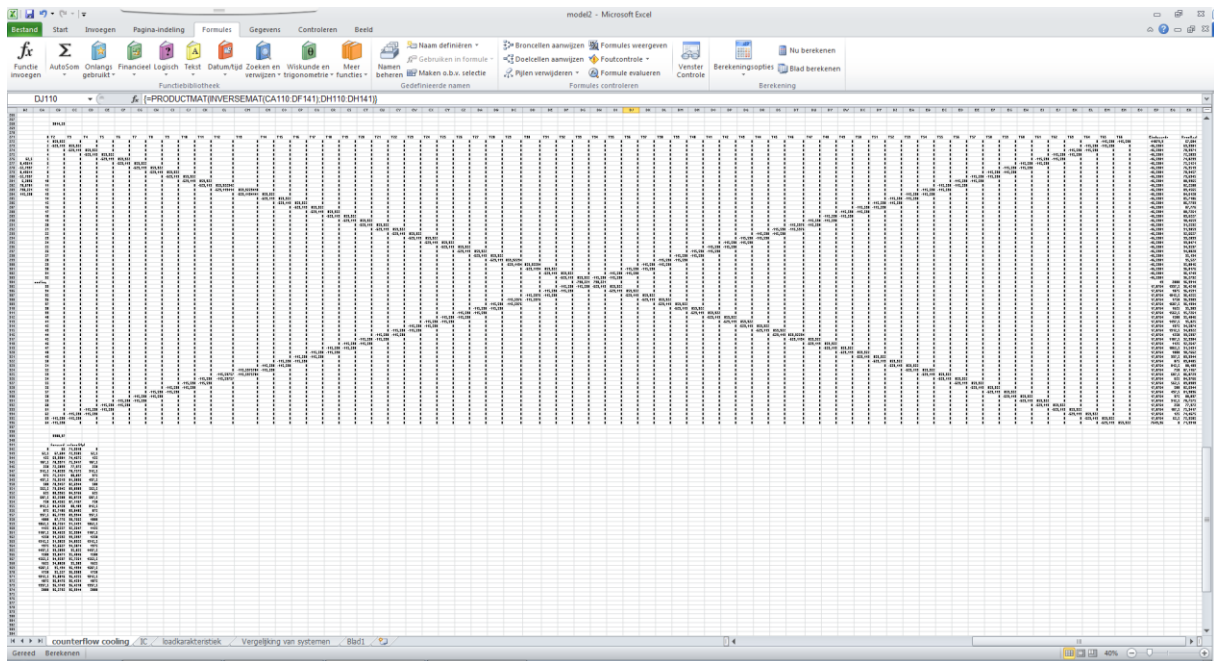


Figure B-6 Excel calculation matrix for double sided cooling

## Appendix C. Model results

In this appendix the model results are tabulated. All results are achieved by optimizing the input parameters to minimal losses at the given conditions of copper cross section, critical current and heat intrusion. Cooling capacity at zero current is calculated by using the model parameters and lowering system pressure drop to a value so that the maximum temperature at zero current does not exceed the maximum temperature at nominal current. For double sided cooled systems the pressure drop over the outer flow is tabulated since this is the highest system pressure drop. For single sided cooled systems the total system pressure drop is tabulated. The tables are colour coded, red values do not offer fault recovery, orange values offer delayed fault recovery, green values offer immediate fault recovery.

### C.1 Dry PPLP

#### C.1.1 Norris correction 0.9

Table 6 System parameters for copper cross sections 150 mm<sup>2</sup> and 200 mm<sup>2</sup> with double sided cooling

Copper Core (mm <sup>2</sup> )	Critical current (A)	Heat intrusion (W·m <sup>-2</sup> )	Cooling capacity at nominal current (kW) ± 5 kW	Cooling capacity at zero current (kW) ± 5 kW	Maximum temperature (K) ± 0.7 K	$\tau$ outer flow (s) ± 1 s	$\tau$ inner flow (s) ± 3 s	Adiabatic Temperature after fault (K) ± 0.7 K	Adiabatic $I_c$ (A)	Maximum temperature after 3 $\tau$ (K) ± 0.7 K	Cooling capacity after fault (kW) ± 5 kW	Pressure drop at nominal current (10 <sup>5</sup> Pa)	Pressure drop at zero current (10 <sup>5</sup> Pa)	Former Diameter (mm)	Dielectric Field strength (kV·mm <sup>-1</sup> )
150	2000	3	165	106	68.8	6	13	100	N/A	73.5	208	5	3	34	11
		4	189	119	70.6	4	10	102	N/A	N/A	N/A	7	4	29	13
		5	215	143	70.8	4	10	102	N/A	N/A	N/A	8	5	29	13
	3000	3	124	87	72.4	4	11	104	N/A	N/A	N/A	6	4	25	13
		4	147	115	71.5	4	11	103	N/A	N/A	N/A	6	5	27	14
		5	171	135	72.6	4	10	104	N/A	N/A	N/A	6	5	27	15
	4000	3	107	87	72.2	3	9	104	N/A	N/A	N/A	8	7	23	13
		4	128	107	72.9	3	8	104	N/A	N/A	N/A	9	8	23	14
		5	151	123	74.6	3	8	106	N/A	N/A	N/A	11	9	22	15
200	2000	3	169	111	68.6	5	13	86	140 ± 140	71.8	191	5	3	35	10
		4	192	122	70.8	4	11	88	N/A	77.0	290	7	4	29	12
		5	221	146	71.1	4	10	89	N/A	76.9	314	8	5	29	13
	3000	3	125	93	70.9	4	10	89	N/A	77.5	177	7	5	26	12
		4	151	113	72.5	3	9	90	N/A	N/A	N/A	8	6	25	13
		5	174	139	71.8	3	9	89	N/A	78.7	245	9	7	26	14
	4000	3	110	89	72.8	3	9	90.5	N/A	N/A	N/A	8	7	23	13
		4	134	110	73.9	4	10	91.5	N/A	N/A	N/A	7	6	24	14
		5	157	133	73.8	4	10	91.5	N/A	N/A	N/A	7	6	25	15

Table 7 System parameters for copper cross sections 250 mm<sup>2</sup>, 300 mm<sup>2</sup> and 350 mm<sup>2</sup> with double sided cooling

Copper Core (mm <sup>2</sup> )	Critical current (A)	Heat intrusion (W·m <sup>-2</sup> )	Cooling capacity at nominal current (kW) ± 5 kW	Cooling capacity at zero current (kW) ± 5 kW	Maximum temperature (K) ± 0.7 K	τ <sub>outer</sub> flow (s) ± 1 s	τ <sub>inner</sub> flow (s) ± 3 s	Adiabatic Temperature after fault (K) ± 0.7 K	Adiabatic I <sub>c</sub> (A)	Maximum temperature after 3 τ (K) ± 0.7 K	Cooling capacity after fault (kW) ± 5 kW	Pressure drop at nominal current (10 <sup>5</sup> Pa)	Pressure drop at zero current (10 <sup>5</sup> Pa)	Former Diameter (mm)	Dielectric Field strength (kV·mm <sup>-1</sup> )
250	2000	3	167	105	69.7	4	12	81.0	1200 ± 140	73.0	195.3	6	4	31	11
		4	199	124	71.2	4	11	82.5	910 ± 140	75.6	258.6	7	4	29	12
		5	224	151	70.9	4	9	82.2	970 ± 140	74.7	268.9	9	5	29	13
	3000	3	129	95	71.3	4	10	82.6	1320 ± 210	75.6	154.6	7	5	26	12
		4	154	119	71.8	3	10	83.1	1170 ± 210	76.5	187.5	8	6	26	13
		5	179	140	72.9	3	10	84.2	840 ± 210	N/A	N/A	8	6	26	14
	4000	3	113	94	72.0	3	10	83.3	1490 ± 280	76.9	132.2	8	7	24	12
		4	137	116	72.8	3	9	84.1	1150 ± 280	78.0	163.1	9	8	24	14
		5	161	140	72.7	3	9	84.0	1200 ± 280	77.3	185.0	9	8	25	15
300	2000	3	169	107	69.9	5	13	77.7	1860 ± 140	72.4	191.5	5	3	32	11
		4	199	132	70.6	4	12	78.4	1720 ± 140	73.3	227.3	6	4	31	12
		5	228	159	70.7	4	11	78.6	1690 ± 140	73.4	255.2	7	5	31	13
	3000	3	131	97	71.7	4	11	79.5	2250 ± 210	75.8	156.1	7	5	26	12
		4	158	124	71.3	4	10	79.1	2360 ± 210	74.3	173.8	8	6	27	13
		5	186	143	73.4	3	10	81.2	1730 ± 210	77.7	227.2	8	6	26	13
	4000	3	116	96	72.5	3	10	80.3	2670 ± 280	76.4	132.4	8	7	24	12
		4	141	120	72.7	3	10	80.5	2600 ± 280	76.2	156.6	8	7	25	13
		5	165	141	74.0	3	9	81.8	2070 ± 280	78.6	197.7	10	9	24	14
350	2000	3	172	109	70.0	5	14	75.8	2250 ± 140	72.0	187.3	5	3	32	10
		4	202	134	70.8	4	12	76.6	2090 ± 140	72.9	222.0	6	4	31	12
		5	231	162	70.9	4	11	76.7	2070 ± 140	73.0	250.3	7	5	31	12
	3000	3	134	102	71.7	4	12	77.5	2870 ± 210	74.3	148.3	6	5	27	11
		4	162	127	72.2	4	11	78.0	2710 ± 210	74.7	175.1	7	6	27	12
		5	190	150	73.4	4	11	79.2	2340 ± 210	76.4	215.1	7	6	27	13
	4000	3	119	98	73.0	3	10	78.7	3310 ± 280	76.3	133.8	8	7	24	12
		4	145	126	72.0	3	10	77.7	3710 ± 280	74.5	152.8	8	7	26	13
		5	170	146	73.8	3	9	79.6	2980 ± 280	76.8	184.0	9	8	25	14

Table 8 System parameters for copper cross sections 150 mm<sup>2</sup> and 200 mm<sup>2</sup> with single sided cooling

Copper Core (mm <sup>2</sup> )	Critical current (A)	Heat intrusion (W·m <sup>-2</sup> )	Cooling capacity at nominal current (kW) ± 5 kW	Cooling capacity at zero current (kW) ± 5 kW	Maximum temperature (K) ± 0.7 K	τ <sub>outer</sub> flow (s) ± 2 s	τ <sub>inner</sub> flow (s) ± 4 s	Adiabatic Temperature after fault (K) ± 0.7 K	Adiabatic I <sub>c</sub> (A)	Maximum temperature after 3 τ (K) ± 0.7 K	Cooling capacity after fault (kW) ± 5 kW	Pressure drop at nominal current (10 <sup>5</sup> Pa)	Pressure drop at zero current (10 <sup>5</sup> Pa)	Former Diameter (mm)	Dielectric Field strength (kV·mm <sup>-1</sup> )
150	2000	3	189	116	70.9	5	13	102.3	N/A	N/A	N/A	6.91	4.62	36	9
		4	224	146	70.6	5	12	101.9	N/A	75.6	292	9.29	4.66	37	10
		5	255	179	70.8	5	12	102.2	N/A	75.3	319	7.05	4.71	39	11
	3000	3	146	108	71.5	4	11	102.8	N/A	N/A	N/A	8.03	5.75	32	10
		4	174	132	72.6	4	11	104.0	N/A	N/A	N/A	8.08	5.78	32	11
		5	203	159	73.9	4	11	105.3	N/A	N/A	N/A	8.12	6.96	32	12
	4000	3	129	108	71.6	5	12	103.0	N/A	77.6	156	6.93	5.78	32	11
		4	155	131	72.9	4	11	104.3	N/A	N/A	N/A	8.09	6.94	31	12
		5	182	152	75.0	4	9	106.4	N/A	N/A	N/A	10.38	9.23	29	13
200	2000	3	194	121	69.7	5	13	87.3	N/A	72.5	218	6.96	3.49	39	9
		4	225	151	70.8	5	13	88.4	N/A	74.0	259	6.99	4.67	38	10
		5	259	183	70.9	5	12	88.5	N/A	74.2	301	8.19	5.87	38	11
	3000	3	147	115	71.0	5	12	88.6	N/A	74.8	167	6.93	5.78	34	10
		4	178	142	71.9	4	11	89.6	N/A	76.4	211	8.05	6.91	33	10
		5	209	165	72.7	4	10	90.4	N/A	77.8	257	10.42	8.12	32	12
	4000	3	130	109	71.9	5	12	89.6	N/A	75.9	144	6.93	5.78	32	11
		4	158	135	73.0	4	11	90.6	N/A	77.75	184	8.01	6.87	31	10
		5	187	160	73.9	4	10	91.5	N/A	N/A	N/A	9.28	8.13	31	13

Table 9 System parameters for copper cross sections 250 mm<sup>2</sup>, 300 mm<sup>2</sup> and 350 mm<sup>2</sup> with single sided cooling

Copper Core (mm <sup>2</sup> )	Critical current (A)	Heat intrusion (W·m <sup>-2</sup> )	Cooling capacity at nominal current (kW) ± 5 kW	Cooling capacity at zero current (kW) ± 5 kW	Maximum temperature (K) ± 0.7 K	τ outer flow (s) ± 2 s	τ inner flow (s) ± 4 s	Adiabatic Temperature after fault (K) ± 0.7 K	Adiabatic I <sub>c</sub> (A)	Maximum temperature after 3 τ (K) ± 0.7 K	Cooling capacity after fault (kW) ± 5 kW	Pressure drop at nominal current (10 <sup>5</sup> Pa)	Pressure drop at zero current (10 <sup>5</sup> Pa)	Former Diameter (mm)	Dielectric Field strength (kV·mm <sup>-1</sup> )
250	2000	3	194	121	70.7	5	13	82.0	1000 ± 140	73.5	224	6.91	4.62	37	9
		4	229	149	70.9	5	12	82.2	960 ± 140	73.6	258	8.11	4.65	37	10
		5	264	177	71.8	4	11	83.1	790 ± 140	74.9	304	9.29	5.82	36	11
	3000	3	149	114	72.0	5	12	83.3	1110 ± 210	75.5	172	6.89	5.74	33	10
		4	182	143	72.5	4	11	83.8	970 ± 210	75.8	203	8.07	6.93	33	11
		5	212	168	72.8	4	10	84.1	860 ± 210	76.3	241	9.26	6.96	33	12
	4000	3	133	111	72.2	5	13	83.5	1390 ± 280	75.2	144	5.74	4.60	33	10
		4	162	136	73.7	4	11	84.9	820 ± 280	77.6	184	8.03	6.89	31	11
		5	190	164	73.9	4	10	85.2	720 ± 280	77.7	213	9.17	8.03	31	11
300	2000	3	195	127	70.0	6	15	77.8	1840 ± 140	71.8	209	5.75	3.46	40	8
		4	231	157	70.6	5	13	78.5	1710 ± 140	72.5	249	6.97	4.66	39	10
		5	265	183	71.9	5	13	79.7	1460 ± 140	74.2	299	6.96	4.65	38	10
	3000	3	152	118	71.5	5	13	79.4	2300 ± 210	73.9	163	6.89	5.75	34	10
		4	184	144	72.8	5	12	80.7	1910 ± 210	75.6	203	6.92	5.78	34	11
		5	215	175	72.9	4	11	80.7	1890 ± 210	75.5	234	8.07	6.92	34	11
	4000	3	135	112	72.6	5	14	80.4	2640 ± 280	74.9	142	5.73	4.59	33	10
		4	165	141	72.9	5	12	80.8	2500 ± 280	75.3	175	6.91	5.76	33	11
		5	195	169	73.9	4	12	81.8	2090 ± 280	76.6	209	7.98	6.85	32	10
350	2000	3	198	125	70.6	6	15	76.4	2120 ± 140	72.4	214	5.77	3.47	39	9
		4	234	159	70.8	5	13	76.5	2090 ± 140	72.5	250	6.96	4.65	39	10
		5	268	191	71.0	5	13	76.8	2050 ± 140	72.5	284	7.00	4.68	40	11
	3000	3	154	118	71.9	5	14	77.7	2800 ± 210	73.9	163	5.75	4.60	35	10
		4	186	150	72.0	5	13	77.8	2770 ± 210	73.9	196	6.89	5.75	35	10
		5	218	178	73.0	5	13	78.8	2470 ± 210	75.0	231	6.89	5.75	35	11
	4000	3	136	113	72.9	5	14	78.7	3340 ± 280	74.9	143	5.71	4.58	33	10
		4	168	146	73.6	5	13	79.3	3070 ± 280	75.5	176	5.76	5.76	34	11
		5	199	172	73.7	4	11	79.5	3010 ± 280	75.7	207	8.06	6.92	33	12

Table 10 System comparison between single and double sided cooling for copper cross sections 150 mm<sup>2</sup> and 200 mm<sup>2</sup>

Copper Core (mm <sup>2</sup> )	Critical Current (A)	Heat intrusion (W·m <sup>-2</sup> )	Cooling Capacity at nominal current (kW)			Cooling capacity at zero current (kW)			Fault recovery		Cooling capacity after fault (kW)		
			Double sided ± 5 kW	Single sided ± 5 kW	Difference ± 10 kW	Double sided ± 5 kW	Single sided ± 5 kW	Difference ± 10 kW	Double sided	Single sided	Double sided ± 5 kW	Single sided ± 5 kW	Difference ± 10 kW
150	2000	3	165	189	24	106	116	10	Some	None	208	N/A	N/A
		4	189	224	35	119	146	27	None	Some	N/A	292	N/A
		5	215	255	41	143	179	36	None	Some	N/A	319	N/A
	3000	3	124	146	21	87	108	21	None	None	N/A	N/A	N/A
		4	147	174	27	115	132	17	None	None	N/A	N/A	N/A
		5	171	203	32	135	159	24	None	None	N/A	N/A	N/A
	4000	3	107	129	22	87	108	21	None	Some	N/A	156	N/A
		4	128	155	26	107	131	24	None	None	N/A	N/A	N/A
		5	151	182	30	123	152	29	None	None	N/A	N/A	N/A
200	2000	3	169	194	25	111	121	10	Some	Some	191	218	27
		4	192	225	33	122	151	29	Some	Some	290	259	-31
		5	221	259	38	146	183	37	Some	Some	314	301	-13
	3000	3	125	147	22	93	115	22	Some	Some	177	167	-10
		4	151	178	27	113	142	29	None	Some	N/A	211	N/A
		5	174	209	35	139	165	26	Some	Some	245	257	11
	4000	3	110	130	20	89	109	20	None	Some	N/A	144	N/A
		4	134	158	25	110	135	25	None	Some	N/A	184	N/A
		5	157	187	30	133	160	27	None	None	N/A	N/A	N/A

Table 11 System comparison between single and double sided cooling for copper cross sections 250 mm<sup>2</sup>, 300 mm<sup>2</sup> and 350 mm<sup>2</sup>

Copper Core	Critical Current	Heat intrusion	Cooling Capacity at nominal current			Cooling capacity at zero current			Fault recovery		Cooling capacity after fault		
			Double sided ± 5 kW	Single sided ± 5 kW	Difference ± 10 kW	Double sided ± 5 kW	Single sided ± 5 kW	Difference ± 10 kW	Double sided	Single sided	Double sided ± 5 kW	Single sided ± 5 kW	Difference ± 10 kW
250	2000	3	167	194	27	105	121	16	Full	Full	195	224	29
		4	199	229	30	124	149	25	Some	Some	259	258	0
		5	224	264	40	151	177	25	Some	Some	269	304	35
	3000	3	129	149	20	95	114	18	Full	Full	155	172	17
		4	154	182	28	119	143	24	Full	Some	187	203	16
		5	179	212	33	140	168	28	None	Some	N/A	241	N/A
	4000	3	113	133	20	94	111	17	Full	Full	132	144	11
		4	137	162	24	116	136	20	Full	Some	163	184	21
		5	161	190	29	140	164	24	Full	Some	185	213	28
300	2000	3	169	195	26	107	127	20	Full	Full	191	209	18
		4	199	231	32	132	157	25	Full	Full	227	249	22
		5	228	265	38	159	183	24	Full	Full	255	299	44
	3000	3	131	152	21	97	118	21	Full	Full	156	163	7
		4	158	184	25	124	144	20	Full	Full	174	203	30
		5	186	215	29	143	175	32	Full	Full	227	234	7
	4000	3	116	135	18	96	112	16	Full	Full	132	142	9
		4	141	165	24	120	141	21	Full	Full	157	175	18
		5	165	195	30	141	169	28	Full	Full	198	209	11
350	2000	3	172	198	26	109	125	16	Full	Full	187	214	27
		4	202	234	31	134	159	25	Full	Full	222	250	28
		5	231	268	37	162	191	30	Full	Full	250	284	34
	3000	3	134	154	20	102	118	17	Full	Full	148	163	15
		4	162	186	24	127	150	23	Full	Full	175	196	21
		5	190	218	28	150	178	29	Full	Full	215	231	16
	4000	3	119	136	18	98	113	16	Full	Full	134	143	9
		4	145	168	23	126	146	21	Full	Full	153	176	24
		5	170	199	29	146	172	26	Full	Full	184	207	23

C.1.2 Norris correction 0.5

Table 12 System parameters for copper cross sections 150 mm<sup>2</sup> and 200 mm<sup>2</sup> with double sided cooling

Copper Core (mm <sup>2</sup> )	Critical current (A)	Heat intrusion (W·m <sup>-2</sup> )	Cooling capacity at nominal current (kW) ± 5 kW	Cooling capacity at zero current (kW) ± 5 kW	Maximum temperature (K) ± 0.7 K	τ outer flow (s) ± 1 s	τ inner flow (s) ± 3 s	Adiabatic Temperature after fault (K) ± 0.7 K	Adiabatic I <sub>c</sub> (A)	Maximum temperature after 3 τ (K) ± 0.7 K	Cooling capacity after fault (kW) ± 5 kW	Pressure drop at nominal current (10 <sup>5</sup> Pa)	Pressure drop at zero current (10 <sup>5</sup> Pa)	Former Diameter (mm)	Dielectric Field strength (kV·mm <sup>-1</sup> )
150	2000	3	133	97	70.1	5	12	101.5	N/A	78.0	212	5	4	29	12
		4	156	118	70.9	4	11	102.3	N/A	N/A	N/A	6	5	28	13
		5	185	150	70.0	4	10	101.4	N/A	76.0	228	7	6	30	13
	3000	3	107	88	71.7	4	10	103.1	N/A	N/A	N/A	7	6	24	12
		4	130	110	71.9	4	10	103.3	N/A	N/A	N/A	7	6	25	14
		5	153	134	72.0	4	10	103.3	N/A	N/A	N/A	7	6	26	14
	4000	3	98	88	72.0	4	11	103.4	N/A	N/A	N/A	6	6	24	13
		4	118	106	73.9	4	10	105.3	N/A	N/A	N/A	7	7	23	14
		5	140	128	73.9	4	9	105.3	N/A	N/A	N/A	7	7	24	15
200	2000	3	134	95	70.8	3	10	88.4	N/A	78.0	211	8	6	26	12
		4	163	125	69.9	3	9	87.6	N/A	74.7	193	9	7	28	13
		5	186	146	70.9	3	9	88.5	N/A	76.4	236	10	8	27	14
	3000	3	110	91	71.9	4	11	89.5	N/A	79.0	151	6	5	25	12
		4	133	112	72.9	3	9	90.6	N/A	N/A	N/A	8	7	24	14
		5	156	135	72.9	3	9	90.6	N/A	N/A	N/A	8	7	25	15
	4000	3	100	89	73.0	3	10	90.6	N/A	N/A	N/A	7	7	23	13
		4	122	109	73.8	3	9	91.4	N/A	N/A	N/A	8	7	23	14
		5	145	133	73.9	3	9	91.5	N/A	N/A	N/A	8	8	24	16

Table 13 System parameters for copper cross sections 250 mm<sup>2</sup>, 300 mm<sup>2</sup> and 350 mm<sup>2</sup> with double sided cooling

Copper Core (mm <sup>2</sup> )	Critical current (A)	Heat intrusion (W·m <sup>-2</sup> )	Cooling capacity at nominal current (kW) ± 5 kW	Cooling capacity at zero current (kW) ± 5 kW	Maximum temperature (K) ± 0.7 K	τ outer flow (s) ± 1 s	τ inner flow (s) ± 3 s	Adiabatic Temperature after fault (K) ± 0.7 K	Adiabatic I <sub>c</sub> (A)	Maximum temperature after 3 τ (K) ± 0.7 K	Cooling capacity after fault (kW) ± 5 kW	Pressure drop at nominal current (10 <sup>5</sup> Pa)	Pressure drop at zero current (10 <sup>5</sup> Pa)	Former Diameter (mm)	Dielectric Field strength (kV·mm <sup>-1</sup> )
250	2000	3	137	103	70.0	4	12	81.3	1150 ± 140	73.4	156	6	5	29	11
		4	166	129	69.9	4	10	81.2	1160 ± 140	73.2	185	8	6	29	12
		5	189	147	71.9	4	10	83.2	760 ± 140	76.4	234	7	6	28	14
	3000	3	113	94	72.0	3	10	83.2	1130 ± 210	76.8	133	8	7	24	11
		4	138	119	71.8	4	10	83.1	1170 ± 210	75.8	152	7	6	26	13
		5	161	140	73.0	4	10	84.3	820 ± 210	77.5	186	7	6	26	14
	4000	3	104	93	73.0	4	11	84.3	1090 ± 280	77.8	118	6	6	24	11
		4	127	114	73.9	4	10	85.2	740 ± 280	79.0	146	7	7	24	14
		5	150	138	73.9	4	10	85.2	720 ± 280	78.5	168	7	7	25	15
300	2000	3	140	102	70.3	4	11	78.2	1770 ± 140	73.2	157	7	5	28	11
		4	169	134	70.0	4	11	77.8	1840 ± 140	72.5	181	7	6	30	12
		5	195	154	70.8	4	10	78.7	1670 ± 140	73.5	211	8	6	29	13
	3000	3	115	97	72.0	4	11	79.8	2160 ± 210	75.6	128	7	6	25	12
		4	142	125	71.9	4	11	79.8	2170 ± 210	74.9	151	6	6	27	12
		5	166	145	72.7	3	10	80.6	1930 ± 210	75.9	178	8	7	26	14
	4000	3	106	96	72.7	3	10	80.5	2600 ± 280	76.3	115	7	7	24	12
		4	131	118	74.0	4	11	81.8	2080 ± 280	77.6	143	6	6	25	13
		5	156	143	73.9	5	12	81.8	2060 ± 280	77.2	167	6	6	26	13
350	2000	3	143	109	69.8	4	12	75.6	2280 ± 140	71.9	152	6	5	30	11
		4	170	130	71.0	4	10	76.7	2060 ± 140	73.4	185	8	6	28	12
		5	198	160	70.9	4	11	76.7	2070 ± 140	73.0	209	7	6	30	13
	3000	3	119	104	71.0	4	13	76.8	3070 ± 210	73.3	125	5	5	28	11
		4	145	124	72.7	4	11	78.4	2570 ± 210	75.4	155	7	6	26	13
		5	170	149	73.0	3	10	78.7	2480 ± 210	75.6	181	8	7	26	12
	4000	3	109	98	72.8	4	11	78.5	3390 ± 280	75.4	115	6	6	25	12
		4	135	124	73.0	4	12	78.8	3230 ± 280	75.5	140	6	6	26	12
		5	159	147	73.9	3	10	79.7	2930 ± 280	76.6	166	8	8	25	13

Table 14 System parameters for copper cross sections 150 mm<sup>2</sup> and 200 mm<sup>2</sup> with single sided cooling

Copper Core (mm <sup>2</sup> )	Critical current (A)	Heat intrusion (W·m <sup>-2</sup> )	Cooling capacity at nominal current (kW) ± 5 kW	Cooling capacity at zero current (kW) ± 5 kW	Maximum temperature (K) ± 0.7 K	τ <sub>outer</sub> flow (s) ± 2 s	τ <sub>inner</sub> flow (s) ± 4 s	Adiabatic Temperature after fault (K) ± 0.7 K	Adiabatic I <sub>c</sub> (A)	Maximum temperature after 3 τ (K) ± 0.7 K	Cooling capacity after fault (kW) ± 5 kW	Pressure drop at nominal current (10 <sup>5</sup> Pa)	Pressure drop at zero current (10 <sup>5</sup> Pa)	Former Diameter (mm)	Dielectric Field strength (kV·mm <sup>-1</sup> )
150	2000	3	154	114	71.0	6	15	102.4	N/A	76.0	194	4.68	3.51	37	10
		4	186	146	70.9	6	14	102.3	N/A	75.6	224	5.84	4.68	37	10
		5	218	176	71.0	5	12	102.4	N/A	75.6	255	7.04	5.87	37	11
	3000	3	127	104	72.6	5	13	103.9	N/A	N/A	N/A	5.89	4.64	32	11
		4	155	131	72.9	4	11	104.3	N/A	N/A	N/A	8.12	6.97	31	12
		5	186	163	72.3	4	10	103.7	N/A	78.5	224	9.30	8.15	32	12
	4000	3	115	102	73.9	4	11	105.3	N/A	N/A	N/A	6.89	6.89	29	11
		4	141	124	74.9	4	10	106.3	N/A	N/A	N/A	9.20	8.05	28	12
		5	167	150	74.9	4	10	106.3	N/A	N/A	N/A	9.22	8.08	29	12
200	2000	3	157	117	70.9	5	14	88.5	N/A	74.4	182	5.81	4.65	36	10
		4	189	149	70.9	5	12	88.6	N/A	74.4	213	6.96	5.81	36	10
		5	219	174	72.0	5	12	89.6	N/A	75.8	252	7.03	5.87	36	12
	3000	3	129	106	73.0	5	13	90.6	N/A	78.8	167	5.78	4.63	32	11
		4	159	133	73.7	4	10	91.3	N/A	N/A	N/A	9.22	8.07	30	12
		5	186	160	74.0	4	10	91.6	N/A	N/A	N/A	10.36	9.22	30	12
	4000	3	118	101	74.8	4	11	92.5	N/A	N/A	N/A	7.98	6.84	28	11
		4	145	126	75.8	4	10	93.4	N/A	N/A	N/A	9.16	8.02	28	12
		5	173	153	75.6	3	9	93.2	N/A	N/A	N/A	11.49	10.34	28	13

Table 15 System parameters for copper cross sections 250 mm<sup>2</sup> and 300 mm<sup>2</sup> with single sided cooling

Copper Core (mm <sup>2</sup> )	Critical current (A)	Heat intrusion (W·m <sup>-2</sup> )	Cooling capacity at nominal current (kW) ± 5 kW	Cooling capacity at zero current (kW) ± 5 kW	Maximum temperature (K) ± 0.7 K	τ outer flow (s) ± 2 s	τ inner flow (s) ± 4 s	Adiabatic Temperature after fault (K) ± 0.7 K	Adiabatic I <sub>c</sub> (A)	Maximum temperature after 3 τ (K) ± 0.7 K	Cooling capacity after fault (kW) ± 5 kW	Pressure drop at nominal current (10 <sup>5</sup> Pa)	Pressure drop at zero current (10 <sup>5</sup> Pa)	Former Diameter (mm)	Dielectric Field strength (kV·mm <sup>-1</sup> )
250	2000	3	160	116	70.9	5	12	82.2	960 ± 140	73.7	177	6.92	4.63	35	10
		4	191	146	72.0	5	12	83.3	740 ± 140	75.3	221	6.96	5.81	35	11
		5	223	179	71.9	4	12	83.2	760 ± 140	74.8	245	8.07	6.92	35	10
	3000	3	132	110	72.9	4	12	84.2	840 ± 210	76.7	149	6.80	5.67	31	9
		4	161	135	73.9	3	11	85.2	540 ± 210	78.7	196	8.07	6.92	31	12
		5	190	164	73.9	4	11	85.2	540 ± 210	77.6	213	8.09	6.94	32	12
	4000	3	120	106	75.0	4	12	86.2	300 ± 280	N/A	N/A	6.80	6.80	29	10
		4	149	131	74.8	4	10	86.1	360 ± 280	79.0	167	9.16	8.02	29	12
		5	176	159	76.0	4	11	87.3	N/A	N/A	N/A	8.04	8.04	30	12
300	2000	3	161	121	70.9	6	16	78.8	1650 ± 140	72.9	172	4.62	3.47	38	9
		4	195	151	71.6	5	14	79.4	1510 ± 140	73.6	208	5.79	4.64	37	10
		5	227	182	71.9	6	14	79.8	1450 ± 140	73.9	240	5.83	4.67	38	11
	3000	3	134	115	72.6	5	14	80.4	1980 ± 210	74.9	142	5.73	5.73	33	10
		4	165	141	72.9	5	12	80.8	1870 ± 210	75.3	175	6.91	5.76	33	11
		5	195	166	74.7	4	10	82.6	1330 ± 210	77.9	215	9.18	8.04	31	12
	4000	3	124	110	74.5	5	13	82.3	1880 ± 280	77.4	134	5.73	5.73	31	11
		4	152	138	74.8	4	11	82.6	1760 ± 280	77.7	163	7.98	7.98	30	11
		5	181	167	74.8	4	11	82.6	1750 ± 280	77.5	191	8.00	8.00	31	11

Table 16 System comparison between single and double sided cooling for copper cross sections 150 mm<sup>2</sup> and 200 mm<sup>2</sup>

Copper Core (mm <sup>2</sup> )	Critical Current (A)	Heat intrusion (W·m <sup>-2</sup> )	Cooling Capacity at nominal current (kW)			Cooling capacity at zero current (kW)			Fault recovery		Cooling capacity after fault (kW)		
			Double sided ± 5 kW	Single sided ± 5 kW	Difference ± 10 kW	Double sided ± 5 kW	Single sided ± 5 kW	Difference ± 10 kW	Double sided	Single sided	Double sided ± 5 kW	Single sided ± 5 kW	Difference ± 10 kW
150	2000	3	133	154	22	97	114	17	Some	Some	212	194	-18
		4	156	186	30	118	146	27	None	Some	N/A	224	N/A
		5	185	218	33	150	176	26	Some	Some	228	255	26
	3000	3	107	127	20	88	104	16	None	None	N/A	N/A	N/A
		4	130	155	25	110	131	21	None	None	N/A	N/A	N/A
		5	153	186	33	134	163	29	None	Some	N/A	224	N/A
	4000	3	98	115	17	88	102	14	None	None	N/A	N/A	N/A
		4	118	141	23	106	124	18	None	None	N/A	N/A	N/A
		5	140	167	27	128	150	22	None	None	N/A	N/A	N/A
200	2000	3	134	157	22	95	117	21	Some	Some	211	182	-30
		4	163	189	26	125	149	23	Some	Some	193	213	20
		5	186	219	33	146	174	28	Some	Some	236	252	16
	3000	3	110	129	19	91	106	15	Some	Some	151	167	16
		4	133	159	26	112	133	21	None	None	N/A	N/A	N/A
		5	156	186	30	135	160	25	None	None	N/A	N/A	N/A
	4000	3	100	118	18	89	101	12	None	None	N/A	N/A	N/A
		4	122	145	23	109	126	17	None	None	N/A	N/A	N/A
		5	145	173	28	133	153	20	None	None	N/A	N/A	N/A

Table 17 System comparison between single and double sided cooling for copper cross sections 250 mm<sup>2</sup> and 300 mm<sup>2</sup>

Copper Core (mm <sup>2</sup> )	Critical Current (A)	Heat intrusion (W·m <sup>-2</sup> )	Cooling Capacity at nominal current (kW)			Cooling capacity at zero current (kW)			Fault recovery		Cooling capacity after fault (kW)		
			Double sided ± 5 kW	Single sided ± 5 kW	Difference ± 10 kW	Double sided ± 5 kW	Single sided ± 5 kW	Difference ± 10 kW	Double sided	Single sided	Double sided ± 5 kW	Single sided ± 5 kW	Difference ± 10 kW
250	2000	3	137	160	22	103	116	13	Full	Some	156	177	20
		4	166	191	25	129	146	17	Full	Some	185	221	37
		5	189	223	34	147	179	31	Some	Some	234	245	11
	3000	3	113	132	19	94	110	15	Full	Some	133	149	17
		4	138	161	24	119	135	17	Full	Some	152	196	45
		5	161	190	29	140	164	24	Some	Some	186	213	27
	4000	3	104	120	17	93	106	13	Full	None	118	N/A	N/A
		4	127	149	22	114	131	17	Some	Some	146	167	21
		5	150	176	26	138	159	21	Some	None	168	N/A	N/A
300	2000	3	140	161	21	102	121	19	Full	Full	157	172	15
		4	169	195	26	134	151	17	Full	Full	181	208	26
		5	195	227	32	154	182	28	Full	Full	211	240	30
	3000	3	115	134	19	97	115	19	Full	Full	128	142	14
		4	142	165	23	125	141	17	Full	Full	151	175	24
		5	166	195	29	145	166	21	Full	Full	178	215	38
	4000	3	106	124	17	96	110	14	Full	Full	115	134	19
		4	131	152	21	118	138	19	Full	Full	143	163	20
		5	156	181	25	143	167	23	Full	Full	167	191	24

## C.2 Wet PPLP

### C.2.1 Norris correction 0.9

Table 18 System parameters for copper cross sections 200 mm<sup>2</sup>, 250 mm<sup>2</sup> and 300 mm<sup>2</sup> with double sided cooling

Copper Core (mm <sup>2</sup> )	Critical current (A)	Heat intrusion (W·m <sup>-2</sup> )	Cooling capacity at nominal current (kW) ± 5 kW	Cooling capacity at zero current (kW) ± 5 kW	Maximum temperature (K) ± 0.7 K	τ outer flow (s) ± 2 s	τ inner flow (s) ± 4 s	Adiabatic Temperature after fault (K) ± 0.7 K	Adiabatic I <sub>c</sub> (A)	Maximum temperature after 3 τ (K) ± 0.7 K	Cooling capacity after fault (kW) ± 5 kW	Pressure drop at nominal current (10 <sup>5</sup> Pa)	Pressure drop at zero current (10 <sup>5</sup> Pa)	Former Diameter (mm)	Dielectric Field strength (kV·mm <sup>-1</sup> )
200	2000	3	192	128	69.9	6	14	87.5	N/A	72.7	216	5	4	40	9
		4	226	152	70.9	5	13	88.6	N/A	74.4	269	6	4	38	9
		5	261	179	71.9	5	13	89.5	N/A	75.8	319	6	4	38	10
	3000	3	149	114	71.8	5	13	89.5	N/A	75.7	172	5	4	35	10
		4	180	145	71.9	5	12	89.6	N/A	75.6	203	6	5	35	10
		5	211	172	73.0	4	11	90.6	N/A	77.6	255	7	6	34	10
	4000	3	131	112	72.8	5	13	90.5	N/A	77.0	149	5	5	33	10
		4	162	141	73.6	5	13	91.2	N/A	77.8	184	5	5	34	11
		5	191	165	73.9	4	10	91.5	N/A	78.7	224	8	7	32	12
250	2000	3	194	127	70.6	6	14	81.9	1030 ± 140	73.0	215	5	4	39	9
		4	229	159	71.0	6	14	82.3	950 ± 140	73.4	255	5	4	40	10
		5	264	194	70.9	5	13	82.1	970 ± 140	73.2	290	6	5	40	10
	3000	3	151	117	71.9	5	12	83.2	1130 ± 210	75.0	168	6	5	34	10
		4	185	147	72.5	4	11	83.8	960 ± 210	75.6	205	7	6	34	11
		5	216	177	72.6	5	11	83.9	920 ± 210	75.5	235	7	6	35	11
	4000	3	135	114	73.3	5	13	84.6	950 ± 280	76.6	149	5	5	33	10
		4	165	139	73.8	5	12	85.1	770 ± 280	77.0	179	6	5	33	11
		5	195	169	73.9	4	11	85.2	710 ± 280	77.0	209	7	6	33	11
300	2000	3	196	128	70.7	6	14	78.6	1680 ± 140	72.7	214	5	4	39	9
		4	231	162	71.0	6	15	78.8	1640 ± 140	72.8	249	5	4	40	9
		5	268	198	70.8	6	14	78.6	1680 ± 140	72.4	284	5	4	42	10
	3000	3	154	119	71.7	5	14	79.5	2250 ± 210	73.7	164	5	4	36	10
		4	187	148	72.9	5	14	80.7	1880 ± 210	75.3	204	5	4	36	10
		5	219	179	73.0	4	12	80.8	1850 ± 210	75.4	237	7	6	35	11
	4000	3	137	115	73.8	5	14	81.6	2160 ± 280	76.5	150	5	5	33	10
		4	168	142	74.0	5	12	81.8	2080 ± 280	76.6	181	6	5	33	10
		5	199	170	74.8	4	11	82.7	1740 ± 280	77.6	217	7	6	33	12

Table 19 System parameters for copper cross sections 200 mm<sup>2</sup>, 250 mm<sup>2</sup> and 300 mm<sup>2</sup> with single sided cooling

Copper Core (mm <sup>2</sup> )	Critical current (A)	Heat intrusion (W·m <sup>-2</sup> )	Cooling capacity at nominal current (kW) ± 5 kW	Cooling capacity at zero current (kW) ± 5 kW	Maximum temperature (K) ± 0.7 K	τ <sub>outer flow</sub> (s) ± 3 s	τ <sub>inner flow</sub> (s) ± 6 s	Adiabatic Temperature after fault (K) ± 0.7 K	Adiabatic I <sub>c</sub> (A)	Maximum temperature after 3 τ (K) ± 0.7 K	Cooling capacity after fault (kW) ± 5 kW	Pressure drop at nominal current (10 <sup>5</sup> Pa)	Pressure drop at zero current (10 <sup>5</sup> Pa)	Former Diameter (mm)	Dielectric Field strength (kV·mm <sup>-1</sup> )
200	2000	3	231	155	71.0	9	21	88.6	N/A	72.7	248	3.54	2.36	55	7
		4	278	202	70.9	8	18	88.5	N/A	72.5	295	4.70	3.53	54	7
		5	322	237	72.0	8	18	89.6	N/A	73.8	344	4.74	3.56	54	8
	3000	3	184	142	72.6	7	17	90.3	N/A	74.9	197	4.69	3.52	47	8
		4	226	191	73.0	8	17	90.6	N/A	75.2	243	4.74	4.74	49	9
		5	266	216	74.0	7	15	91.7	N/A	76.6	291	5.90	4.73	47	9
	4000	3	165	143	73.7	7	17	91.4	N/A	76.4	178	4.62	4.62	44	7
		4	203	177	75.0	7	17	92.6	N/A	77.9	222	4.67	4.67	45	8
		5	242	216	74.9	6	15	92.6	N/A	77.6	260	5.88	5.88	45	9
250	2000	3	235	161	70.6	8	18	81.9	1010 ± 140	72.0	246	4.69	3.52	53	7
		4	281	197	71.9	8	18	83.2	770 ± 140	73.4	300	4.73	3.55	53	8
		5	327	242	71.9	7	16	83.2	760 ± 140	73.4	346	5.89	4.72	52	8
	3000	3	186	155	71.8	9	21	83.1	1175 ± 210	73.3	194	3.51	3.51	51	7
		4	228	193	72.8	7	17	84.1	870 ± 210	74.5	239	4.70	4.70	49	8
		5	270	221	73.8	6	16	85.1	560 ± 210	75.7	284	5.84	4.68	47	8
	4000	3	166	145	73.6	7	17	84.9	860 ± 280	75.5	174	4.67	4.67	45	8
		4	206	181	74.9	7	17	86.2	340 ± 280	76.8	217	4.71	4.71	46	9
		5	247	217	75.9	7	15	87.2	N/A	78.7	271	5.90	5.90	45	10
300	2000	3	236	162	70.9	7	19	78.8	1650 ± 140	72.2	250	4.63	3.47	52	6
		4	285	203	71.9	7	19	79.8	1450 ± 140	73.3	303	4.63	3.47	52	6
		5	329	244	71.8	8	18	79.7	1470 ± 140	72.9	340	4.73	3.56	55	8
	3000	3	189	155	72.4	7	17	80.3	2020 ± 210	73.8	195	4.68	4.68	48	8
		4	230	191	73.8	7	17	81.7	1600 ± 210	75.5	244	4.68	4.68	48	8
		5	274	224	73.8	7	15	81.6	1610 ± 210	75.4	287	5.88	4.71	48	9
	4000	3	168	146	73.8	7	17	81.7	2130 ± 280	75.4	175	4.66	4.66	45	8
		4	209	184	74.7	7	17	82.5	1790 ± 280	76.3	218	4.67	4.67	46	8
		5	249	224	75.0	6	14	82.8	1670 ± 280	76.6	259	7.00	7.00	44	9

Table 20 System comparison between single and double sided cooling for copper cross sections 200 mm<sup>2</sup>, 250 mm<sup>2</sup> and 300 mm<sup>2</sup>

Copper Core (mm <sup>2</sup> )	Critical Current (A)	Heat intrusion (W·m <sup>-2</sup> )	Cooling Capacity at nominal current (kW)			Cooling capacity at zero current (kW)			Fault recovery		Cooling capacity after fault (kW)		
			Double sided ± 5 kW	Single sided ± 5 kW	Difference ± 10 kW	Double sided ± 5 kW	Single sided ± 5 kW	Difference ± 10 kW	Double sided	Single sided	Double sided ± 5 kW	Single sided ± 5 kW	Difference ± 10 kW
200	2000	3	192	231	39	128	155	27	Some	Some	216	248	31
		4	226	278	52	152	202	50	Some	Some	269	295	26
		5	261	322	62	179	237	59	Some	Some	319	344	25
	3000	3	149	184	36	114	142	28	Some	Some	172	197	25
		4	180	226	46	145	191	46	Some	Some	203	243	40
		5	211	266	55	172	216	44	Some	Some	255	291	36
	4000	3	131	165	33	112	143	30	Some	Some	149	178	29
		4	162	203	41	141	177	37	Some	Some	184	222	37
		5	191	242	51	165	216	51	Some	Some	224	260	36
250	2000	3	194	235	41	127	161	34	Full	Full	215	246	30
		4	229	281	52	159	197	39	Some	Some	255	300	45
		5	264	327	62	194	242	48	Some	Some	290	346	56
	3000	3	151	186	35	117	155	39	Full	Full	168	194	27
		4	185	228	43	147	193	47	Some	Some	205	239	34
		5	216	270	54	177	221	44	Some	Some	235	284	49
	4000	3	135	166	32	114	145	31	Some	Some	149	174	25
		4	165	206	41	139	181	41	Some	Some	179	217	37
		5	195	247	52	169	217	48	Some	Some	209	271	62
300	2000	3	196	236	40	128	162	34	Full	Full	214	250	36
		4	231	285	54	162	203	41	Full	Full	249	303	54
		5	268	329	61	198	244	46	Full	Full	284	340	56
	3000	3	154	189	35	119	155	36	Full	Full	164	195	32
		4	187	230	44	148	191	43	Full	Full	204	244	40
		5	219	274	55	179	224	45	Full	Full	237	287	50
	4000	3	137	168	31	115	146	31	Full	Full	150	175	25
		4	168	209	41	142	184	41	Full	Full	181	218	37
		5	199	249	50	170	224	53	Full	Full	217	259	42

C.2.2 Norris correction 0.5

Table 21 System parameters for copper cross sections 200 mm<sup>2</sup>, 250 mm<sup>2</sup> and 300 mm<sup>2</sup> with double sided cooling

Copper Core (mm <sup>2</sup> )	Critical current (A)	Heat intrusion (W·m <sup>-2</sup> )	Cooling capacity at nominal current (kW) ± 5 kW	Cooling capacity at zero current (kW) ± 5 kW	Maximum temperature (K) ± 0.7 K	τ outer flow (s) ± 2 s	τ inner flow (s) ± 5 s	Adiabatic Temperature after fault (K) ± 0.7 K	Adiabatic I <sub>c</sub> (A)	Maximum temperature after 3 τ (K) ± 0.7 K	Cooling capacity after fault (kW) ± 5 kW	Pressure drop at nominal current (10 <sup>5</sup> Pa)	Pressure drop at zero current (10 <sup>5</sup> Pa)	Former Diameter (mm)	Dielectric Field strength (kV·mm <sup>-1</sup> )
200	2000	3	159	119	70.8	6	14	88.4	N/A	74.0	177	5	4	37	10
		4	191	147	72.0	6	13	89.6	N/A	75.7	222	5	4	37	11
		5	223	174	72.7	5	12	90.4	N/A	76.9	266	6	5	36	11
	3000	3	131	112	72.8	5	13	90.5	N/A	77.0	149	5	5	33	10
		4	162	141	73.6	5	13	91.2	N/A	77.8	185	5	5	34	11
		5	191	161	75.0	4	11	92.6	N/A	N/A	N/A	7	6	32	12
	4000	3	121	109	73.5	5	13	91.2	N/A	77.7	133	5	5	32	11
		4	149	129	76.0	4	10	93.6	N/A	N/A	N/A	8	7	29	12
		5	176	157	76.0	4	10	93.6	N/A	N/A	N/A	8	7	30	12
250	2000	3	161	121	71.0	6	14	82.3	940 ± 140	73.5	176	5	4	37	10
		4	194	150	71.8	5	13	83.1	780 ± 140	74.6	214	6	5	36	10
		5	227	177	73.0	5	11	84.3	540 ± 140	76.6	266	7	6	35	11
	3000	3	134	112	72.9	4	13	84.2	850 ± 210	76.3	150	6	5	32	9
		4	165	139	73.8	5	12	85.1	580 ± 210	77.0	179	6	5	33	11
		5	195	169	73.9	4	11	85.2	530 ± 210	77.3	216	7	6	33	11
	4000	3	123	111	73.8	5	13	85.1	780 ± 280	76.8	131	5	5	32	10
		4	152	136	76.0	4	11	87.3	N/A	N/A	N/A	7	7	30	11
		5	182	168	74.8	4	10	86.1	350 ± 280	78.4	197	8	8	31	11
300	2000	3	163	123	70.9	6	16	78.7	1660 ± 140	72.7	173	4	3	39	9
		4	198	158	71.9	6	16	79.8	1450 ± 140	73.8	210	4	4	39	9
		5	231	187	71.8	6	14	79.7	1470 ± 140	73.7	243	5	4	39	10
	3000	3	137	118	72.6	5	14	80.5	1960 ± 210	74.9	144	5	5	34	10
		4	169	148	73.4	5	13	81.3	1720 ± 210	75.7	177	5	5	35	11
		5	199	170	74.8	4	11	82.7	1300 ± 210	77.6	217	7	6	33	12
	4000	3	126	112	74.9	6	15	82.7	1710 ± 280	77.6	136	4	4	33	10
		4	155	141	75.0	4	11	82.8	1670 ± 280	77.8	165	7	7	31	11
		5	185	169	75.8	4	10	83.7	1340 ± 280	78.8	199	8	8	31	12

Table 22 System parameters for copper cross sections 200 mm<sup>2</sup>, 250 mm<sup>2</sup> and 300 mm<sup>2</sup> with single sided cooling

Copper Core (mm <sup>2</sup> )	Critical current (A)	Heat intrusion (W·m <sup>-2</sup> )	Cooling capacity at nominal current (kW) ± 5 kW	Cooling capacity at zero current (kW) ± 5 kW	Maximum temperature (K) ± 0.7 K	τ outer flow (s) ± 2 s	τ inner flow (s) ± 6 s	Adiabatic Temperature after fault (K) ± 0.7 K	Adiabatic I <sub>c</sub> (A)	Maximum temperature after 3 τ (K) ± 0.7 K	Cooling capacity after fault (kW) ± 5 kW	Pressure drop at nominal current (10 <sup>5</sup> Pa)	Pressure drop at zero current (10 <sup>5</sup> Pa)	Former Diameter (mm)	Dielectric Field strength (kV·mm <sup>-1</sup> )
200	2000	3	196	144	72.7	7	18	90.4	N/A	75.5	222	4.65	3.49	47	7
		4	239	198	72.0	7	18	89.6	N/A	73.8	251	4.67	4.67	50	7
		5	281	225	72.9	7	15	90.6	N/A	75.2	275	5.92	4.74	49	9
	3000	3	165	144	73.3	7	17	90.9	N/A	75.7	174	4.67	4.67	45	8
		4	204	179	74.5	7	17	92.2	N/A	76.9	216	4.72	4.72	46	9
		5	244	206	76.0	5	14	93.6	N/A	N.A	N/A	6.95	5.80	42	8
	4000	3	151	134	75.9	7	16	93.5	N/A	79.9	174	4.68	4.68	42	9
		4	188	172	75.7	6	15	93.4	N/A	78.7	202	5.85	5.85	42	9
		5	225	206	76.9	5	13	94.5	N/A	N/A	N/A	6.99	6.99	41	9
250	2000	3	197	148	72.0	7	17	83.3	750 ± 140	73.7	209	4.70	3.53	49	8
		4	241	201	71.9	8	18	83.2	760 ± 140	73.5	252	4.71	4.71	51	8
		5	284	229	72.8	7	16	84.1	590 ± 140	74.5	299	5.86	4.70	49	8
	3000	3	166	145	73.6	7	17	84.9	650 ± 210	75.5	174	4.67	4.67	45	8
		4	207	181	74.8	6	15	86.1	280 ± 210	76.9	218	5.85	5.85	44	9
		5	247	222	74.7	6	14	86.0	310 ± 210	76.6	258	7.02	7.02	44	9
	4000	3	153	139	74.7	7	17	86.0	420 ± 280	76.7	159	4.65	4.65	43	8
		4	192	173	76.3	6	15	87.6	N/A	78.6	203	5.83	5.93	42	9
		5	231	212	76.2	5	13	87.5	N/A	78.4	242	6.99	6.99	42	9
300	2000	3	199	151	71.8	7	18	79.6	1470 ± 140	73.1	209	4.65	3.49	49	7
		4	243	198	72.8	8	18	80.6	1280 ± 140	74.2	256	4.70	4.70	50	8
		5	287	235	74.0	8	18	81.8	1040 ± 140	75.6	305	4.70	4.70	50	8
	3000	3	168	146	73.8	7	17	81.7	1600 ± 210	75.5	175	4.66	4.66	45	8
		4	209	184	74.7	7	17	82.5	1350 ± 210	76.4	219	4.67	4.67	46	8
		5	249	224	75.0	6	14	82.8	1250 ± 210	76.6	259	7.00	7.00	44	9
	4000	3	154	140	75.0	7	17	82.8	1670 ± 280	76.7	160	4.64	4.64	43	8
		4	194	175	76.7	6	15	84.6	980 ± 280	78.8	205	5.82	5.82	42	9
		5	233	214	76.6	5	14	84.4	1030 ± 280	78.5	244	6.98	6.98	42	9

Table 23 System comparison between single and double sided cooling for copper cross sections 200 mm<sup>2</sup>, 250 mm<sup>2</sup> and 300 mm<sup>2</sup>

Copper Core (mm <sup>2</sup> )	Critical Current (A)	Heat intrusion (W·m <sup>-2</sup> )	Cooling Capacity at nominal current (kW)			Cooling capacity at zero current (kW)			Fault recovery		Cooling capacity after fault (kW)		
			Double sided ± 5 kW	Single sided ± 5 kW	Difference ± 10 kW	Double sided ± 5 kW	Single sided ± 5 kW	Difference ± 10 kW	Double sided	Single sided	Double sided ± 5 kW	Single sided ± 5 kW	Difference ± 10 kW
200	2000	3	159	196	37	119	144	24	Some	Some	177	222	44
		4	191	239	48	147	198	52	Some	Some	222	251	29
		5	223	281	58	174	225	51	Some	Some	266	275	9
	3000	3	131	165	34	112	144	31	Some	Some	149	174	25
		4	162	204	42	141	179	39	Some	Some	185	216	31
		5	191	244	53	161	206	45	None	None	N/A	N/A	N/A
	4000	3	121	151	30	109	134	25	Some	Some	133	174	40
		4	149	188	39	129	172	42	None	Some	N/A	202	N/A
		5	176	225	49	157	206	49	None	None	N/A	N/A	N/A
250	2000	3	161	197	37	121	148	28	Some	Some	176	209	33
		4	194	241	47	150	201	51	Some	Some	214	252	38
		5	227	284	57	177	229	52	Some	Some	266	299	32
	3000	3	134	166	32	112	145	33	Some	Some	150	174	25
		4	165	207	42	139	181	42	Some	Some	179	218	38
		5	195	247	53	169	222	53	Some	Some	216	258	42
	4000	3	123	153	30	111	139	28	Some	Some	131	159	28
		4	152	192	40	136	173	38	None	Some	N/A	203	N/A
		5	182	231	49	168	212	44	Some	Some	197	242	45
300	2000	3	163	199	36	123	151	28	Full	Full	173	209	36
		4	198	243	45	158	198	40	Full	Full	210	256	46
		5	231	287	55	187	235	48	Full	Full	243	305	62
	3000	3	137	168	31	118	146	28	Full	Full	144	175	31
		4	169	209	40	148	184	36	Full	Full	177	219	41
		5	199	249	50	170	224	53	Full	Full	217	259	42
	4000	3	126	154	28	112	140	28	Full	Full	136	160	24
		4	155	194	39	141	175	33	Full	Some	165	205	40
		5	185	233	48	169	214	45	Full	Full	199	244	44

## Appendix D. Sensitivity Analysis

To determine the accuracy of the model a sensitivity analysis is made. In this analysis the various input parameters of the model are varied within their known accuracy and the relevance of the parameter on the model is determined. When this is done for all the input parameters an overall accuracy of the model can be determined.

There are two types of influences on the accuracy of the model. First there are the accuracies inherent to the model. These are for example the number of elements used, linearization of quantities or approximations made to certain equations. Examples are the use of the Haaland approximation for the friction factor, or the linearization of AC-losses in YBCO tapes. These types of inaccuracies are inherent to the model and form a fundamental limitation to the accuracy that can be acquired by the model.

Less fundamental are the inaccuracies originating from (yet) unknown variables. Examples of this are the roughness of the piping, or the correction on AC-losses of the Norris equation. Since these are design parameters they influence the accuracy of the model only as long as these parameters are not known. Once these parameters are specified their influence on the overall accuracy is reduced. For example the correction on the Norris equation ranges from 0.5 to 1. While this leaves for a wide range of possible AC-losses that could be expected, once the cable design is specified the correction factor is an exact known variable and is thus of small influence on the total accuracy.

This appendix will address both types of inaccuracies, since they are both relevant to the model predictions. In the results however it should be noted which accuracies are fundamental to the model that is used and which accuracies rely on input parameters. Table 24 and Table 25 shows the input parameters that are used in the model and are the baseline reference for the variations. Only one of these input parameters is varied at a time. The parameters are either model or material properties or design parameters that might be chosen.

**Table 24 Model input parameters**

Parameter	Property/Design	Value	Varied between	Unit
Nitrogen density	Property	840	810-860	kg·m <sup>-3</sup>
Nitrogen viscosity	Property	0.2	0.14-0.28	mPa·s
Nitrogen heat capacity	Property	2010	2000-2040	J·kg <sup>-1</sup> ·K <sup>-1</sup>
Copper heat capacity	Property	170		J·kg <sup>-1</sup> ·K <sup>-1</sup>
Copper thermal conductivity	Property	500	500-600	W·K <sup>-1</sup> ·m <sup>-1</sup>
PPLP thermal conductivity	Property	0.05 and 0.25		W·K <sup>-1</sup> ·m <sup>-1</sup>
PPLP tangent delta	Property	6·10 <sup>-4</sup>		
PPLP K-factor	Property	2.6		
MLI heat intrusion	Design	3.4 and 5		W·m <sup>-2</sup>
Cryostat roughness	Design/property	0.03	0.015-0.030	mm
AC coupling	Property	1		
Norris correction	Design	0.5 and 0.9		
Linearization range	Property	66 – 77	None, 3, 5 and 10	K
Cooling penalty	Property	20		

**Table 25 Model input parameters**

Parameter	Property/Design	Value	Varied between	Unit
Maximum pressure head	Design	0.30-1.15		MPa
Inlet temperature	Design	66		K
System critical current	Design	2000, 3000 and 4000		A
System nominal current	Design	1000		A
System length	Design	2000, 3000 and 4000		M
System frequency	Design	50		Hz
System voltage/Phase voltage	Design	150/87		kV
Maximum allowed electric field	Design	6-16		kV·mm <sup>-1</sup>
Copper cross section	Design	150-350		mm <sup>2</sup>
Former diameter	Design	30		mm
Number of element	Property	64	4-64	

### D.1 Number of elements

The accuracy of the model depends on the assumptions made and the number of elements that are calculated. To determine the desired accuracy of the model several amounts of elements are calculated with the same assumptions. By doing this the (in)accuracy for the assumptions made is the same for every amount of elements. Only the amount of elements used contributes to the overall accuracy. The number of elements used are 4,8,16,32 and 64 elements. The total heat loss for the cable system is calculated and compared.

**Table 26 Comparison between element numbers**

Number of elements	Cooling power <i>P</i> (kW)	Change in Power <i>P</i> (kW)
4	164.52	
8	169.30	5.22
16	169.87	0.47
32	170.02	0.15
64	170.06	0.04

Table 26 shows the calculated cooling power required with different amount of elements. The accuracy of these calculations in general is limited by the assumptions and accuracy of the source data. It can thus be argued that the accuracy increase from 8 to 64 elements is beyond the accuracy of the calculations in general.

Although this is the case for the total cooling power required this is not the case for the temperature distribution along the cable. Figure D-1 shows that the 4 and 8 element calculations show a difference between the temperature distribution along the cable. The 16, 32 and 64 element models show comparable temperature distributions and maximum temperatures.

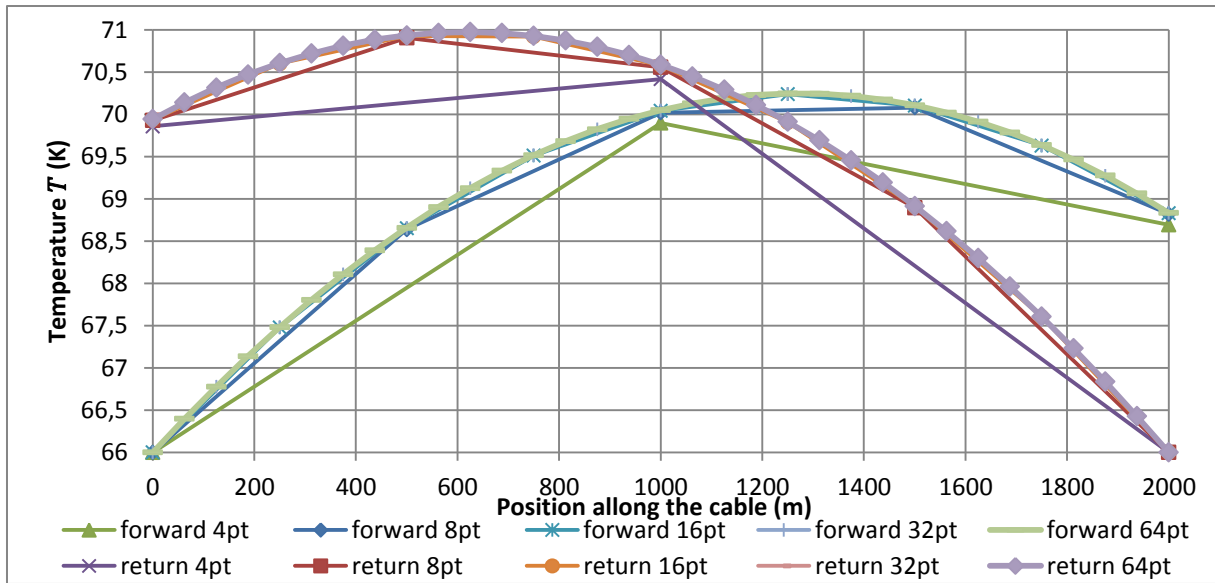


Figure D-1 Temperature distribution along the cable for different amount of elements modelled

Table 27 Maximum cable temperature and location for different number of elements

Number of elements	Maximum Temperature $T$ (K)	Location of the maximum (m)
8	70.91	500
16	70.93	500
32	70.97	625
64	70.97	625

Figure D-2 and Table 27 compare the location of the maximum. It can be seen that although the temperature difference between the number of elements is small, the location of the maximum varies. Only the 32 and 64 element show a maximum at the same position of the cable. For this reason the 64 element method is used in all calculations.

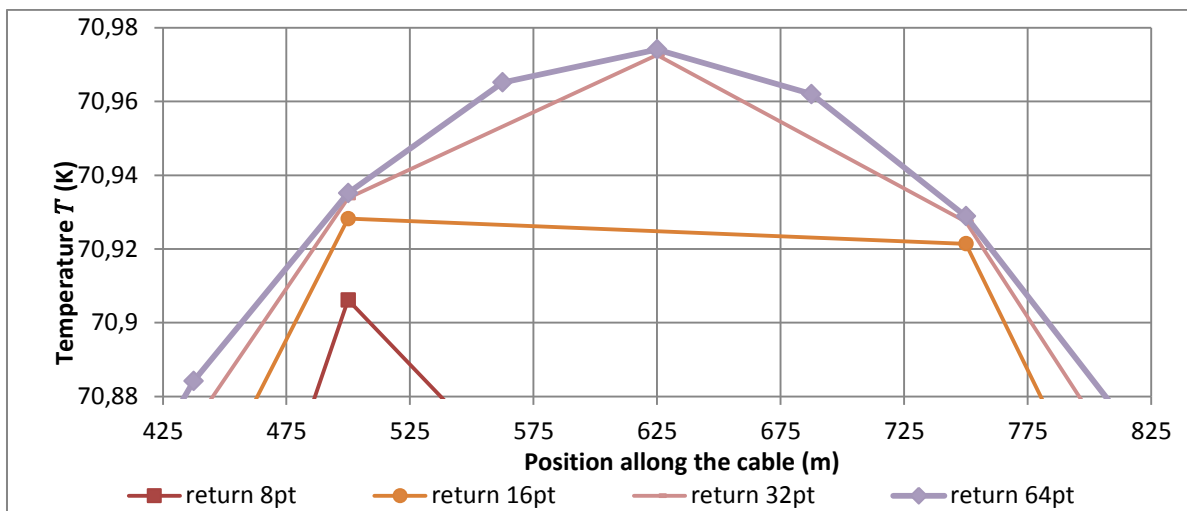


Figure D-2 Comparison of maximum temperature location

This accuracy is a fundamental model accuracy. The accuracy of the model can never exceed this accuracy. With the use of 64 elements the location accuracy can be expressed by equation (41)

$$\Delta L_{T_{\max}} = \frac{L}{32} \quad (41)$$

For a 2000 meter long cable this means that the maximum accuracy of the location of the maximum temperature is 63 meter. The accuracy for the temperature of the model is  $\pm 0.01$  K and for the cooling power  $\pm 0.1$  kW. These accuracies are the accuracies determined by the number of elements used. The accuracy of the model as a whole is smaller since other parameters also influence this accuracy.

### D.2 YBCO properties

The property of the YBCO tape that is most of influence on the accuracy of the model is the temperature dependency of the AC-losses in the wire. When no linearization is applied the difference at 66K is 502% with an average of 278% difference in the interval from 66 K to 77 K. When comparing the linearized AC-losses with the actual AC-losses at a given temperature the maximum difference between real and linearized losses is 151% with an average of 131% when linearized between 66 and 77 Kelvin. This can be seen in Figure D-3.

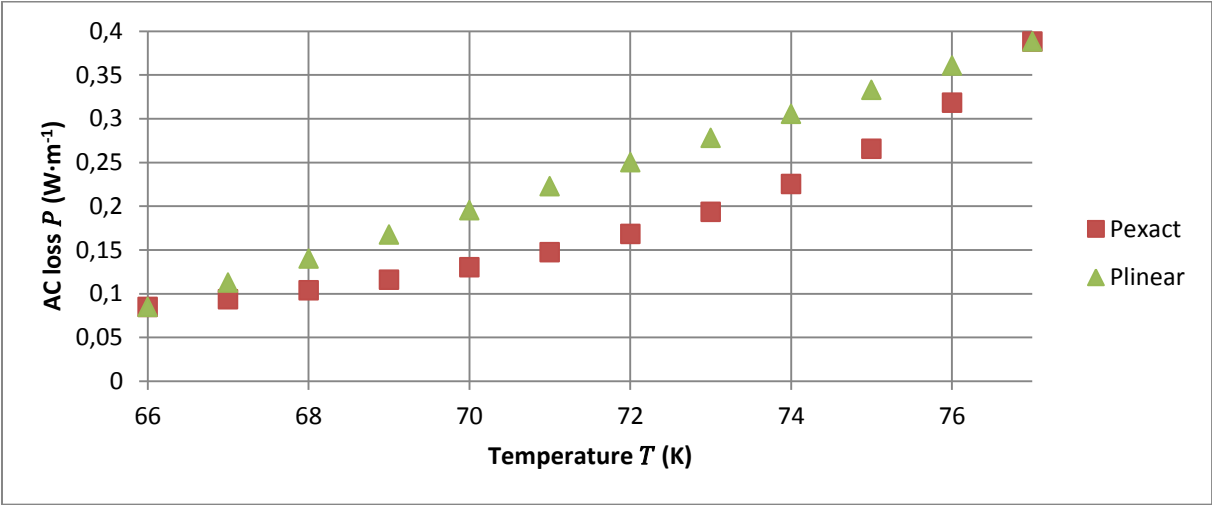


Figure D-3 Exact AC-loss and linearized AC-loss for 66 to 77 Kelvin

When the linearized segment is reduced to 66 and 71 Kelvin the maximum difference between real and linearized loss is 113% and the average is 107%.

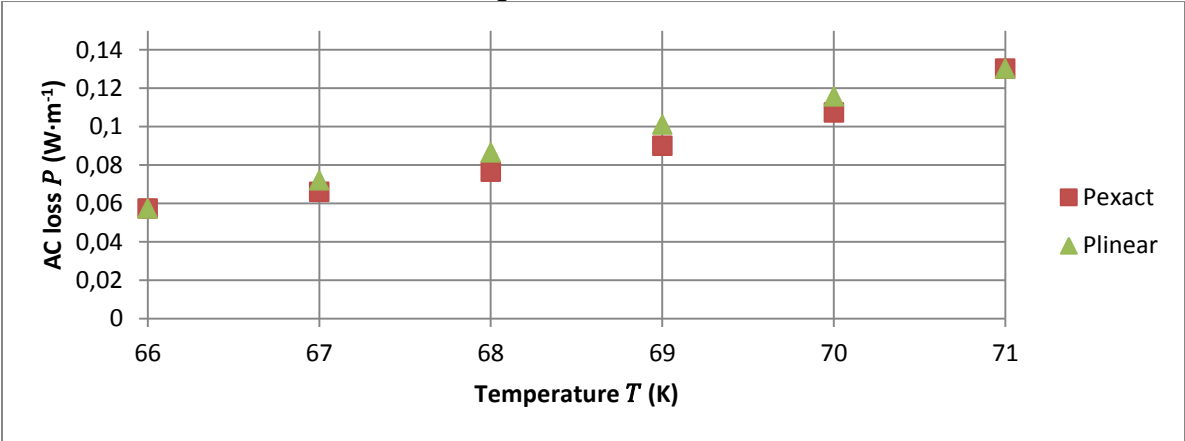


Figure D-4 Exact AC-loss and linearized AC-loss for 66 to 71 Kelvin

As can be seen in Figure D-4 reducing the linearized section increases the accuracy of the linearization. For a cold side temperature of 66 Kelvin 4 calculations are made based upon the 64 point model. A calculation using no linearization and only the 77K AC-loss is made, a 10K linearization is made and the 5K linearization is made. A final linearization is done in the 66 K to 69 K region to

reach 97% difference between average linearized loss and exact calculated loss. This is done to determine the influence of the linearization on the total accuracy of the model.

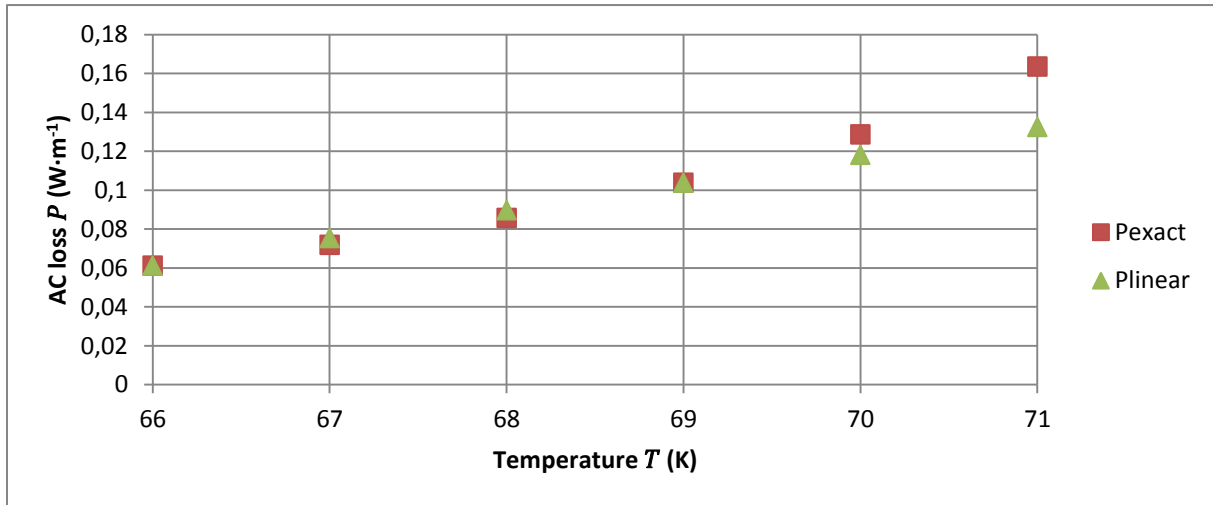


Figure D-5 Exact AC-loss and linearized AC-loss for 66 to 69 Kelvin

Table 28 Comparison between linearization methods

Linearization	Cooling power $P$ (kW)	Maximum Temperature $T$ (K)	$Q_{\text{Linear}}/Q_{\text{Exact}}$	$Q_{\text{AC}}/Q_{\text{total}}$
None (77 K)	215.06	72.22	278%	39%
66 K – 77 K	170.06	70.97	131%	23%
66 K – 71 K	158.23	70.64	107%	17%
66 K – 69 K (71 K)	156.69	70.60	97%	16%

The accuracy of the linearization is very dependent on the temperature range that is linearized. For smaller temperature ranges the accuracy of the linearization is increased. Table 28 also shows that even a linearization over a large temperature range yields better results than no linearization at all.

Since the final result lies in the range of the smaller linearization ranges, these results are the most accurate. For this set of input parameters the linearization result yield a cooling power required between 156.69 and 158.23 kW. This gives a cooling power  $\pm 2$  kW and a maximum temperature of  $\pm 0.04$  Kelvin.

It should also be noted that the different linearization intervals showed no change in position for the maximum temperature. This accuracy is a fundamental accuracy and is not likely to be increased because of the limitations of the linearization.

### D.3 Copper properties

Some of the properties of copper are assumed constant at the temperature. In reality these properties are temperature dependent. An analysis of these properties has to be made to determine their influence on the accuracy of the model. The main property of influence is the thermal conductivity. In the model a thermal conductivity of  $500 \text{ W}\cdot\text{K}^{-1}\cdot\text{m}^{-1}$  is used. This is the conductivity at 77 K. At 65 K the thermal conductivity is  $600 \text{ W}\cdot\text{K}^{-1}\cdot\text{m}^{-1}$ . A comparison of the results is made using the 64 element model. Table 29 shows that the thermal conductivity of the copper is of negligible influence on the parameters of the cable. This property is fundamental to the model, but it is shown that it does not harm the accuracy of the model.

Table 29 comparison between thermal conductivity of copper

Thermal conductivity ( $W \cdot K^{-1} \cdot m^{-1}$ )	Cooling power $P$ (kW)	Maximum Temperature $T$ (K)	Position of the maximum (m)
500	170.06	70.97	625
525	170.06	70.97	625
550	170.06	70.97	625
575	170.06	70.97	625
600	170.06	70.97	625

#### D.4 Nitrogen properties

The properties of nitrogen are described in chapter A.3. The properties that influence the accuracy of the model are the density and the viscosity. Since both are considered a temperature independent property the inaccuracy caused by this consideration is an inaccuracy inherent to the model. The effect of this consideration is determined by varying the density and viscosity independently.

Table 30 Influence of nitrogen density

Density ( $kg \cdot m^{-3}$ )	Cooling power $P$ (kW)	Maximum Temperature $T$ (K)	Position of the maximum (m)
860	169.51	70.87	625
850	169.78	70.92	625
840	170.06	70.97	625
830	170.34	71.03	625
820	170.63	71.08	625
810	170.93	71.14	625

Table 31 Influence of nitrogen viscosity

Viscosity (mPa·s)	Cooling power $P$ (kW)	Maximum Temperature $T$ (K)	Position of the maximum (m)
0.14	169.30	70.76	625
0.20	170.06	70.97	625
0.28	171.01	71.25	625

Table 30 and Table 31 show a range 1.7 kW for the cooling power and 0.5 K for the temperature maximum. It can thus be stated that the temperature dependency of the nitrogen properties is justly neglected.

The heat capacity of nitrogen is varied from 2000 to 2040  $J \cdot kg^{-1} \cdot K^{-1}$ . It can be seen in Table 32 that the influence of nitrogen heat capacity is less than  $\pm 1$  kW for the cooling power and less than  $\pm 0.2$  K for the temperature maximum. Heat capacity is correctly assumed of negligible influence.

Table 32 Influence of nitrogen heat capacity

Heat capacity (J·kg <sup>-1</sup> ·K <sup>-1</sup> )	Cooling power <i>P</i> (kW)	Maximum Temperature <i>T</i> (K)	Position of the maximum (m)
2000	170.23	71.01	625
2010	170.06	70.97	625
2020	169.88	70.93	625
2030	169.71	70.90	625
2040	169.54	70.86	625

## D.5 Orders of magnitude of heat transfer

One of the assumptions that are made is neglecting of the convective heat transfer in the total heat transfer balance during steady state operation. From the calculations it is shown that the convective heat transfer is 300 times bigger than the conductive heat transfer. The conductive heat transfer is thus correctly determined as the limiting factor and the convective heat transfer is correctly ignored.

## D.6 Critical current at adiabatic temperature

The critical current at a given temperature is given by equation (34), to determine the accuracy the partial derivative is used. For this partial derivative only the accuracy of the temperature is relevant, since the other values are input values and are exactly known.

$$\Delta I_c = I_{c(T_{ref})} k \Delta T \quad (42)$$

Equation (42) gives the accuracy for the critical current.

## D.7 RC time

The accuracy of the RC time is determined using its partial derivative. Since the diameter is an input parameter, the resulting area is exactly known and the accuracy of the surface area can be ignored. The same is true for the hydraulic diameter  $D_h$ .

$$\tau_{RC} = \frac{m C_p}{A h} \quad (43)$$

$$\Delta \tau_{RC} = \sqrt{\left| \frac{C_p}{A h} \right|^2 \cdot |\Delta m|^2 + \left| \frac{m}{A h} \right|^2 \cdot |\Delta C_p|^2 + \left| \frac{m C_p}{A h^2} \right|^2 \cdot |\Delta h|^2} \quad (44)$$

$$m = A v \rho \quad (45)$$

$$\Delta m = \sqrt{|A v|^2 \cdot |\Delta \rho|^2 + |A \rho|^2 \cdot |\Delta v|^2} \quad (46)$$

$$h = \frac{Nu \cdot k}{D_h} \quad (47)$$

$$\Delta h = \sqrt{\left| \frac{Nu}{D_h} \right|^2 \cdot |\Delta k|^2 + \left| \frac{k}{D_h} \right|^2 \cdot |\Delta Nu|^2} \quad (48)$$

$$Nu = \frac{\left(\frac{f}{8}\right) (Re - 1000) Pr}{1 + 12.7 \left(\frac{f}{8}\right)^{\frac{1}{2}} \left(Pr^{\frac{2}{3}} - 1\right)} \quad (49)$$

$$\begin{aligned}
\Delta Nu = & \left( \left| \frac{\left( 1 + 12.7 \left( \frac{f}{8} \right)^{\frac{1}{2}} \left( Pr^{\frac{2}{3}} - 1 \right) \right) \left( \frac{f}{8} \right) (Re - 1000) - \left( \frac{f}{8} \right) (Re - 1000) Pr \left( \frac{2}{3} 12.7 \left( \frac{f}{8} \right)^{\frac{1}{2}} Pr^{-\frac{1}{3}} \right)}{\left( 1 + 12.7 \left( \frac{f}{8} \right)^{\frac{1}{2}} \left( Pr^{\frac{2}{3}} - 1 \right) \right)^2} \right|^2 \cdot |\Delta Pr|^2 \right. \\
& + \left. \left| \frac{\left( \frac{f}{8} \right) Pr}{1 + 12.7 \left( \frac{f}{8} \right)^{\frac{1}{2}} \left( Pr^{\frac{2}{3}} - 1 \right)} \right|^2 \cdot |\Delta Re|^2 \right. \\
& \left. + \left( \left| \frac{\left( 1 + 12.7 \left( \frac{f}{8} \right)^{\frac{1}{2}} \left( Pr^{\frac{2}{3}} - 1 \right) \right) \frac{Pr}{8} (Re - 1000) - \frac{12.7}{16} \left( \frac{f}{8} \right)^{\frac{1}{2}} Pr (Re - 1000) \left( Pr^{\frac{2}{3}} - 1 \right)}{\left( 1 + 12.7 \left( \frac{f}{8} \right)^{\frac{1}{2}} \left( Pr^{\frac{2}{3}} - 1 \right) \right)^2} \right|^2 \cdot |\Delta f|^2 \right)^{1/2}
\end{aligned} \tag{50}$$

$$Re = \frac{\rho v D_h}{\mu} \tag{51}$$

$$\Delta Re = \sqrt{\left| \frac{v D_h}{\mu} \right|^2 \cdot |\Delta \rho|^2 + \left| \frac{\rho v D_h}{\mu^2} \right|^2 \cdot |\Delta \mu|^2 + \left| \frac{\rho D_h}{\mu} \right|^2 \cdot |\Delta v|^2} \tag{52}$$

$$Pr = \frac{C_p \mu}{k} \tag{53}$$

$$\Delta Pr = \sqrt{\left| \frac{C_p}{k} \right|^2 \cdot |\Delta \mu|^2 + \left| \frac{\mu}{k} \right|^2 \cdot |\Delta C_p|^2 + \left| \frac{C_p \mu}{l^2} \right|^2 \cdot |\Delta k|^2} \tag{54}$$

$$\Delta f = 2\%$$

The other accuracies are the ranges of variation as tabulated in Table 24. The accuracy of the RC time is calculated using equations (43) to (54). Using these equations the accuracy is now calculated. The accuracies for the different RC times can be found in Appendix C.

## D.8 Conclusions

Table 33 Sum of accuracies

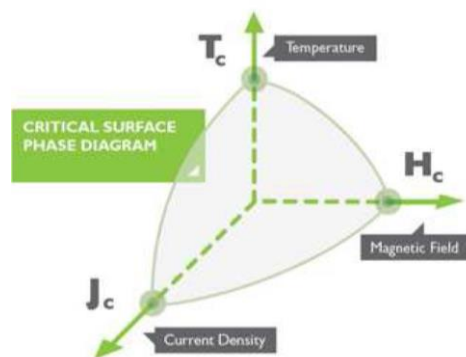
Source	Cooling power accuracy (kW)	Temperature accuracy (K)
Number of elements	± 0.1	± 0.01
YBCO properties	± 2	± 0.4
Copper properties	± 2	± 0.2
Nitrogen properties	± 0.5	± 0.1
<b>Total</b>	<b>± 5</b>	<b>± 0.7</b>

When all the before mentioned accuracies are combined the total accuracy of the model can be acquired. The accuracy for the maximum temperature is ± 0.7 K. For the cooling power the accuracy is ± 5 kW.

## Appendix E. Graduation Assignment

TenneT onderzoekt de mogelijkheid supergeleidende (cryogene) kabels toe te passen in het Nederlandse hoogspanningsnet. Supergeleiding betekent elektrische geleiding zonder weerstand. In de elektrotechniek is alles steeds beperkt door warmteontwikkeling als gevolg elektrische weerstand. Het fenomeen supergeleiding is ontdekt bij een temperatuur nabij het absolute nulpunt ( 0 Kelvin). Momenteel zijn er materialen ontwikkeld die supergeleitend zijn bij hogere temperatuur (77 Kelvin). Dit komt overeen met de temperatuur van vloeibare stikstof. High Temperature Superconducting (HTS) kan voor een revolutie zorgen in de energievoorziening maar er dient nog veel in detail te worden uitgezocht. Een van de onderwerpen is de specificering van een HTS kabel.

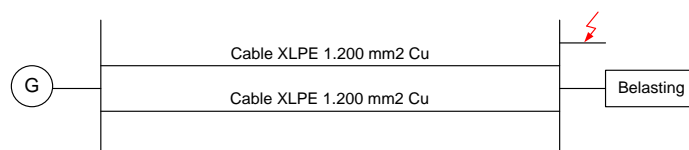
Een HTS kabel blijft in de supergeleidende modus zolang de volgende kritische grenzen niet worden overschreden, dit zijn: temperatuur, stroomdichtheid en magneetveld waarin de supergeleider zich bevindt, Figuur 1.



Figuur 1 Voorwaarden voor supergeleiding.

Bij een kortsluiting in een supergeleidende kabel moet deze de kortsluitstroom kunnen verwerken en mag de kabel geen schade ondervinden anders dan op de foutplaats zelf. Raakt de HTS kabel als gevolg van de kortsluitstroom uit de supergeleidende modus dan heeft de kabel wel weerstand en ontstaat er als gevolg van stroomdoorgang warmteontwikkeling. De ontwikkelde warmte en daarmee gepaard gaande temperatuursverhoging zal de kabel-isolatie niet beschadigen, als gevolg van de aanwezige vloeibare stikstof. De temperatuur van de stikstof zelf gaat wel omhoog en komt boven de kritische temperatuur. De kabel wordt bij een normaal functionerende beveiliging binnen 100 ms afgeschakeld. Mocht de eerste beveiliging niet werken dan treden de volgende beveiligingen in werken en volgt afschakeling na maximaal 1 seconde, maar ook dan is er geen schade.

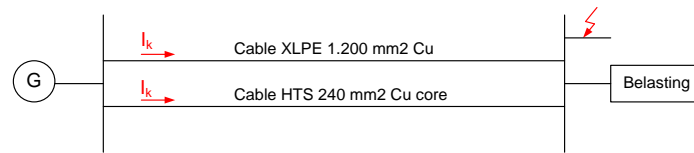
Een supergeleidende kabel moet kunnen worden ingepast in het bestaande hoogspanningsnet. Dit betekent dat zowel onder normaal bedrijf als tijdens kortsluiting de supergeleidende kabel de juiste eigenschappen moet hebben voor een bestaand net. Figuur 2 toont een generator die een belasting voedt via twee standaard XLPE kabels. Bij het falen van één van de kabelverbindingen zorgt de tweede kabelverbinding er voor dat de belasting gevoed blijft.



Figuur 2 Standaard XLPE kabels voeden de belasting / een kortsluiting.

Bij een kortsluiting aan de zijde van de belasting zullen de kabels samen de kortsluiting voeden. Nadat de fout is afgeschakeld zijn de kabels opgewarmd maar blijven verder gewoon in bedrijf.

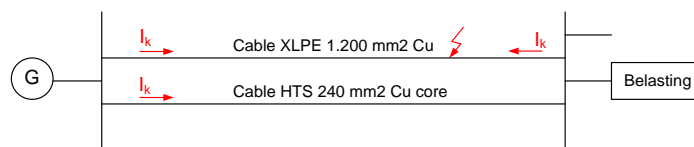
In Figuur 3 is dezelfde situatie nogmaals weergegeven maar nu is een van de kabels supergeleidend (aangevuld met een kleine koperen kern).



**Figuur 3 HTS kabel parallel aan standaard XLPE kabel.**

Door de kortsluitstroom raakt de HTS kabel uit supergeleiding (stroomdichtheid). Hierdoor wordt de vloeibare stikstof opgewarmd ( $I^2.R$ ) en nadat de kortsluiting is afgeschakeld duurt het enige tijd voordat de kabel weer onder de kritische temperatuur komt.

In Figuur 4 ontstaat een kortsluiting in de XLPE kabel. De kortsluiting wordt mede gevoed door de HTS kabel en deze raakt daarbij uit de supergeleidende modus.



**Figuur 4 Kortsluiting in de XLPE kabel waarbij HTS kabel uit supergeleiding.**

De XLPE kabel wordt afgeschakeld door de beveiliging en de HTS kabel voedt nu alleen de belasting, maar kan uit supergeleiding geraken. De HTS-kabel heeft een geleider die bestaat uit HTS-materiaal en uit koper. Het koper dient om de stroom over te nemen zodra het HTS-materiaal uit supergeleiding raakt. Het koper is dus een reservegeleider. Een tweede functie kan de warmtecapaciteit van koper geven als koude-buffer die nog geoptimaliseerd kan worden. Door de warmteontwikkeling ( $I^2.R$ ) in de kabel kan deze niet terug meer terug keren in supergeleiding als de kritische temperatuur is overschreden. De transportcapaciteit van de HTS kabel is gebaseerd op de maximale stroomdichtheid bij supergeleiding en niet op de elektrische weerstand van de koperen kern, maar die zou wel betrokken worden in de berekening zowel qua stroombegrenzing als koudebuffer. De toestand waarin de kabel veel warmte produceert kan niet blijven bestaan. Het leidt tot onacceptabele gasvorming in de kabel, zorgt dat de kabel niet direct ingeschakeld kan worden en kan ook leiden tot beschadiging van de isolatie.

Onderzoeksvragen:

Hoofdvraag:

- Hoe ziet een HTS kabel specificatie eruit, zodat deze bij een doorgaande kortsluitstroom (kortsluitsluiting buiten de kabel) niet uit supergeleiding raakt.

Sub vragen:

- Hoeveel warmte wordt er in een supergeleidende kabel ontwikkeld bij een doorgaande kortsluiting en tot welke temperatuursverhoging leidt dit?
- Hoeveel HTS-materiaal en hoeveel koper moet er aan de kern van de kabel worden toegevoegd om de HTS kabel bij een doorgaande kortsluitstroom supergeleidend te houden?
- Kan de stroombegrenzende eigenschap van een HTS kabel (overschrijding kritische magneetveldsterkte) hierin een verbetering bewerkstellingen?

Optionele vraag:

- Welke ontwikkeling in efficiency van koeling voor supergeleidende kabel mag er nog verwacht?
- Zijn er alternatieve strategieën om deze situatie het hoofd te bieden? Bijvoorbeeld FCL (Fault Current Limiters)?

Benodigd kennis/onderzoek:

- Traditionele hoogspanningskabelsystemen
- Internationale normen Kortsluitberekeningen
- Supergeleidende kabels, opbouw en koeling
- Warmtemodellen

Onderzoeksduur:

- Circa 17 weken.